AD

USAAVLABS TECHNICAL REPORT 69-99

A PRELIMINARY DESIGN STUDY OF A QUIET LIGHT OBSERVATION HELICOPTER

By

E. L. Brown
C. R. Cox
D. R. Halwes

December 1969

U. S. ARMY AVIATION MATERIEL LABORATORIES
FORT EUSTIS, VIRGINIA

CONTRACT DAAJ02-68-C-0095
BELL HELICOPTER COMPANY
A TEXTRON COMPANY
FORT WORTH, TEXAS

16

Disclaimers

The findings in this report are not to be construed as an official Department of the Army position unless so designated by other authorized documents.

When Government drawings, specifications, or other data are used for any purpose other than in connection with a definitely related Government procurement operation, the United States Government thereby incurs no responsibility nor any obligation whatsoever; and the fact that the Government may have formulated, furnished, or in any way supplied the said drawings, specifications, or other data is not to be regarded by implication or otherwise as in any manner licensing the holder or any other person or corporation, or conveying any rights or permission, to manufacture, use, or sell any patented invention that may in any way be related thereto.

Disposition Instructions

Destroy this report when no longer needed. Do not return it to the originator.

DEPARTMENT OF THE ARMY
U. S. ARMY AVIATION MATERIEL LABORATORIES
FORT EUSTIS, VIRGINIA 23604

This report has been prepared by Bell Helicopter Company under the terms of Contract DAAJ02-68-C-0095. This effort was a preliminary design study and analytical investigation of an LOH helicopter. The purpose was to establish the degree of quietening possible and to determine what penalties in performance and mission capabilities are associated with the application of noise-reduction measures.

As a result of the work accomplished, design data for four configurations are presented. Two of the configurations maintain the same gross weight as the baseline helicopter and are compared on the basis of mission useful load, range and endurance, and speed and/or maneuvering capability, versus noise reduction. The other two configurations maintain the payload and performance of the base helicopter and show required increase in gross weight to maintain a comparable noise reduction.

The design data contained herein are concurred in by this Command. This concurrence is limited to the technical feasibility and does not imply the practicality of the proposed design or the use of such designs on current Army aircraft.

Task 1F162203A14081
Contract DAAJ02-68-C-0095
USAAVLABS Technical Report 69-99
December 1969

A PRELIMINARY DESIGN STUDY OF A QUIET LIGHT OBSERVATION HELICOPTER

Final Report

Bell Helicopter Report 299-099-526

By

E. L. Brown
C. R. Cox
D. R. Halwes

Prepared by

Bell Helicopter Company
A Textron Company
Fort Worth, Texas

for

U. S. ARMY AVIATION MATERIEL LABORATORIES
FORT EUSTIS, VIRGINIA

SUMMARY

This report, prepared for USAAVLABS under Contract DAAJ02-68-C-0095, presents the results of a preliminary design study and an analytical investigation of noise-reduction measures for the OH-58A Light Observation Helicopter. The purpose was to establish what degree of quieting is possible and what penalties in performance and mission capabilities are associated with the application of noise-reduction measures.

Design data are presented for four configurations. Two are test/demonstrator versions suitable for a 10-hour test program to verify the predicted noise reductions. The primary test configuration has modified main- and tail-rotor blades, reduced rotor speeds, a four-bladed tail rotor, and engine-exhaust silencers for maximum practical reduction in perceived noise level. The alternate test configuration has main-rotor blades that are further modified for additional noise reduction.

On both test configurations, noise reduction degrades performance. The quieting features result in 6- to 14-percent increases in empty weight. If gross weight is increased so as to retain the OH-58A's mission useful load, range and endurance are unaffected, but hover ceiling, maneuvering capability, and speed are degraded. Reducing the fuel load to preserve the hover ceiling degrades endurance and range. Further reducing useful load to improve speed and/or maneuvering capability increases hover ceiling but substantially reduces payload, endurance, and range.

The other two configurations show the redesign and the increase in weight necessary to give an operational LOH the performance and payload of the OH-58A. Their noise levels are similar to those of the test/demonstrator versions. The quieting features result in 15- to 27-percent increases in empty weight.

Perceived noise levels are affected by the helicopter's flight conditions and gross weight and the observer's aspect and distance. Perceived levels 200 feet from the test configurations at design gross weight are at least 5 PNdb, and as much as 13 PNdb, lower than those of the OH-58A. The minimum level at this distance is 77 PNdb. At 4000 feet the reductions are greater--ranging from 10 to 26 PNdb, for a minimum perceived noise level of 28 PNdb. The resulting noise levels are still above the initial design goals by 12 and 8 PNdb, respectively.

Design data, performance, and noise levels for all the study configurations are summarized (Tables XIII and XXXIV through XXXVII). A program of design modification and tests to confirm the predicted noise reductions is presented.

TABLE OF CONTENTS

		Page
SUMMARY		iii
LIST OF ILLUSTRATIONS		vii
LIST OF TABLES		x
LIST OF SYMBOLS		xiii
I.	OBJECTIVES AND APPROACH	1
II.	NOISE ANALYSIS AND CORRELATION	3
	A. Introduction	3
	B. Problem Areas	3
	C. Rotor Noise	4
	D. Engine and Drive System Noise	13
	E. Sound-Transmission Losses	17
	F. Perceived Noise Level	17
	G. Correlation	26
III.	NOISE REDUCTION TECHNIQUES	49
IV.	EFFECTS OF PARAMETERS	54
	A. Introduction	54
	B. Main Rotor	54
	C. Tail Rotor	54
V.	DESIGN ALTERNATIVES AND SELECTION OF COMPONENT PARAMETERS AND CONFIGURATIONS	63
VI.	DESIGN DESCRIPTIONS	67
	A. Test Version--Primary Configuration	67
	B. Test Version--Alternate Configuration	76
	C. Operational Version--Primary Configuration	86
	D. Operational Version--Alternate Configuration	93
VII.	COMPARISONS WITH CH-58A	102
	A. Performance	102
	B. Noise Comparisons	117
VIII.	DESIGN MODIFICATIONS AND TEST PROGRAM	121
	A. Engine-Silencer Evaluation	125
	B. Component Tests	125
	C. Hover and Flyover Noise Measurements	125
	D. Aural-Detection Tests	126

Page

E. Acoustical Instrumentation 127
F. Report 127

LITERATURE CITED 128

APPENDIX, DRAWINGS 131

DISTRIBUTION 141

LIST OF ILLUSTRATIONS

Figure		Page
1	Flow Chart for Development of Helicopter Noise Calculation	6
2	Assumed Filter Shape for Octave-Band-Level Calculation	10
3	Assumed Filter Shapes for the Preferred Octave Bands	12
4	Allison T63-A-5A Engine Noise Spectrum at $\psi = 0°$	15
5	Allison T63-A-5A Engine Noise Spectrum at $\psi = 150°$	16
6	Azimuth Distribution of Allison T63-A-5A Engine Noise	19
7	Excess Attenuation Over Open, Level Terrain	21
8	Extrapolation of Noy Curves Below 50 Hz	23
9	Extension of Perceived Noise Level for N_T Less Than 1.0	25
10	Microphone Location and Azimuth Heading for Hover and Flyover Noise Measurements	27
11	Main-Rotor and Engine Noise Spectra at $\psi = 0°$	30
12	Tail-Rotor and Engine Noise Spectra at $\psi = 150°$	31
13	OH-58A Main-Rotor Rotational-Noise Correlation	32
14	Measured and Predicted Variation of Main-Rotor Rotational Noise With Tip Speed	33
15	Tail-Rotor Rotational-Noise Correlation in Front and to Rear of Hovering OH-58A Helicopter	35
16	Tail-Rotor Rotational-Noise Correlation to Sides of Hovering OH-58A Helicopter	36

Figure		Page
17	Measured and Predicted Variation of Tail-Rotor Rotational Noise With Tip Speed	37
18	OH-58A Hover Noise Correlation at $\psi = 0°$	39
19	OH-58A Hover Noise Correlation at $\psi = 90°$	40
20	OH-58A Hover Noise Correlation at $\psi = 270°$ . . .	41
21	OH-58A Forward-Flight Noise Correlation at 45 Knots	42
22	OH-58A Forward-Flight Noise Correlation at 102 Knots	43
23	OH-58A Forward-Flight Noise Correlation at 113 Knots	44
24	Effects of Vertical Fin on OH-58A Tail-Rotor Noise	50
25	Comparison of UH-1 Square-Tip and Double-Swept-Tip Blades on Tail-Rotor Whirl Stand	52
26	Sample Computer Program Output	55
27	Effects of Tip Speed and Diameter on Two-Bladed Main-Rotor Noise	56
28	Effects of Tip Speed and Diameter on Four-Bladed Main-Rotor Noise	57
29	Effects of Tip Speed and Number of Blades on Tail-Rotor Noise	58
30	Effects of Thrust and Torque on Tail-Rotor Noise	60
31	Effects of Torque and Diameter on Tail-Rotor Noise	61
32	Variation of Tail-Rotor Noise for Different Headings	62
33	Main-Rotor Natural Frequencies, Primary Test Configuration	69
34	Main-Rotor Natural Frequencies, Atlernate Test Configuration	79

Figure		Page
35	Fatigue Life of Blade Grip, Alternate Test Configuration	81
36	Hovering Ceilings, Test Configurations	104
37	Speed at Maximum Continuous Power, Test Configurations	105
38	Specific Range, Test Configurations	106
39	Payload-Range, OH-58A	108
40	Payload-Range, Primary Test Configuration	109
41	Payload-Range, Alternate Test Configuration	110
42	Hovering Ceilings, Operational Configurations	112
43	Speed at Maximum-Continuous Power, Operational Configurations	113
44	Specific Range, Operational Configurations	114
45	Payload-Range, Primary Operational Configuration	115
46	Payload-Range, Alternate Operational Configuration	116
47	Noisiness as a Function of Perceived Noise Level	120
48	Test Program, Plan of Performance	123
49	Tapered-Tip OH-58A Main-Rotor Blade	131
50	Modified UH-1 Main-Rotor Blade	133
51	Four-Bladed Tail Rotor	135
52	Powerplant Installation	137
53	Three-View, Quiet Helicopter	139

LIST OF TABLES

Table		Page
I	Steps in Development of Rotor-Noise Calculation	5
II	Measured Noise Levels of Allison T63-A-5A Engine	18
III	Extrapolated Noy Values for Octave Bands Centered at 16 and 31.5 Hertz	24
IV	OH-58A Octave-Band Sound-Pressure Levels	28
V	Rotor Corrections To Be Added to Rotor-Only Correlation	46
VI	Engine Corrections To Be Added to Engine-Only Correlations	47
VII	Rotor Corrections To Be Added to Rotor-and-Engine Correlation	47
VIII	Engine Corrections To Be Added to Rotor-and-Engine Correlation	47
IX	Comparison of OH-58A Perceived Noise Levels (PNdb) for Different Types of Corrections	48
X	Noise Reductions for Blade-Planform Modifications	53
XI	Perceived Noise Levels for Alternate Combinations of Parameters	64
XII	Combined Noise of Complete Helicopter	65
XIII	Design Data	68
XIV	Weight and Moment Changes, Primary Test Configuration	73
XV	Group Weight Statement, Primary Test Configuration	74
XVI	Weight and Balance, Primary Test Configuration	75

Table		Page
XVII	Performance Summary, Primary Test Configuration	77
XVIII	Installation Losses, Primary Test Configuration	78
XIX	Weight and Moment Changes, Alternate Test Configuration	83
XX	Weight and Balance, Alternate Test Configuration	84
XXI	Performance Summary, Alternate Test Configuration	85
XXII	Installation Losses, Alternate Test Configuration	86
XXIII	Weight and Moment Changes, Primary Operational Configuration	89
XXIV	Group Weight Statement, Primary Operational Configuration	90
XXV	Weight and Balance, Primary Operational Configuration	92
XXVI	Performance Summary, Primary Operational Configuration	93
XXVII	Installation Losses, Primary Operational Configuration	94
XXVIII	Gross Weight and Rotor Thrust, OH-58A and Alternate Operational Configuration	96
XXIX	Weight and Moment Changes, Alternate Operational Configuration	97
XXX	Group Weight Statement, Alternate Operational Configuration	98
XXXI	Weight and Balance, Alternate Operational Configuration	99
XXXII	Performance Summary, Alternate Operational Configuration	100
XXXIII	Installation Losses, Alternate Operational Configuration	101

Table		Page
XXXIV	Performance Comparisons, Test Configurations, Observation Mission	.103
XXXV	Performance Comparisons, Operational Configurations	.111
XXXVI	Perceived Noise Levels at 200 Feet (PNdb) . . .	.118
XXXVII	Perceived Noise Levels at 4000 Feet (PNdb) . .	.119

LIST OF SYMBOLS

A	rotor disc area, πR^2, ft^2
a_o	speed of sound in air, ft/sec
a_g	absorption over the ground, db
a_{mB}, b_{mB}	sound-pressure-amplitude coefficients of mBth harmonic sound radiation, lb/ft^2
$a_{\lambda,(T,D,C)}$ $b_{\lambda',(T,D,C)}$	aerodynamic loading terms for steady values of thrust, drag, and radial force
a'_{mol}	molecular absorption, db
B	number of blades
C	outboard (radial) component of force, lb
C_m	sound-pressure amplitude, db
C_T	thrust coefficient, $T/2\rho A(\Omega R)^2$
c	blade chord, ft
c_e	effective blade chord, based on thrust, ft
D	total blade drag force, lb
d	directivity increment, db
db	decibels, 20 $\log_{10}$ (pressure ratio), pressure ratio is re 0.0002 $dyne/cm^2$
f	frequency, Hz
f_c	octave-band center frequency, Hz
f_{cj}	center of frequency of jth octave, Hz
f_1, f_{1j}	lower cutoff frequency, Hz
f_2, f_{uj}	upper cutoff frequency, Hz

f_o	frequency at which maximum octave level occurs, Hz
fr	product of frequency times retarded distance, Hz-ft
Hz	cycles per second
i_d	incidence of the rotor disc, deg
J_{mB}	Bessel function of the first kind, order mB
K	frequency coefficient for broadband noise
K_M	hub-material constant
K_T	nondimensional rotor constant
k	loading power-law exponent
L	limiting value for rotational noise summation, $mB(1+M_e)$
l_c	correlation length
M_e	effective rotational Mach number of rotor, ηM_t
M_o	component of the forward-speed flight Mach number of the helicopter in the direction of the observer, $\frac{V}{a_o}$ (cos α)
M_t	rotational Mach number of blade tip, ΩR
m	sound harmonic number
N_B	number of rotor blades
N_{II}	normal operating rotor speed, pct
N_F	limit flight-load factor
N_k	noy value
N_T	total noy value
N_{max}	number of noy in octave band with highest noy value
PNdb	unit of perceived noise level
PNL	perceived noise level
Q	total rotor torque, ft-lb
R	rotor radius, ft

R'	total retarded distance, ft
R_1, R_2	distances of source and observer, ft
r	straight-line distance from observer, ft
r_1	$r(1 - M_o)$, ft
S_m	spectrum shape factor
S_b	total blade planform area, ft^2
SLS	sea level standard day
SPL	sound-pressure level, db
ΔSPL	change in sound-pressure level, db
T	rotor thrust, lb
t_c	thrust coefficient = $2\ C_T/\sigma$
V	forward flight velocity of the helicopter along the flight path, ft/sec
V_{ne}	aircraft speed not to be exceeded in flight, kt
V_t	rotor tip speed, ΩR, ft/sec
W	gross weight, lb
W_{MR}	main-rotor weight, lb
X	for the main rotor, the projected distance between the helicopter and the observer, in the longitudinal direction, in the ground plane, ft
X'	for the main rotor, the retarded distance between the helicopter and the observer, in the lateral direction, in the ground plane, ft
x	axial distance between the observer and the rotor hub, measured positive in the direction of thrust action, ft
Y	for the main rotor, the projected distance between the helicopter and the observer, in the lateral direction, in the ground plane, ft
y	component of r in the rotor-disc plane, ft
Z	vertical distance of the helicopter above the ground, ft

α	exponent defined as 2-2k
β	blade coning angle, deg
η	effective blade loading station, pct of R
θ	angular position of observer from rotor axis, deg
λ	loading harmonic number
ρ	atmospheric density, slug/ft^3
Σ	summation
σ	rotor solidity = $\frac{Bc_e}{\pi R}$
ϕ	angular position of observer from y-axis, deg
ψ	rotor azimuth angle, deg
Ω	rotor rotational speed, rad/sec

I. OBJECTIVES AND APPROACH

The objectives of this study were to delineate the characteristics and parameters that would yield the highest practicable degree of quietness in an operating light observation helicopter, and to compare the predicted performance of the quiet helicopter with that of an operating helicopter without the quieting features. The helicopter selected for the study is the OH-58A. The initial design objective was a noise level of 65 PNdb at a ground range of 200 feet and 20 PNdb at 4000 feet. The details and the costs of a 10-hour test program were also to be determined.

The approach to the problem began with a review of state-of-the-art designs and techniques for noise reduction. Data on the OH-58A and the Bell Model 206A were analyzed to determine octave-band and narrow-bandwidth sound-pressure levels. These levels were then compared with the noise levels predicted by a theory that had been developed by Wyle Laboratories for USAAVLABS. The theory includes the calculation of the rotational noise that arises from steady and oscillatory aerodynamic airloads. It has been refined to include higher harmonics of rotational noise and broadband rotor noise and has been extended to the calculation of sound-transmission losses and perceived noise levels. The noise that had been measured on the OH-58A and the Model 206A was compared with that predicted by the theory, and correction factors were used to correlate the two. On the basis of the corrected theory, means to reduce the observed noise, to the desired levels if possible, were applied. In this way, the theory was used to predict the changes in the noise that would result from altering the parameters of the helicopter.

Some of the variations of the OH-58A that were considered are:

- Main Rotor: tip speed, number of blades, tip shape, diameter, chord, thrust
- Tail Rotor: tip speed, tip shape, planform, number of blades, diameter, thrust, chord
- Engine and Drive System: compartment treatment, exhaust silencing

It was found that all three sources of noise--the main rotor, the tail rotor, and the engine and drive system--must be treated to achieve the maximum of noise reduction. The design must be "balanced" in such a way that all sources of noise are quieted. In a practicable, balanced modification of the OH-58A, the overall perceived noise levels are reduced the most when the tip speed of the main rotor is reduced to 600 feet per second and that of the tail rotor to 530 feet per second, with

tail-rotor-tip modifications and an engine-exhaust noise reduction of 15 db. These are the essential parameters used in the design study for the primary test configuration.

Although a method for including the effects of impulsive and modulated noise in the calculations was not available, limited test data show that a modulated tone 6 db below an unmodulated tone may give the same effective perceived noise level. The modulated noise of the OH-58A's main rotor can be lowered by 6 db by reducing the tip speed to 530 feet per second. By using modified UH-1 blades, this tip speed can be made practicable. Therefore, on the alternate test configuration, such blades are adapted to use on the OH-58A.

The basic conditions established for the modifications of the OH-58A were:

- Maximum attainable noise reduction
- Minimum practical cost
- Some sacrifice of maneuverability
- Adequate safety and performance

Since the performance of the configurations was expected to be degraded by the quieting measures, two operational configurations were defined in order to determine the extent of the redesign and the increase in the weight that would be necessary to maintain the performance, payload, and maneuverability of the OH-58A. The noise levels of the operational configurations were to be similar to those of the test configurations.

Finally, a test program to verify the predicted noise reductions and to provide a sound basis for noise-reduction changes to light observation helicopters was developed.

II. NOISE ANALYSIS AND CORRELATION

A. INTRODUCTION

A comprehensive noise analysis is developed which, when compared and adjusted to the actual recorded noise of the OH-58A, predicts with an accuracy of ±4 PNdb the perceived noise level. Noise-reduction techniques and designs, based on a study of the technical literature, are applied to the OH-58A. The noise generated by the projected quiet LOH is then compared with that of the OH-58A.

The noise analysis is comprised of both measured data and theoretical predictions and was performed at Bell Helicopter Company, except for theoretical work done by Wyle Laboratories, Huntsville, Alabama, under subcontract to BHC. This analysis treats three sources of noise: the main rotor, the tail rotor, and the engine/drive system.

B. PROBLEM AREAS

Problem areas pertinent to the interpretation and evaluation of the subject study are outlined below and are discussed in more detail in later sections.

- Perceived Noise Level Calculation

  Noise levels are calculated using the procedure established by Kryter and Pearsons[1] to obtain the perceived noise level in PNdb. The use of these procedures results in some potential errors. The noy tables do not include the two lowest preferred octave bands. Since the low rotational-noise harmonics of the OH-58A main rotor fall into these octave bands, extrapolations are necessary. The extrapolated values are given in the test. In addition, errors inherent in the noy tables become significant when evaluating relatively low values of PNdb, such as helicopter far-field conditions. For example, the lowest obtainable value using this method is 23.2 PNdb compared with the target design value of 20.0 PNdb.

- Noise Correlation for Entire Helicopter

  In establishing the correlation between measured and calculated perceived noise levels for the complete helicopter, empirical adjustments are required. Factors not explicitly accounted for in the analytical procedures which could contribute to this requirement are:

- inflow disturbances to the tail rotor, and main-rotor and tail-rotor interference noise at forward airspeeds

- wake and tip-vortex disturbances from preceding blades

- increase in engine noise with power

These are the factors to which it is most difficult to ascribe meaningful results.

- Sound Directivity Effects

Rotational and broadband noise produce a dipole pattern with nodes or seminodes occurring in the plane and along the axis of the rotor. Thus, according to theory, an observer in the plane of the rotor would be subjected to relatively low noise. Correlation work has shown that the theory does not accurately predict the sound-pressure level in these regions. Since noise-level calculations in these regions are required, this discrepancy has significant implications with regard to the correlation studies.

C. ROTOR NOISE

The procedure used in the development of the calculation of helicopter rotor noise is given in Table I. The numbered steps relate to the flow chart in Figure 1 and are discussed below.

1. Rotational Noise

The calculation of rotational noise is based on the theory developed by Lowson and Ollerhead[2] and considers both steady and oscillatory airloads acting on the rotor blades. The calculation also includes a method to estimate the harmonic airloads. Rotational noise is calculated in four steps:

- First, the amplitudes of discrete-frequency rotational-noise harmonics are calculated up to the frequency of the harmonic whose number is

$$m = 60/B(1 + M_e) \qquad (1)$$

- Second, the amplitudes are calculated for those higher harmonics necessary to accurately predict the sound-pressure level in the octave band whose center frequency, f_c, is closest to the frequency of the harmonic whose number is $m = 60/B(1 + M_e)$.

TABLE I. STEPS IN DEVELOPMENT OF ROTOR-NOISE CALCULATION

1. Calculation of rotational-noise harmonic levels through $m = 60/B(1+M_e)$ (Equations 2 through 13)
2. Prediction of harmonic levels above $m = 60/B(1+M_e)$
3. Subtraction of atmospheric and terrain losses from the calculated sound-pressure levels (Equations 18, 19, 20, and 21)
4. Calculation of octave-band levels for rotational noise
5. Calculation of peak level of broadband noise (Equation 14)
6. Calculation of characteristic center frequency of broadband noise (Equation 15)
7. Calculation of directivity correction for broadband noise (Equation 17)
8. Calculation of spectral distribution of broadband noise (Equation 16)
9. Correlation with narrow-bandwidth analyses of OH-58A hover data
10. Determination of power-law exponent, correlation length
11. Calculation of octave-band levels for combined noise
12. Conversion of octave-band levels to perceived noise level (Equations 22, 23, and 24 and Table III, plus noy tables[1])
13. Correlation with OH-58A hover and flyover data
14. Addition of empirical adjustments for noise level of entire aircraft (Table VII)

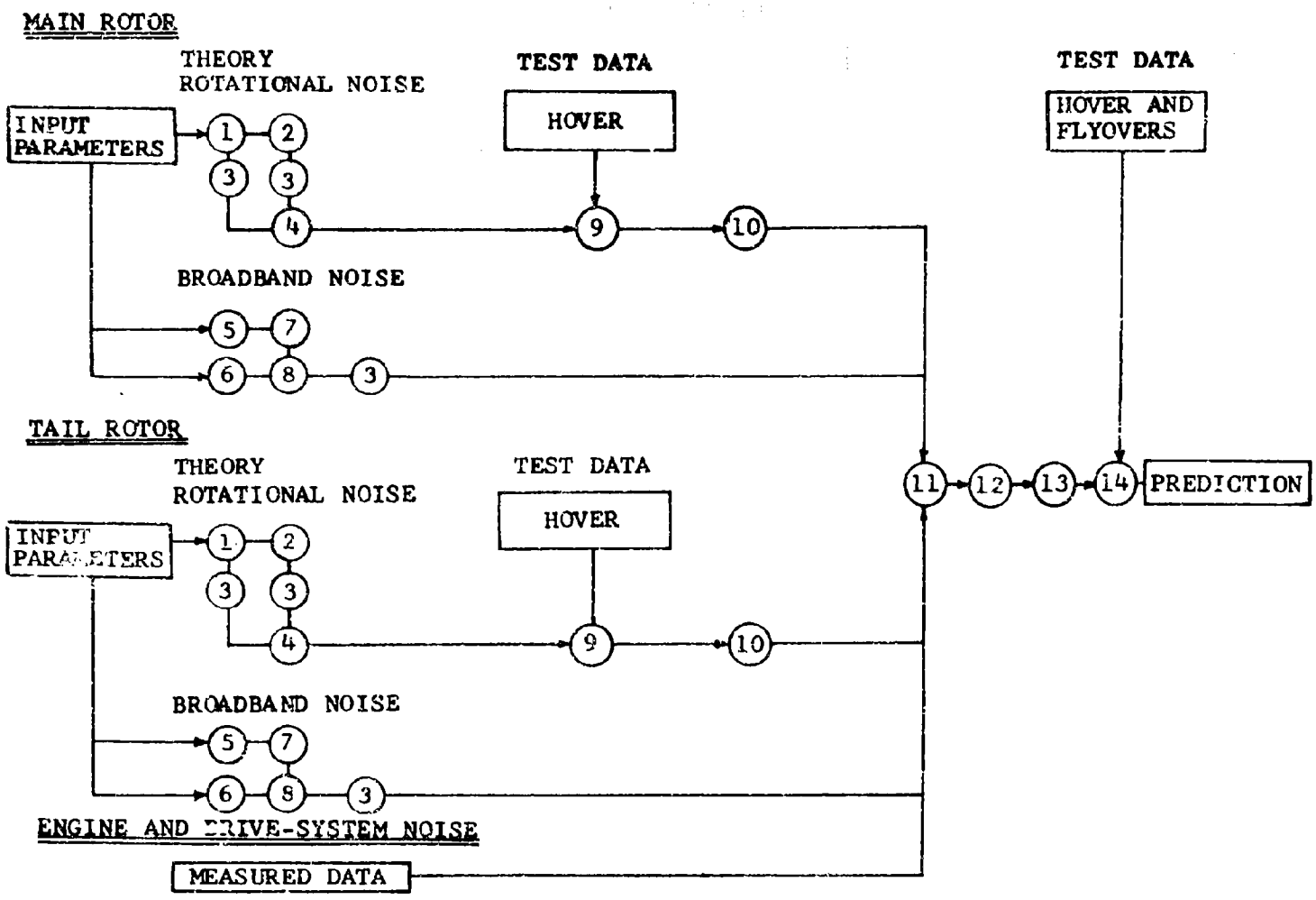

Figure 1. Flow Chart for Development of Helicopter Noise Calculation.

- Third, the octave-band levels of rotational noise are computed for bands up to and including the band containing f_c.

- Fourth, levels in all higher octave bands are calculated on the basis of the level in the band containing f_c.

a. Harmonic Levels up to $m = 60/B(1 + M_e)$

The specific equations used by Lowson and Ollerhead for the sound-pressure amplitude, C_m, due to the steady and oscillatory thrust, drag, and radial forces acting on a blade are

$$C_m = \sum_{\lambda=0}^{L} \sqrt{(a_{mB,\lambda})^2 + (b_{mB,\lambda})^2} \qquad (2)$$

where, when $mB-\lambda$ is odd,

$$a_{mB,\lambda} = \frac{mB\Omega}{4\pi a_o r_1} \left\{ \frac{x a_\lambda T}{r_1} \left(J_{mB-\lambda} + (-1)^\lambda J_{mB+\lambda} \right) \right.$$

$$- \frac{a_\lambda D}{mBM_e} \left\{ (mB-\lambda) J_{mB-\lambda} + (-1)^\lambda (mB+\lambda) J_{mB+\lambda} \right\}$$

$$\left. - \frac{y b_\lambda C}{2r_1} \left\{ J_{mB-\lambda+1} - J_{mB-\lambda-1} - (-1)^\lambda \left(J_{mB+\lambda+1} - J_{mB+\lambda-1} \right) \right\} \right\}$$

$$(-1)^{\left(\frac{mB-\lambda-1}{2} \right)} \qquad (3)$$

and when $mB-\lambda$ is even,

$$a_{mB,\lambda} = \frac{mB\Omega}{4\pi a_o r_1} \left\{ \frac{x b_\lambda T}{r_1} \left(J_{mB-\lambda} - (-1)^\lambda J_{mB+\lambda} \right) \right.$$

$$\left. - \frac{b_\lambda D}{mBM_e} \left\{ (mB-\lambda) J_{mB-\lambda} - (-1)^\lambda (mB+\lambda) J_{mB+\lambda} \right\} \right.$$

$$+ \frac{ya_\lambda C}{2r_1}\left\{J_{mB-\lambda+1}-J_{mB-\lambda-1}+(-1)^\lambda\left(J_{mB+\lambda+1}-J_{mB+\lambda-1}\right)\right\}\Bigg\}(-1)^{\left(\frac{mB-\lambda-2}{2}\right)} \quad (4)$$

where, when $mB-\lambda$ is even,

$$b_{mB,\lambda} = \frac{mB\Omega}{4\pi a_o r_1}\left\{\frac{xa_\lambda T}{r_1}\left(J_{mB-\lambda}+(-1)^\lambda J_{mB+\lambda}\right)\right.$$

$$- \frac{a_\lambda D}{mBM_e}\left\{(mB-\lambda)J_{mB-\lambda}+(-1)^\lambda(mB+\lambda)J_{mB+\lambda}\right\}$$

$$- \frac{yb_\lambda C}{2r_1}\left\{J_{mB-\lambda+1}-J_{mB-\lambda-1}-(-1)^\lambda\left(J_{mB+\lambda+1}-J_{mB+\lambda-1}\right)\right\}\Bigg\}(-1)^{\left(\frac{mB-\lambda}{2}\right)} \quad (5)$$

and when $mB-\lambda$ is odd,

$$b_{mB,\lambda} = \frac{mB\Omega}{4\pi a_o r_1}\left\{\frac{xb_\lambda T}{r_1}\left(J_{mB-\lambda}-(-1)^\lambda J_{mB+\lambda}\right)\right.$$

$$- \frac{b_\lambda D}{mBM_e}\left\{(mB-\lambda)J_{mB-\lambda}-(-1)^\lambda(mB+\lambda)J_{mB+\lambda}\right\}$$

$$- \frac{ya_\lambda C}{2r_1}\left\{J_{mB-\lambda+1}-J_{mB-\lambda-1}+(-1)^\lambda\left(J_{mB+\lambda+1}-J_{mB+\lambda-1}\right)\right\}\Bigg\}(-1)^{\left(\frac{mB-\lambda-1}{2}\right)} \quad (6)$$

This is the magnitude of the sound pressure of the mth harmonic from the complex magnitude given by Lowson's and Ollerhead's Equation 37. The effective Mach number is given by

$$M_e = \eta M_t \quad (7)$$

and the limiting value for the summation is given by

$$L = mB(1+M_e) \quad (8)$$

The argument of all the Bessel functions is $mBM_e y/r_1$.

Equations 2 through 6 show that a wide range of aerodynamic loading harmonics contributes to any one sound harmonic. In fact, the higher the sound harmonic, the greater the number of the aerodynamic harmonics. The theory assumes that the blade loads are concentrated at a single point on the blade, and that chordwise airload variations are of importance only for source frequencies having wavelengths that are small compared with a blade chord.

The amplitude of the aerodynamic loading terms in Equations 3 through 6 is

$$a_{\lambda,(T,D,C)} = (T,D,C)l_c\lambda^{-k}\cos\lambda\phi \qquad (9)$$

$$b_{\lambda,(T,D,C)} = (T,D,C)l_c\lambda^{-k}\sin\lambda\phi \qquad (10)$$

where T, D, and C are the steady values of total rotor thrust, total effective drag of all blades, and radial force at an effective blade-loading station η, respectively; λ is the order of the loading harmonic; l_c is a correlation length; and k is the exponent of the power law. Values for η, l_c, and k are determined by correlation studies.

The angle, $\lambda\phi$, is given by

$$\lambda\phi = \lambda \arctan\left[\frac{-Y}{-X\cos i_d - Z\sin i_d}\right] \qquad (11)$$

and the values of D and C are calculated from

$$D = Q/R \qquad (12)$$

$$C = T\sin\beta \qquad (13)$$

b. Harmonic Levels Greater Than $m = 60/B(1+M_e)$

A method was developed to predict harmonic noise levels above the limiting value of $m = 60/B(1+M_c)$. Instead of calculating each harmonic, the total sound-pressure level of harmonics within a given octave band is computed. The octave-band levels are then assumed to follow the same power-law exponent as used in computing the low harmonics.

c. Calculation of Octave-Band Levels

Octave-band levels of rotational noise are computed from the levels of the discrete-frequency sounds, assuming a filter shape. The assumed shape is shown in Figure 2.

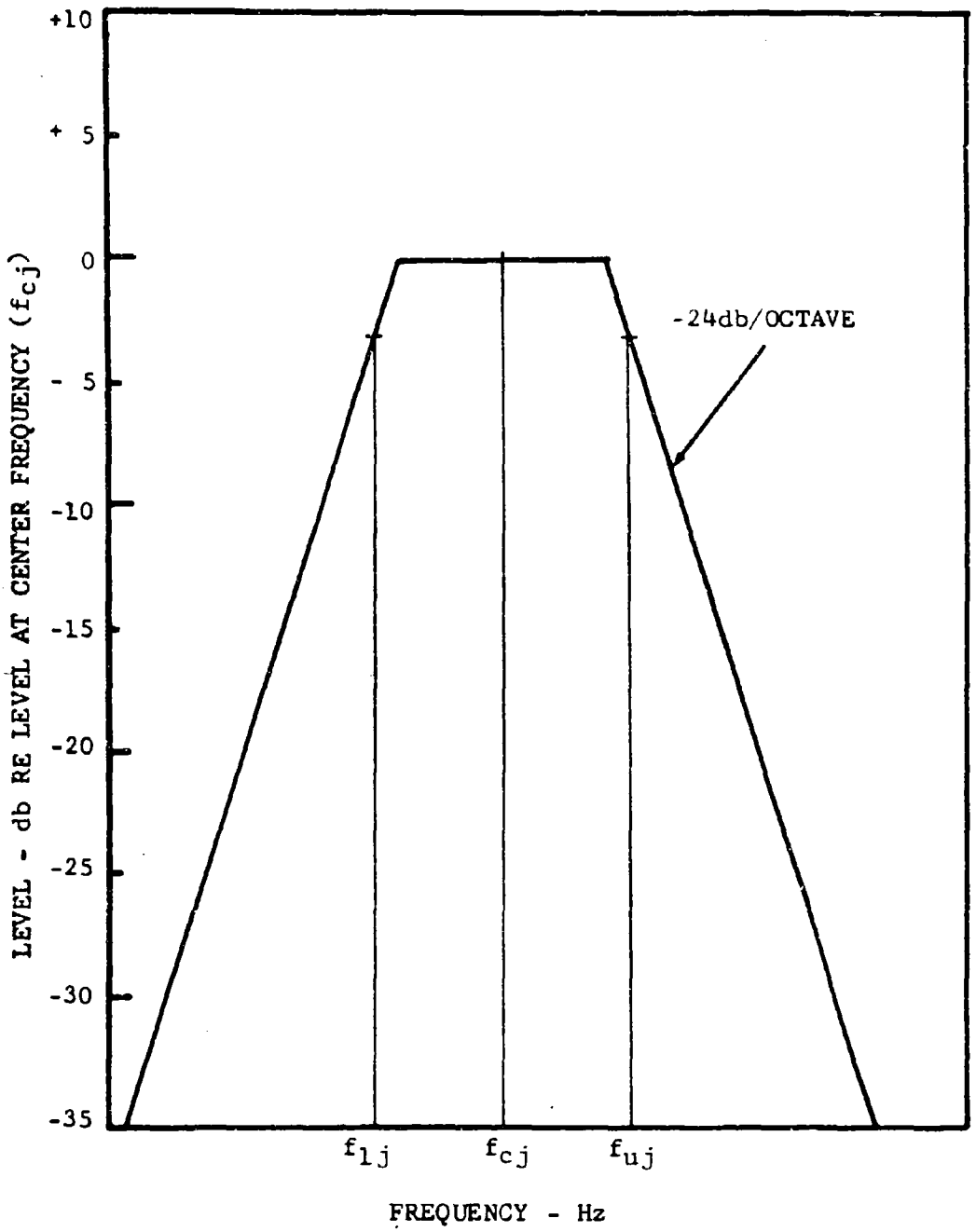

Figure 2. Assumed Filter Shape for Octave-Band-Level Calculation.

The upper and lower cutoff frequencies, f_{uj} and f_{lj}, are taken to be the 3-db-down points; f_{cj} is the center frequency of the jth octave band, and the filter skirts are assumed to drop off at -24 db per octave. The harmonics falling in the flat portion of the filter are unaltered. Those falling outside this flat portion are attenuated an amount determined by their frequency in relation to the center frequency of the band and the filter shape.

The assumed filter shapes for the eight preferred octave bands are shown in Figure 3. The number of sound harmonics necessary to accurately calculate the level of an octave band centered at f_c is equal to the sound harmonic number whose frequency is equal to $2\sqrt{2}\,(f_c)$. At this frequency, the relative level is -27 db compared to the flat portion of the filter, and the contribution of harmonics higher than this frequency is negligibly small.

2. Broadband Noise

It was found early in the development of the noise analysis that, although rotational noise was rigorously treated, it was necessary to include broadband noise in order to correlate measured and calculated main-rotor noise. In the calculation of perceived noise level, it was also found that main-rotor broadband noise results in the maximum noy values attributed to the main rotor, not only for noise at a ground range of 200 feet but also at a range of 4000 feet. Because of the importance of this to the results of the study, the validity of existing broadband-noise prediction methods was reviewed, and new formulas for center frequency, spectral distribution, and directivity were derived and included in the prediction method. The derivations were performed by Lowson.[3] The principal equations for broadband-noise calculation are discussed below.

a. Peak Sound-Pressure Level

The calculation of the peak sound-pressure level of broadband noise is based on an empirical equation given by Schlegel et al.[4] For a range of 500 feet and an angle of 20 degrees below the rotor axis, this equation is

$$db_{500} = 20 \log_{10} V_t + 20 \log_{10} T - 10 \log S_b - 43 \qquad (14)$$

where V_t is the tip speed, T is the thrust, and S_b is the blade area. Levels at other distances are calculated assuming spherical spreading of sound.

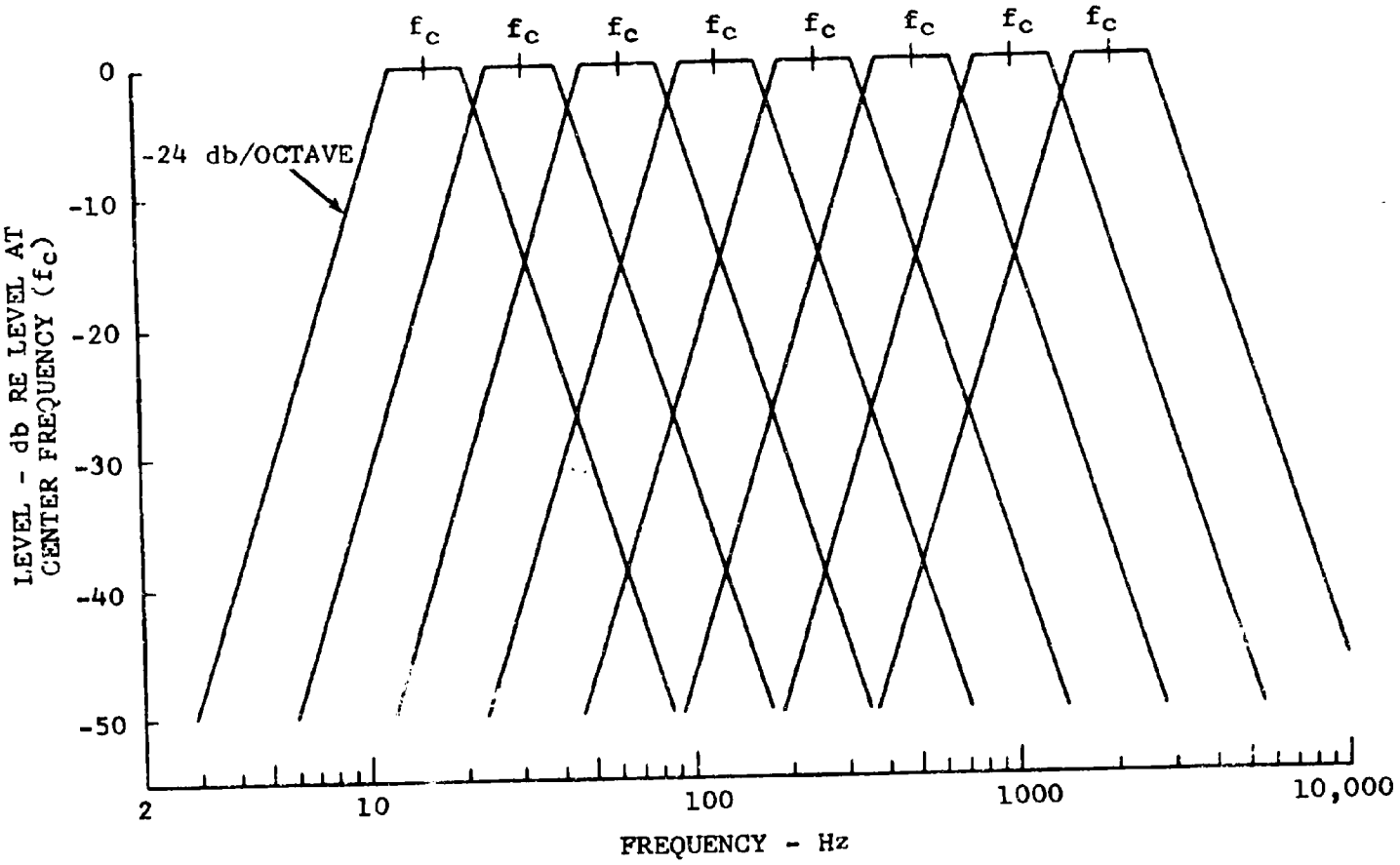

Figure 3. Assumed Filter Shapes for the Preferred Octave Bands.

b. Characteristic Center Frequency

The center frequency, which is the frequency at which the peak sound-pressure level occurs, is given by

$$f_o = V_t/KR \tag{15}$$

where R is the rotor radius, V_t is the tip speed, and K = 0.035.

c. Spectral Distribution

The peak sound-pressure level is multiplied by a spectrum shape factor, S_m, to calculate octave-band levels. The spectrum shape factor is

$$S_m = \frac{\ln\left\{\dfrac{1 + (1+M_t)^2 f_2^2}{1 + (1-M_t)^2 f_2^2} \cdot \dfrac{1 + (1-M_t)^2 f_1^2}{1 + (1+M_t)^2 f_1^2}\right\}}{\ln\left(\dfrac{1+M_t}{1-M_t}\right)^2} \tag{16}$$

where f_1 and f_2 are the octave-band frequency limits divided by the center frequency, f_o, and M_t is the rotational tip Mach number. Equation 16 shows that the spectrum broadens as the Mach number is increased.

d. Directivity

Broadband noise is maximum on the axis perpendicular to the rotor plane and minimum in the plane of rotation. If a dipole distribution is assumed, a null or zero noise is predicted in the plane of rotation. This null can be removed, and the directivity can be accounted for by adding an increment in level, d, in decibels, calculated by

$$d = 10 \log_{10}\left[\frac{\cos^2\theta + 0.1}{\cos^2 70° + 0.1}\right] \tag{17}$$

where θ is the angular position of the observer from the rotor axis. This increment is normalized to the 20-degree angular position to allow direct use of Equation 14 with the directivity term simply added.

D. ENGINE AND DRIVE-SYSTEM NOISE

1. Introduction

Experimental data were used to determine engine and drive-system sources which would require noise-reduction treatments.

Ground tiedown tests were conducted and narrow-band frequency analyses were made in order to find sources that would produce levels high enough to add significantly to the perceived noise level.

2. Noise Sources

Noise spectra of the Allison Model T63-A-5A engine installed in a Bell Model 206A helicopter are shown in Figures 4 and 5 for azimuth positions ψ = 0 and 150 degrees, respectively. The installation is nearly identical to that of the OH-58A except that inertial dust separators are not installed in the 206A inlet. Drive shafts forward of the engine and aft of the fan were removed for the test.

The major noise sources are generally broadband in character, but there are also discrete-frequency tones. At low frequencies, there is in evidence a tone at a frequency of about 100 Hertz which is the fundamental of the engine output rpm. Its source is not explicitly known, but it is either the engine-transmission output gear or shaft, the shaft and bearings between the engine and the engine-transmission oil-cooler fan, or the fan. Broadband noise emanating from the engine exhaust peaks at a frequency of about 270 Hertz and at about 1200 Hertz. Levels of these sources are high, with maximum amplitudes occurring aft.

Between the peaks of exhaust noise is another source at 600 Hertz. This noise is broadband in character to the front and sides of the helicopter, but it is a discrete tone aft of the helicopter. The probable origin is either the engine exhaust or the exiting flow of the oil-cooler fan. At high frequencies, the principal tones in evidence are at 3400 Hertz and between 8000 and 16,000 Hertz. The 3400-Hertz tone is associated with the oil-cooler fan's vane passage, and the latter peaks are associated with engine-compressor blade-passage fundamental tones and harmonics.

Other drive-system noise sources which have been identified are the gear contacts of the main-transmission planetary gears, the main-transmission input-drive pinion, and the engine-transmission power-output-shaft gear. At a distance of 100 feet, these sources are attenuated by the cowling and masked. If engine-exhaust noise is substantially reduced, however, these sources may become important at short distances. Therefore, provisions for evaluation of their contribution and possible cowling treatment are desired in the test aircraft.

Other aspects of engine noise which have been investigated are the effect of rpm and engine power. At flight-idle power, reducing engine rpm to 50 percent reduces engine noise

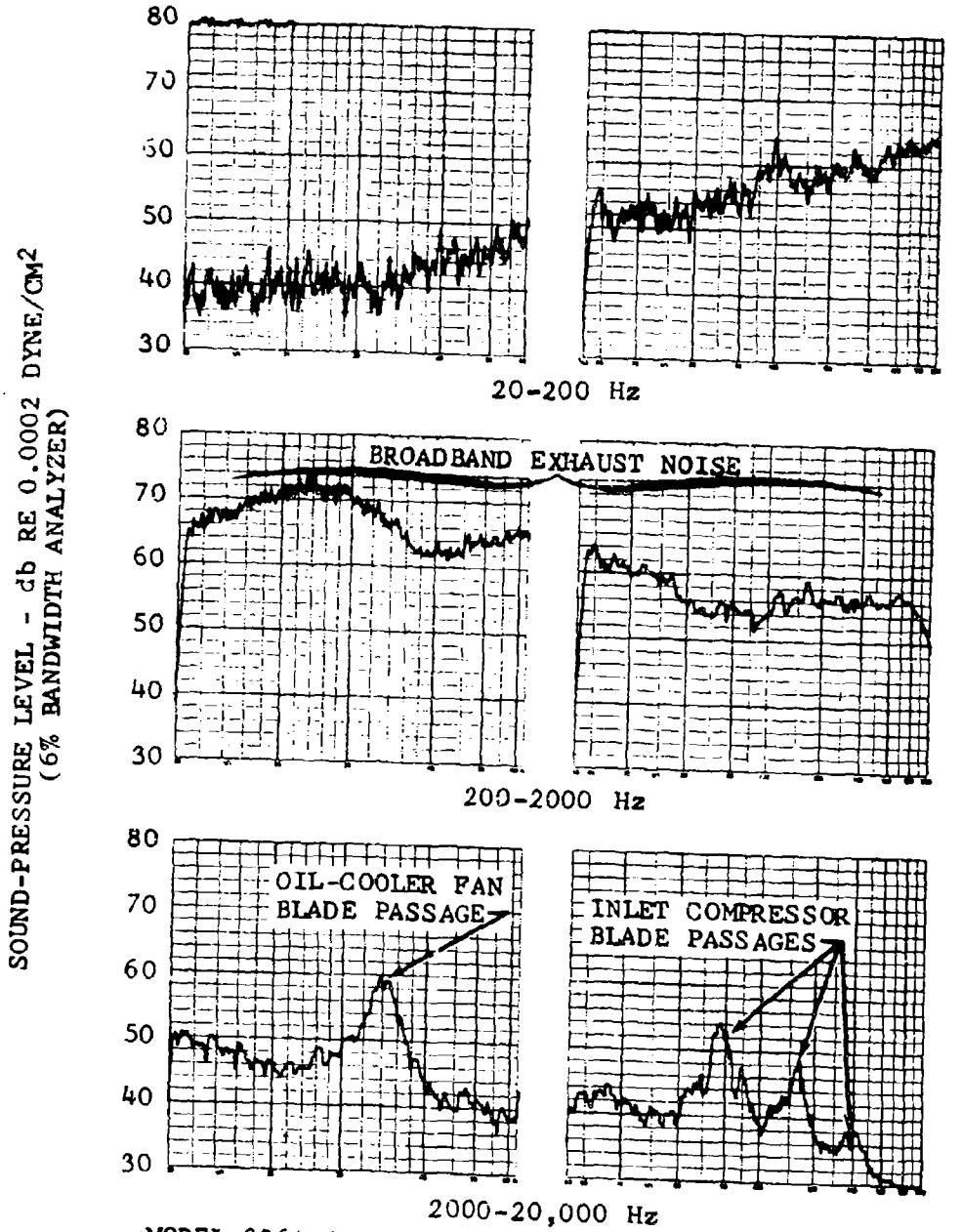

Figure 4. Allison T63-A-5A Engine Noise Spectrum at $\psi = 0°$.

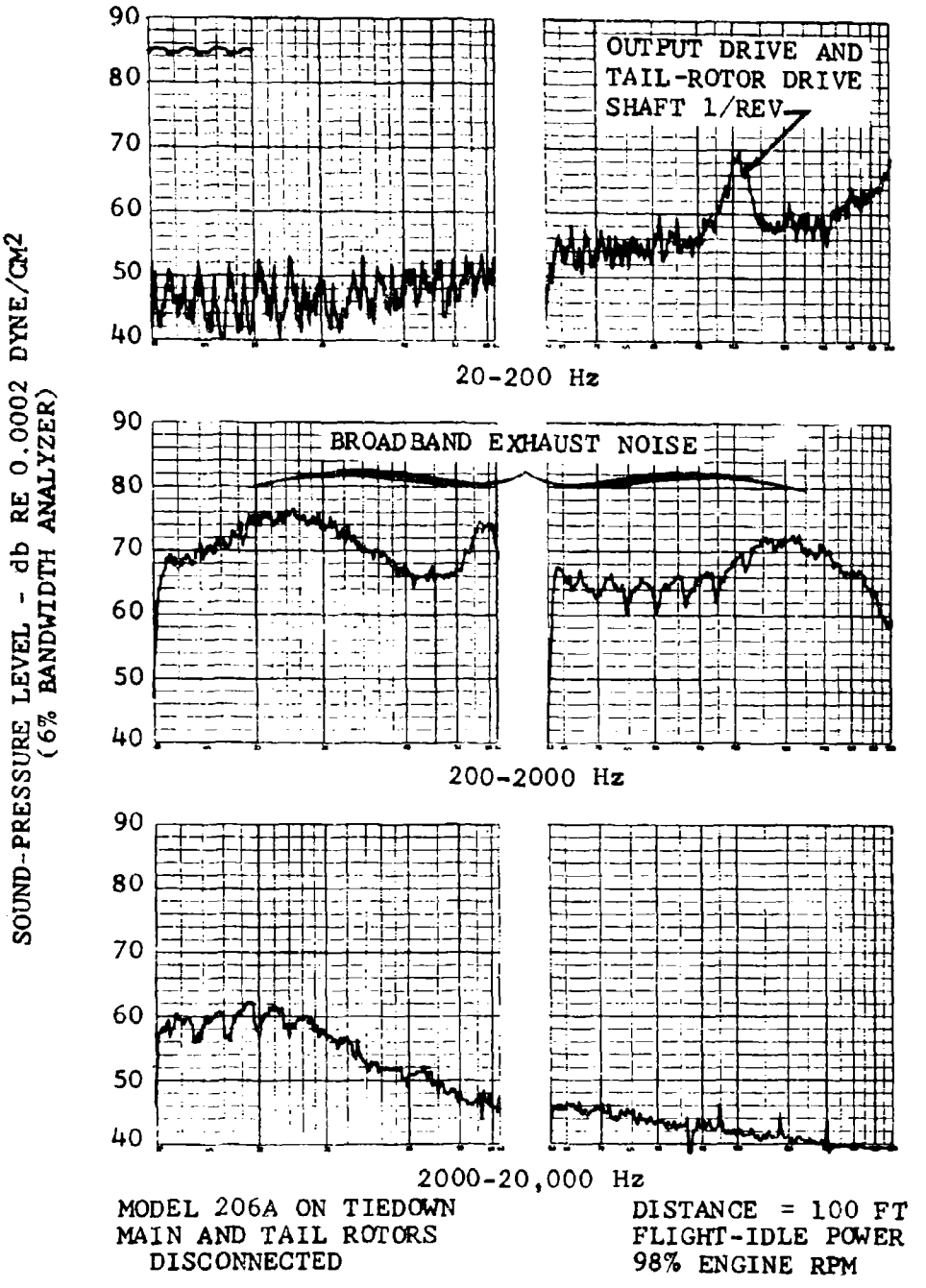

Figure 5. Allison T63-A-5A Engine Noise Spectrum at $\psi = 150°$.

by 7 to 8 PNdb. No significant increase in engine noise is evident for variations of engine power. In addition, the basic frequency distributions shown in Figures 4 and 5 do not substantially change.

3. Combined Noise

In the calculation of the combined noise of the helicopter, the prediction method uses octave-band sound-pressure levels of engine and drive-system noise as measured on the ground at a distance of 100 feet from the helicopter. The engine is at 98 percent of normal output rpm and at flight-idle power setting. The levels are corrected for sound-transmission losses to the retarded distance of the helicopter. The measured noise levels are shown in Table II for fifteen bearings around the helicopter. The azimuth distribution of engine noise is presented in Figure 6.

E. SOUND-TRANSMISSION LOSSES

Five effects attenuate or modify the sound that actually reaches a ground listener:

- Spherical spreading
- Atmospheric absorption
- Refraction due to wind and temperature gradients
- Ground-cover attenuation
- Turbulent scattering

The prediction method includes calculations of four of these effects. Of these, spherical spreading and atmospheric absorption are the largest. Atmospheric absorption has the greatest variation with frequency and the largest effect on high-frequency noise at long range. Ground-cover attenuation is significant, but only at low elevation angles of the source relative to the observer.

1. Spherical Spreading

The helicopter is considered to be a point source, and its total sound power, radiated through an expanding spherical wave front, is taken to be constant over the surface of the sphere. This is considered to be valid in the far field, at sufficiently large distances from the helicopter in the air and out of ground effect. For an ideal medium, the change in sound-pressure level, ΔSPL, is

$$\Delta SPL = -20 \log_{10} \frac{R_2}{R_1} \qquad (18)$$

TABLE II . MEASURED NOISE LEVELS OF ALLISON T63-A-5A ENGINE

Azimuth (deg)	Perceived Noise Level (PNdb)	Sound-Pressure Level (db re 0.0002 dyne/cm^2)								
		Octave Band (Hz)								
		Over-all	20-75	75-150	150-300	300-600	600-1200	1200-2400	2400-4800	4300-10,000
0	87	81	62	68	78	75	69	65	61	56
30	91	84	64	71	78	81	76	70	62	54
60	89	82	65	72	75	78	77	68	64	59
90	88	81	65	72	72	75	76	69	61	55
105	91	83	67	73	73	78	79	73	63	56
120	91	84	65	70	75	81	80	72	61	53
135	92	85	64	71	77	81	79	74	64	54
150	95	87	64	71	82	82	80	77	68	56
165	96	89	65	72	83	82	85	80	66	56
180	95	89	66	71	82	82	85	77	65	55
210	89	84	65	70	80	78	77	70	60	56
240	87	81	66	73	74	75	74	67	60	53
270	89	82	65	74	78	78	74	70	62	53
300	90	83	64	72	78	79	76	70	62	58
330	90	83	61	69	77	80	78	69	59	54

Engine installed on Model 206A, tied down, main and tail rotors disconnected, flight idle, 98% N_{II}, 100-ft distance.

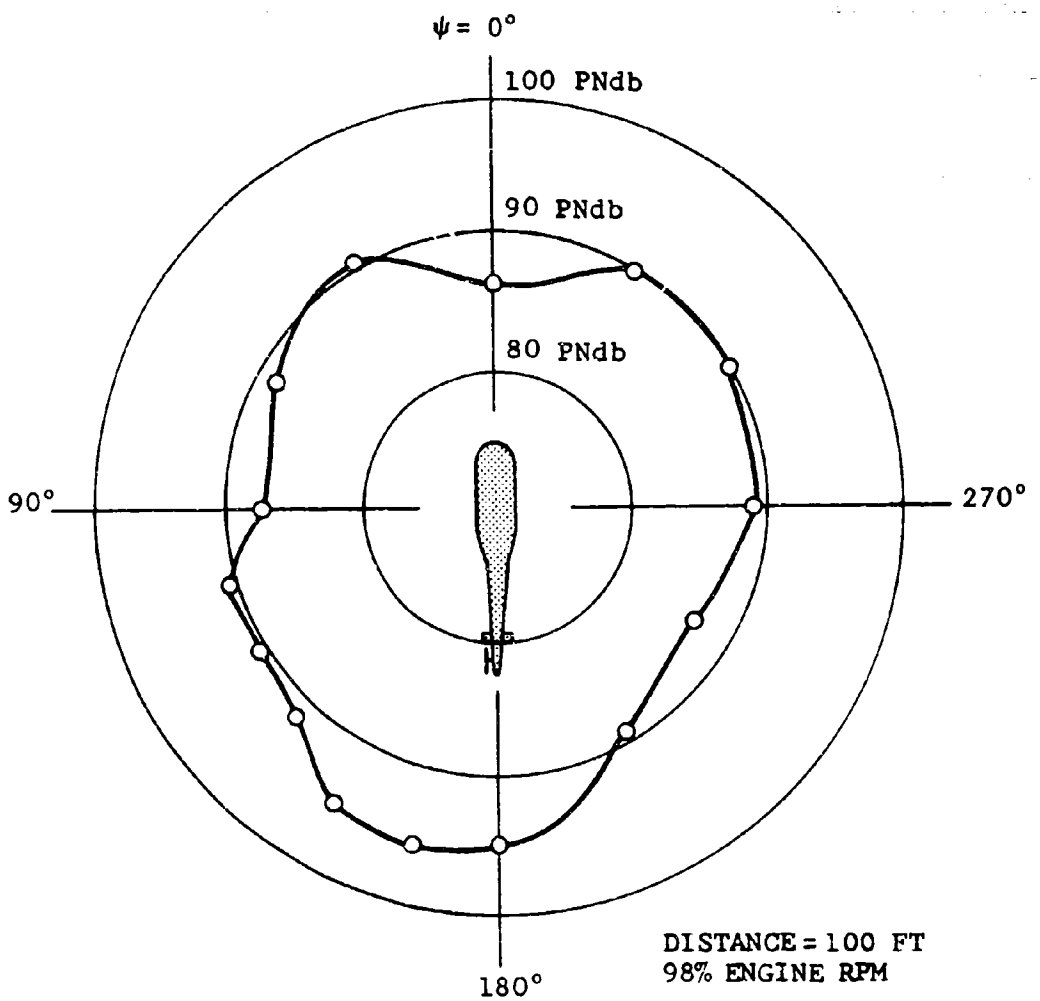

Figure 6. Azimuth Distribution of Allison T63-A-5A Engine Noise.

between any two distances, such as R_1 and R_2. In the prediction method, retarded distances are used. For a doubling of distance from a helicopter in a hover, the equation gives a sound-pressure-level reduction of 6 db.

2. Atmospheric Absorption

Attenuation of sound waves due to absorption by the air is composed of two parts: classical absorption due to viscous and heat-conduction effects and molecular absorption. Of these two, only molecular absorption is important in the audible frequency range, classical absorption being about an order of magnitude less than molecular absorption at 10,000 Hertz.

Sutherland et al.[5] give an expression for molecular absorption based on experimental data and theory discussed by Wiener and Keast[6] and by Kneser.[7] For sea-level-standard conditions of 59°F temperature, 14.7 psi pressure and 50 percent relative humidity, this expression is

$$a'_{mol} = 292.0 \frac{R'}{1000} \left\{ (4.81 \times 10^{-6} f)^2 + \left[\frac{1.43 \times 10^{-9} f^2}{1 + 7.14 \times 10^{-8} f^2} \right] \right\}^{1/2} \quad (19)$$

where a'_{mol} is the molecular absorption in -db, R' is the distance from the observer to the retarded position of the helicopter, and f is the frequency of the sound.

3. Ground-Cover Attenuation

To date, the most definitive data gathered under accurately measured atmospheric conditions appear to be those presented by Wiener and Keast and the preliminary data presented by Guest and Adams.[8] The excess attenuation for downwind propagation is presented in Figure 7. These data have been corrected to remove the effects of spherical spreading and molecular absorption.

The data are approximated by the equations

$$a_g = 0, \text{ for } fr < 4 \times 10^5 \text{ Hz-ft} \quad (20)$$

and

$$a_g = 10 \log_{10} \frac{fr}{4 \times 10^5} \text{ for } fr \geq 4 \times 10^5 \text{ Hz-ft} \quad (21)$$

There are differences in the 300- to 600-Hertz band where some measurements show a substantial increase in excess attenuation at low values of fr. They may have some

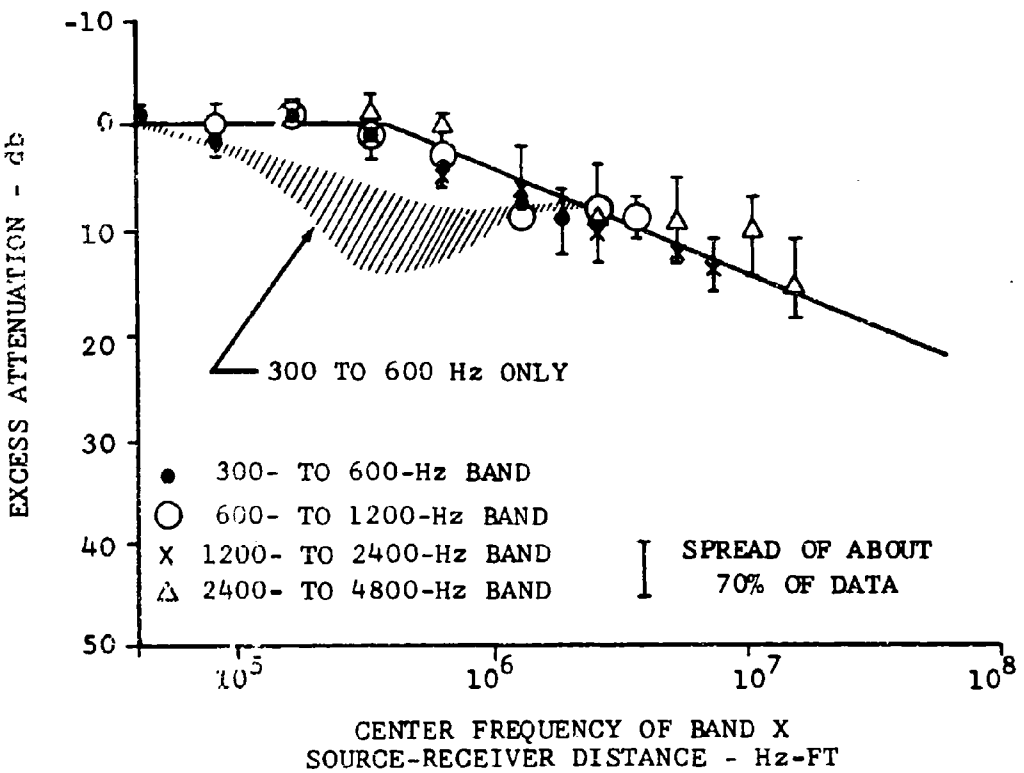

Figure 7. Excess Attenuation Over Open, Level Terrain.

relationship to heights of the source and the microphone above the surface or to variations in ground impedance with frequency.

4. Turbulence Scattering

The propagation of sound waves is influenced by small-scale turbulence in the atmosphere through a process of refraction. The main effect is to fill in gaps in the sound directivity patterns by refracting sound into the dead regions. The approach taken is to consider this effect only at radiation angles slightly above the rotor disc, where a sharp reduction in directivity is theoretically predicted for low-order sound harmonics.

F. PERCEIVED NOISE LEVEL

Calculation of the perceived noise level is based on the procedure and tables given by Kryter and Pearsons.[1] Their tables do not extend below 50 Hertz, and since the low main-rotor harmonics occur below this frequency, it is necessary to extrapolate the noy values for the two octave-bands centered at 16 and 31.5 Hertz. These extrapolations are shown in Figure 8, and the noy values derived from these curves are given in Table III.

The perceived noise level is calculated by converting the sound-pressure level in each octave band to its corresponding noy value (N_k). The quantity N_T is then defined by the relation

$$N_T = N_{max} + 0.3\left[\left(\sum_{k=1}^{10} N_k\right) - N_{max}\right] \qquad (22)$$

where N_{max} is the largest noy value for all the octaves (largest value of N_k).

The ten preferred octave bands having center frequencies from 16 to 8000 Hertz are used. The perceived noise level (PNL) may be obtained from

$$PNL = 40 + 33.3 \log_{10} N_T \text{ , for } N_T \geq 1.0 \qquad (23)$$

and

$$PNL = 16.1\ N_T + 23.2 \text{ , for } N_T < 1.0 \qquad (24)$$

Equation 24 is obtained from Figure 9, which shows the extension of perceived noise level for values of N_T less than 1.0.

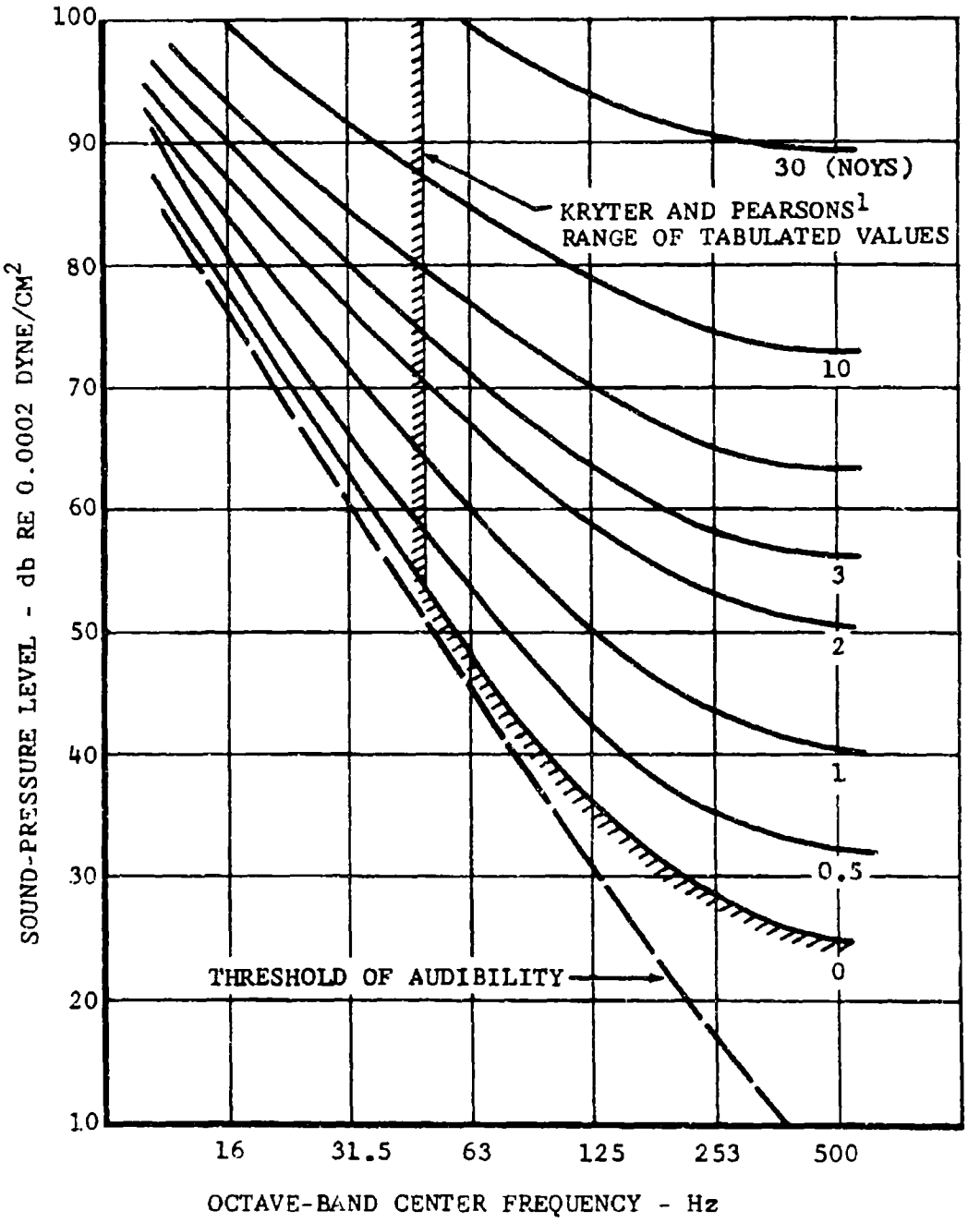

Figure 8. Extrapolation of Noy Curves Below 50 Hertz.

TABLE III. EXTRAPOLATED NOY VALUES FOR OCTAVE BANDS CENTERED AT 16 AND 31.5 HERTZ

Sound-Pressure Level (db)*	Octave (Hz)		Sound-Pressure Level (db)*	Octave (Hz)	
	16	31.5		16	31.5
59	-	-	90	3.2	8.3
60	-	-	91	3.6	9.0
61	-	-	92	4.1	10.0
62	-	0.1	93	4.7	11.0
63	-	0.2	94	5.3	12.0
64	-	0.3	95	6.0	13.0
65	-	0.3	96	6.6	14.0
66	-	0.4	97	7.4	15.0
67	-	0.5	98	8.3	16.0
68	-	0.6	99	9.2	18.0
69	-	0.7	100	10.0	19.0
70	-	0.8	101	11.0	21.0
71	-	0.9	102	12.0	22.0
72	-	1.1	103	13.0	24.0
73	-	1.2	104	14.0	26.0
74	-	1.4	105	15.0	28.0
75	-	1.6	106	16.5	30.0
76	-	1.8	107	18.0	32.0
77	-	2.1	108	19.0	35.0
78	0.1	2.3	109	20.0	37.0
79	0.2	2.6	110	22.0	40.0
80	0.4	2.9	111	24.0	42.0
81	0.6	3.2	112	26.0	45.0
82	0.8	3.6	113	28.0	48.0
83	1.0	4.0	114	30.0	52.0
84	1.2	4.5	115	32.0	56.0
85	1.4	5.0	116	34.0	60.0
86	1.7	5.6	117	36.0	64.0
87	2.0	6.2	118	38.0	68.0
88	2.4	6.8	119	40.0	72.0
89	2.8	7.6	120	43.0	77.0

*re 0.0002 dyne/cm^2

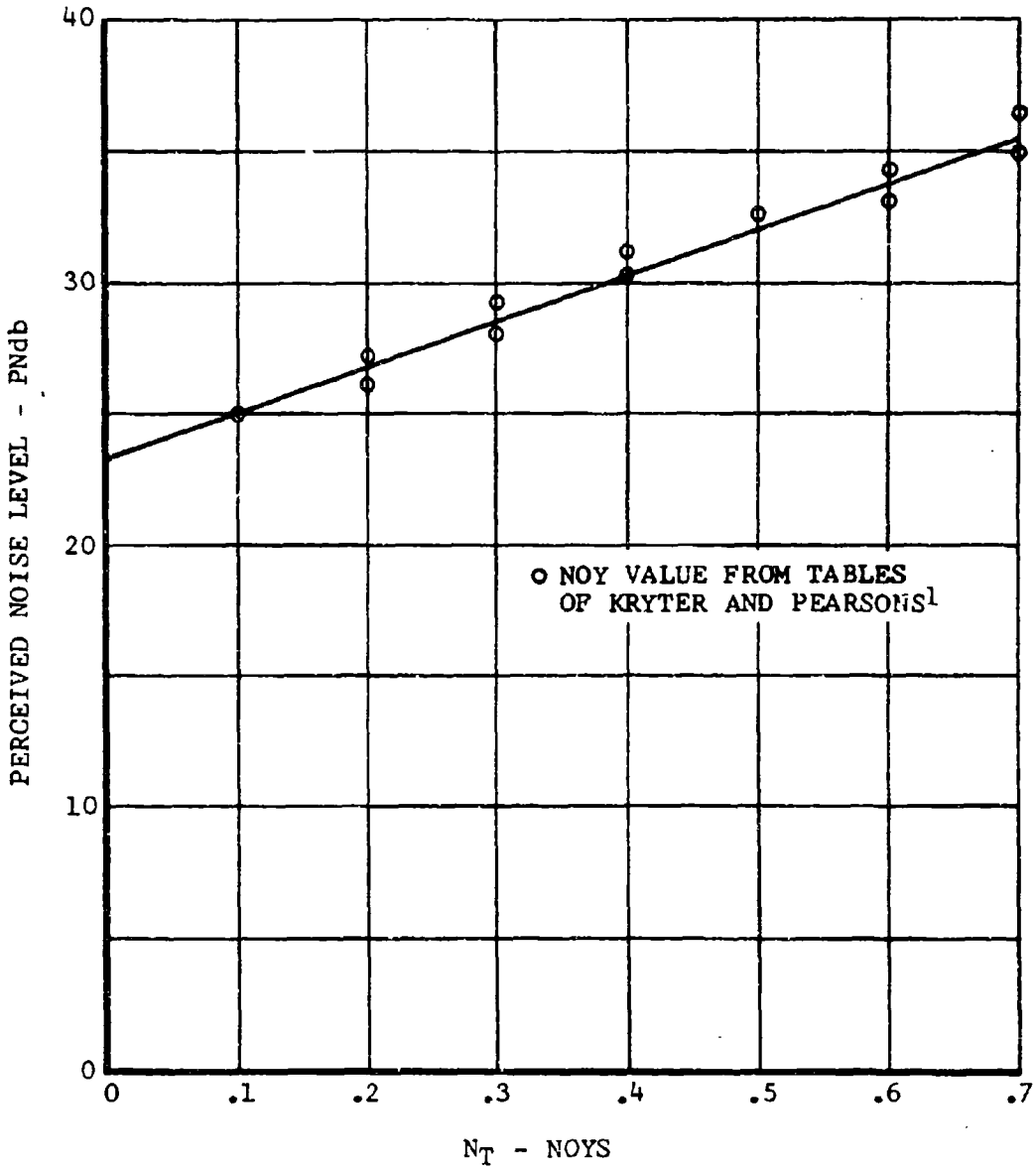

Figure 9. Extension of Perceived Noise Level for N_T Less Than 1.0.

Figure 9 also shows that when N_T is zero, the perceived noise level is 23.2 PNdb. By definition, a noy value of zero is equal to zero PNdb. Thus, the perceived noise level calculation is invalid below 23.2 PNdb.

Since the lowest noy value in Kryter and Pearson's tables is 0.1, the minimum value obtainable for this study is 25.0 PNdb. This is adequate in the sense that the ambient noise in most remote areas will exceed these low levels, but this method negates the possibility of calculating the desired perceived noise level of 20 PNdb.

G. CORRELATION

The noise analysis predicts the noise of the OH-58A in hover or in steady-state forward flight at an altitude of 200 feet above ground level to within an accuracy of ±4 PNdb measured at a ground range of 200 feet from the helicopter. Within the limitations of the available test data and of current techniques to test and to isolate noise of each source in a complex sound field, this analysis should satisfactorily estimate OH-58A noise at a ground range of 4000 feet, and should give a reasonably accurate comparison of OH-58A noise with that of the quiet helicopter.

This section presents comparisons between calculated noise data and two sets of measured data. The first set consists of data measured while the OH-58A hovered and flew over and by the microphone at an altitude of 200 feet. The second set consists of measurements of a Bell Model 206A helicopter on tiedown.

1. Noise Measurements

Hover, flyover, and flyby data were recorded at four headings of the helicopter as shown in Figure 10: 0 degrees (head-on), 90 degrees (left side), 180 degrees (aft), and 270 degrees (right side). Hover recordings were taken for time periods of 10 to 20 seconds while the helicopter was in a steady-state hover, except for control movements required to maintain the helicopter over the spot. The noise produced during steady-state flyovers and flybys was recorded at airspeeds of 45, 102, and 113 knots and a gross weight of 2960 pounds. Table IV shows the OH-58A overall and octave-band sound-pressure levels measured during these tests.

During tiedown tests of the Model 206A, noise measurements were made of the engine, the main rotor and engine, the tail rotor and engine, and the complete helicopter. The objectives of these tests were to isolate the various noise sources and to check the predicted noise trends for each source, particularly with respect to tip-speed reduction. At the same time,

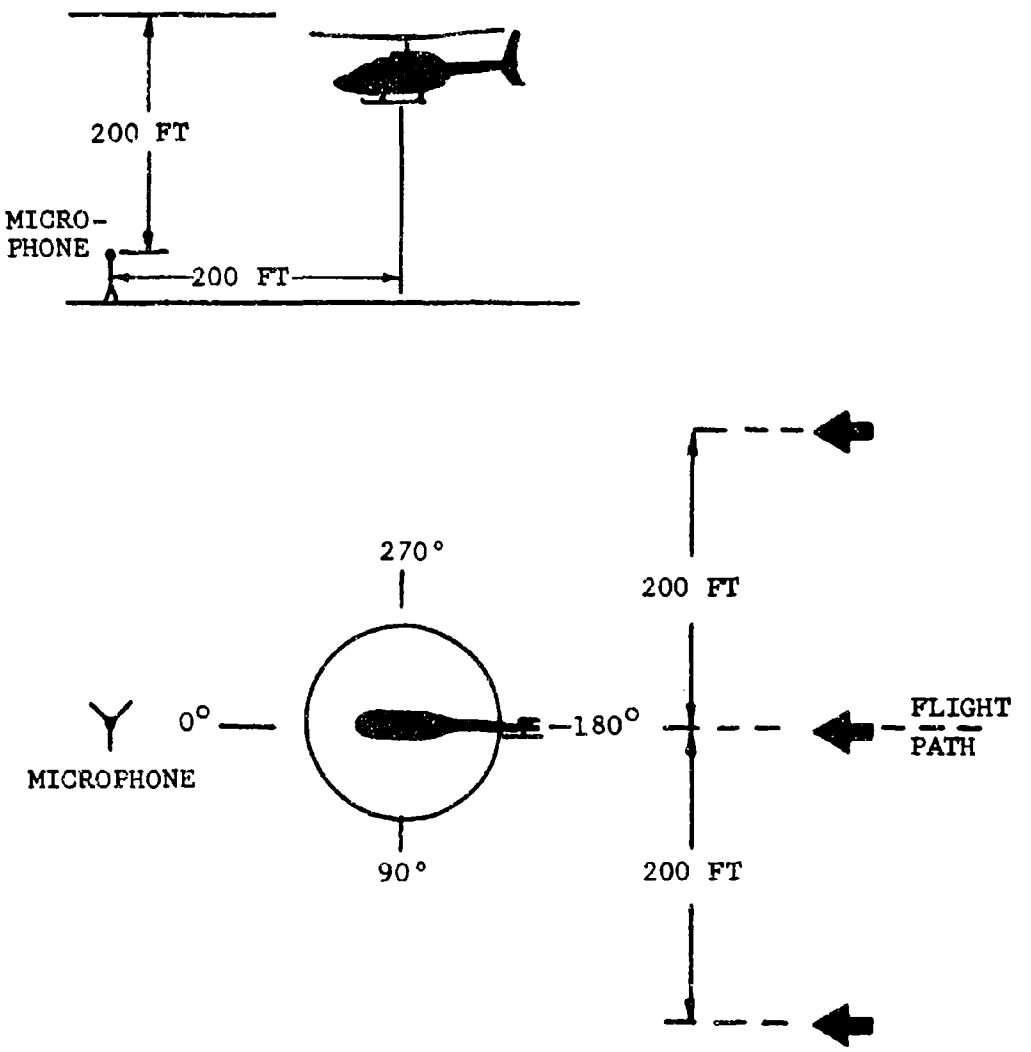

Figure 10. Microphone Location and Azimuth Headings for Hover and Flyover Noise Measurements.

TABLE IV. OH-58A OCTAVE-BAND SOUND-PRESSURE LEVELS

Conditions	Sound-Pressure Level (db re 0.0002 dyne/cm^2)								
		Octave Band (Hz)							
	Over-all	20-75	75-150	150-300	300-600	600-1200	1200-2400	2400-4800	4800-10,000
Hover IGE, 200-Ft Dist									
0° (Head-on)	82	80	76	72	73	73	66	52	55
90° (Left)	84	81	73	73	75	78	74	59	57
180° (Aft)	86	80	79	79	80	79	74	61	57
270° (Right)	86	83	78	77	78	79	73	66	60
Hover at 200-Ft Alt, 200-Ft Dist									
0°	82	78	73	77	72	70	66	61	56
90°	84	79	73	79	76	76	72	64	56
180°	86	80	75	83	79	75	68	60	56
270°	86	80	74	81	79	76	69	60	55
Forward Flight at 200-Ft Alt, 200-Ft Dist									
0° 45 kt	85	82	74	79	76	70	66	61	63
0° 102 kt	90	85	76	81	82	75	68	61	-
0° 113 kt	89	87	78	83	83	77	68	56	-
90° 45 kt	86	85	70	80	75	71	66	55	63
90° 102 kt	88	86	72	82	77	74	69	57	63
90° 113 kt	90	89	74	84	79	77	71	58	63
180° 45 kt	86	83	75	79	75	72	66	63	63
180° 102 kt	89	85	77	83	80	75	68	58	63
180° 113 kt	90	87	77	83	81	77	67	59	-
270° 45 kt	88	87	69	77	76	71	64	54	63
270° 102 kt	89	88	73	81	77	75	67	56	63
270° 113 kt	92	91	73	84	79	77	70	58	63

these tests provided a means for defining the contribution of the engine to the complete noise. Tests were conducted with very low wind conditions (0 to 3 mph) and very low background noise levels. Measurements were made for a variety of conditions, including zero to normal thrust of the main and tail rotors, and at different azimuth positions around the helicopter.

Six-percent narrow-bandwidth analyses of these data were made. Figure 11 shows the frequency spectrum of the main rotor and engine. Rotational-noise harmonics dominate the low end of the spectrum. Harmonics up to the ninth can be identified. The remainder of the spectrum consists of broadband noise components. The component centered at about 270 Hertz is primarily engine-exhaust noise.

Figure 12 shows a similar narrow-bandwidth analysis of the tail-rotor-and-engine noise data. Rotational-noise harmonics up to the seventh can be identified. The other harmonics are masked by engine-exhaust noise.

2. Comparisons Between Measured and Calculated Noise

a. Main Rotor

The measured and calculated levels of main-rotor rotational-noise harmonics are compared in Figure 13. Good correlation is achieved up to the eleventh harmonic. Above the eleventh harmonic, the increase in measured harmonic levels is not predicted. One reason for this is the presence of other noise components in this frequency range, notably main-rotor broadband noise, which adds to the levels of these high harmonics.

The calculated rotational-noise levels of the main rotor are based on the following parameters:

$$k = 2.5$$

$$l_c = 0.7$$

$$\eta = 0.8$$

where k is the loading power-law exponent, l_c is the correlation length, and η is the point loading station.

The theory predicts reasonably well the variation of main-rotor rotational noise with tip speed. This is shown in Figure 14. The measured noise harmonics are summed and compared with those calculated. The predicted rate of noise decrease with tip speed is verified by the measured data. However, theoretical predictions of the absolute levels are

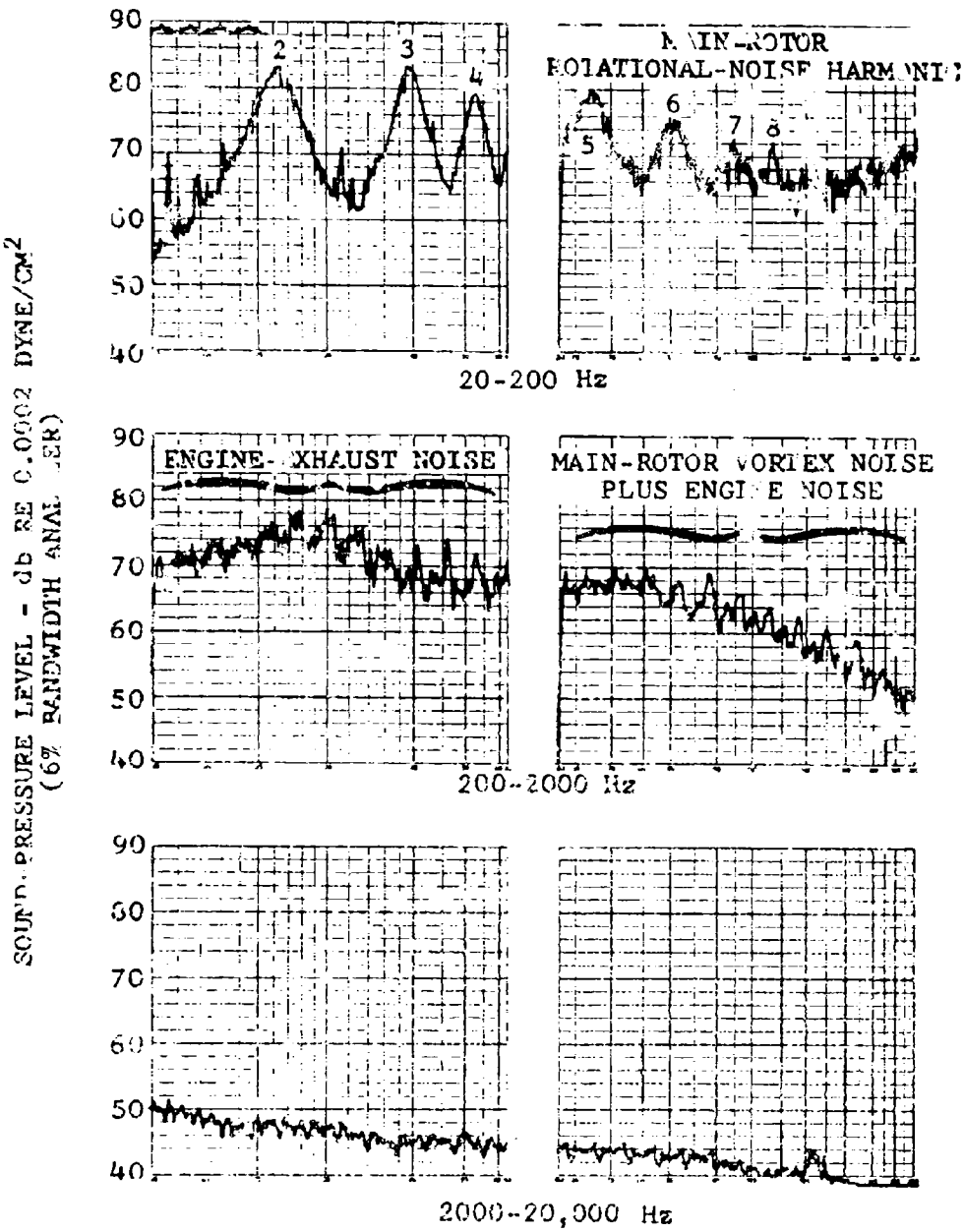

MODEL 206A ON TIEDOWN
TAIL ROTOR DISCONNECTED

DISTANCE = 100 FT
MAIN-ROTOR THRUST = 2540 LB
100% ENGINE RPM

Figure 11. Main-Rotor and Engine Noise Spectra at $\psi = 0^{\circ}$.

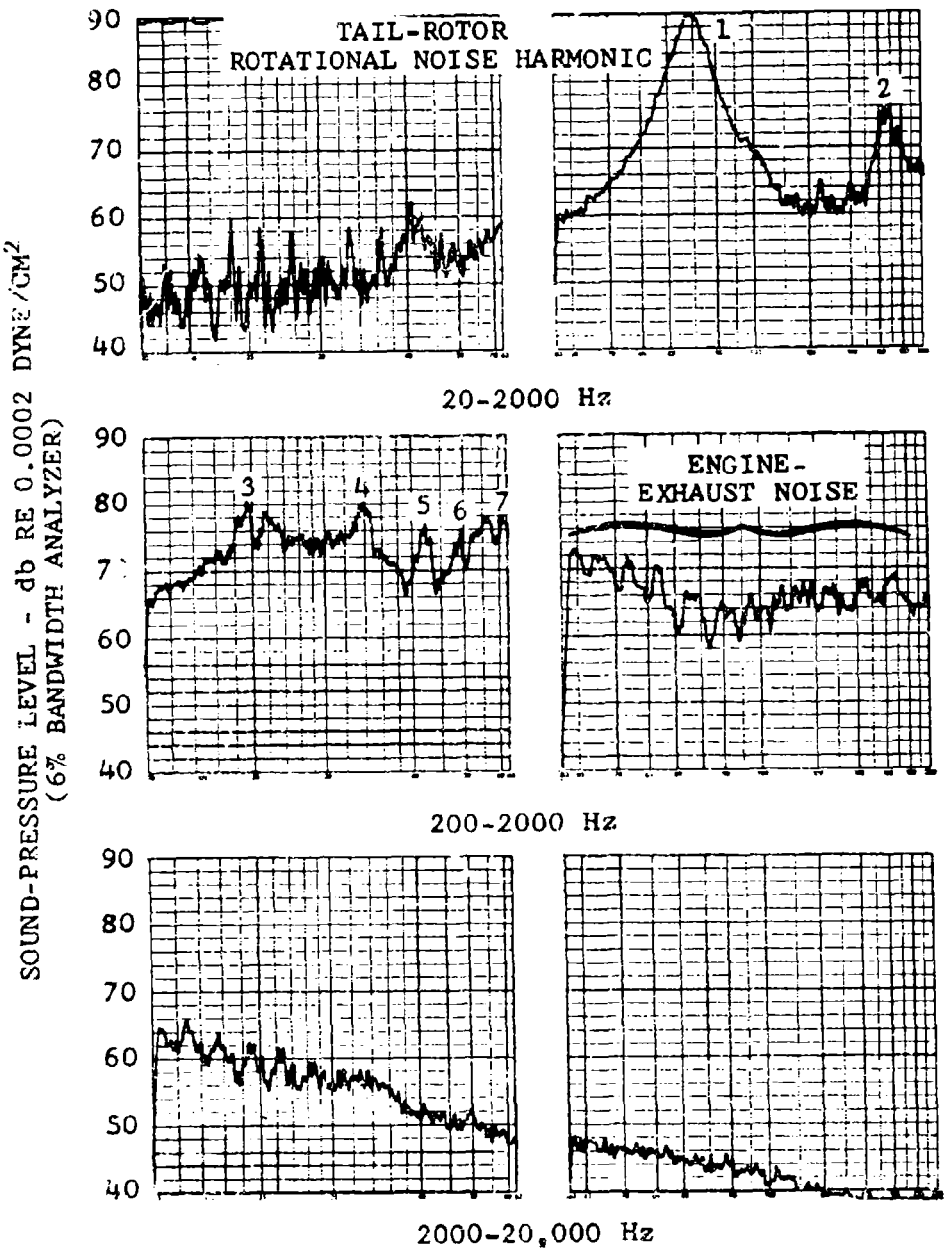

MODEL 206A ON TIEDOWN
MAIN ROTOR DISCONNECTED

DISTANCE = 100 FT
TAIL-ROTOR THRUST = 138 LB
98% ENGINE RPM

Figure 12. Tail-Rotor and Engine Noise Spectra at ψ = 150°.

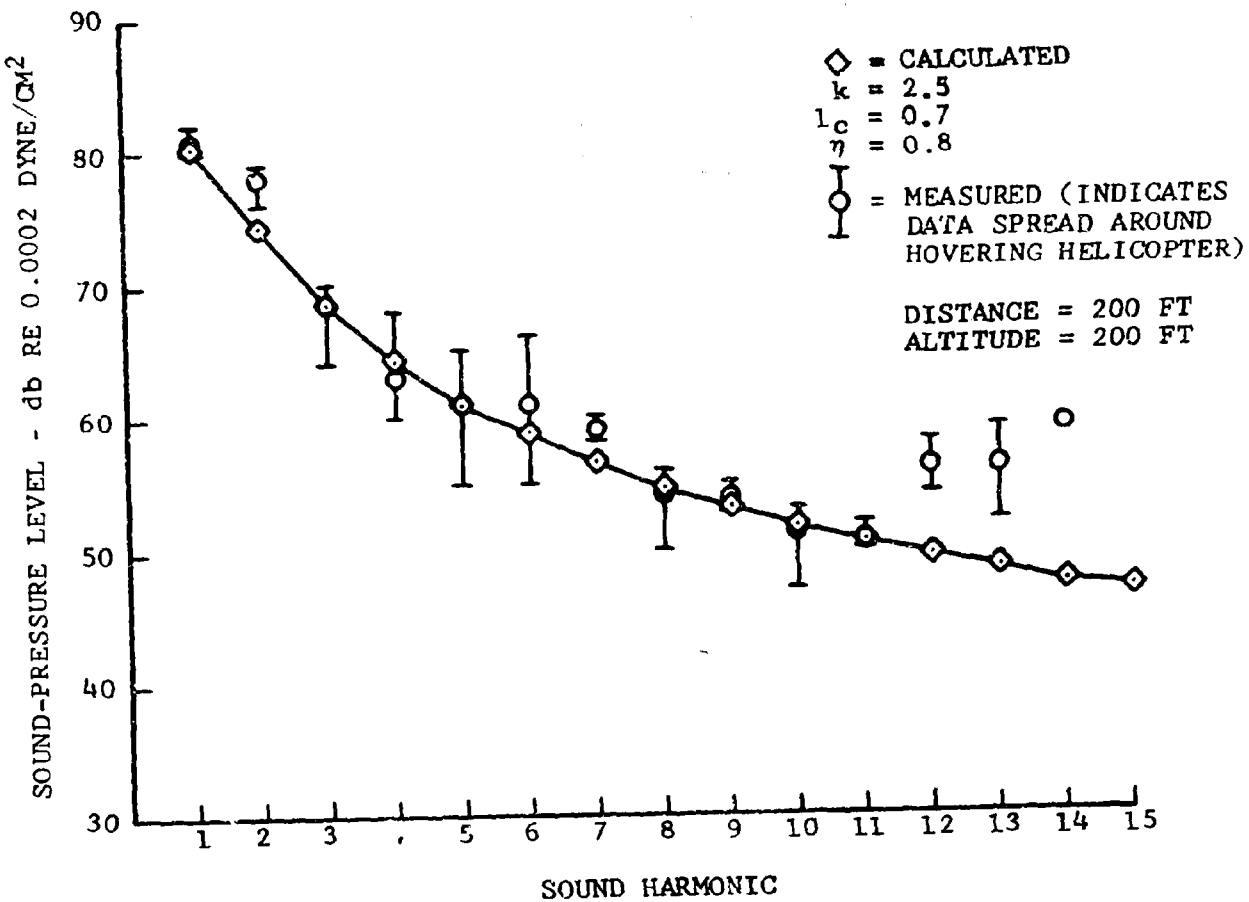

Figure 13. OH-58A Main-Rotor Rotational-Noise Correlation.

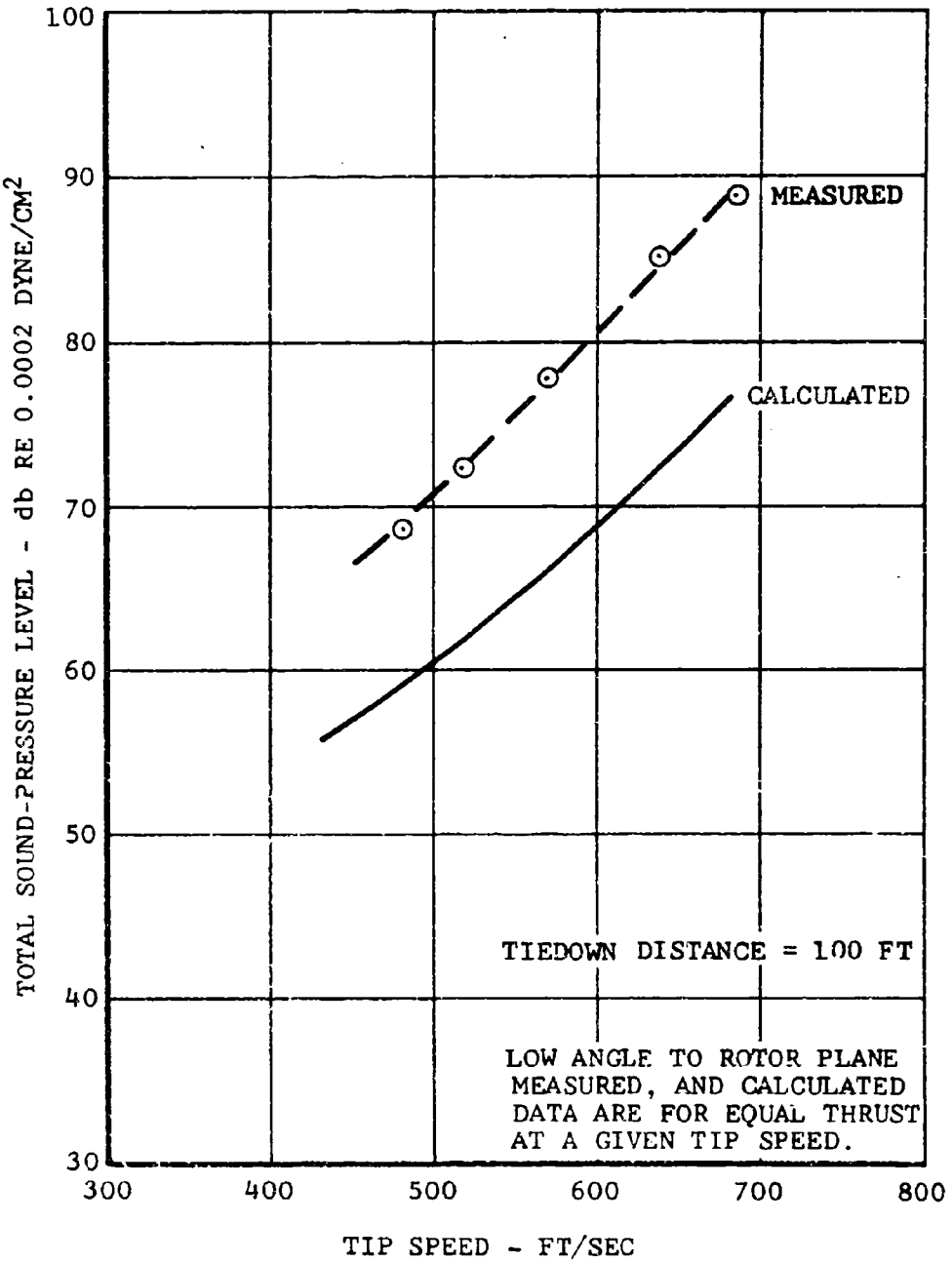

Figure 14. Measured and Predicted Variation of Main-Rotor Rotational Noise With Tip Speed.

approximately 11 db too low. This was found at small angles relative to the rotor plane.

The variation of rotor broadband noise, which is most important for the main rotor, was not determined because of problems in distinguishing it from engine noise. The analysis that could be made indicates that its magnitude directly beneath the rotor (in an overhead hover) is underestimated, but that its order of magnitude at angles of 45 degrees and at 0 degrees (in the plane of the rotor) is about the same as theory predicts. No gross errors were determined in its variation with tip speed, but the data are not conclusive.

b. Tail Rotor

Figure 15 shows a comparison of measured and calculated tail-rotor rotational-noise harmonics for positions forward and aft of the helicopter. The major characteristic of tail-rotor noise is that the measured harmonic levels do not decrease uniformly as predicted. This may be caused by inflow disturbances from the main rotor and by the proximity of the tail boom and fin. One important area where the correlation is seen to break down is in the prediction of the second harmonic, which is higher by an average of 2 db than the first and is 5 to 6 db above the calculated level.

The irregular falloff in harmonic level is more pronounced at the sides of the helicopter, as shown in Figure 16. The calculated levels represent a reasonable compromise.

The calculated rotational-noise levels of the tail rotor are based on the following parameters:

$$k = 2.0$$

$$l_c = 0.7$$

$$\eta = 0.9$$

The value of $\eta = 0.9$ is used for the tail rotor to take into account the effects of untwisted blades. Untwisted blades tend to be loaded more heavily toward the tips than twisted blades; consequently, the point loading station for tail rotors is assumed to be further outboard than for main rotors.

As in the case for a main rotor, the theory predicts reasonably well the variation of tail-rotor rotational noise with tip speed. This is shown in Figure 17. For $\psi = 150°$, the predicted levels are within 3 db of the measured levels for normal hovering thrust. However, at low thrust, theory underestimates tail-rotor noise by approximately 14 db.

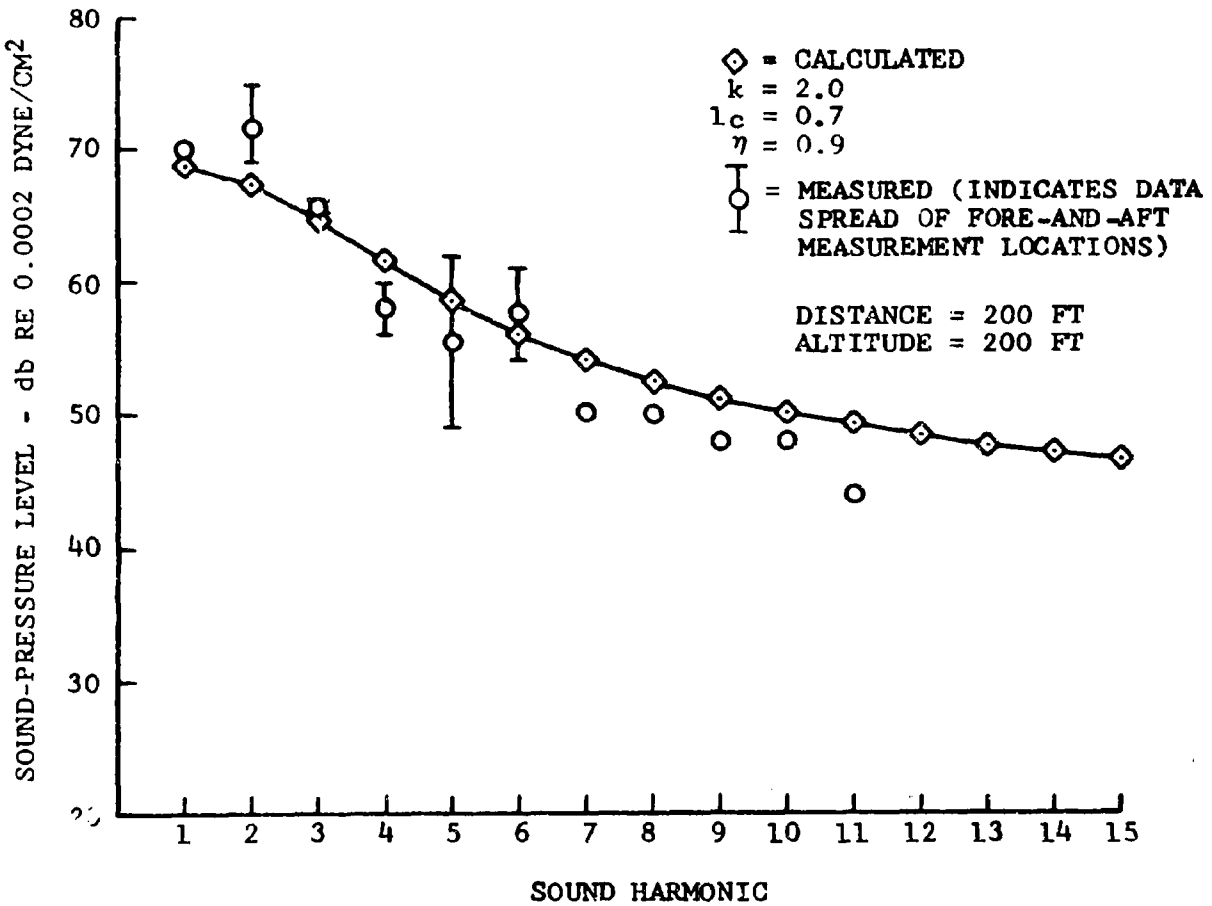

Figure 15. Tail-Rotor Rotational-Noise Correlation in Front and to Rear of Hovering OH-58A Helicopter.

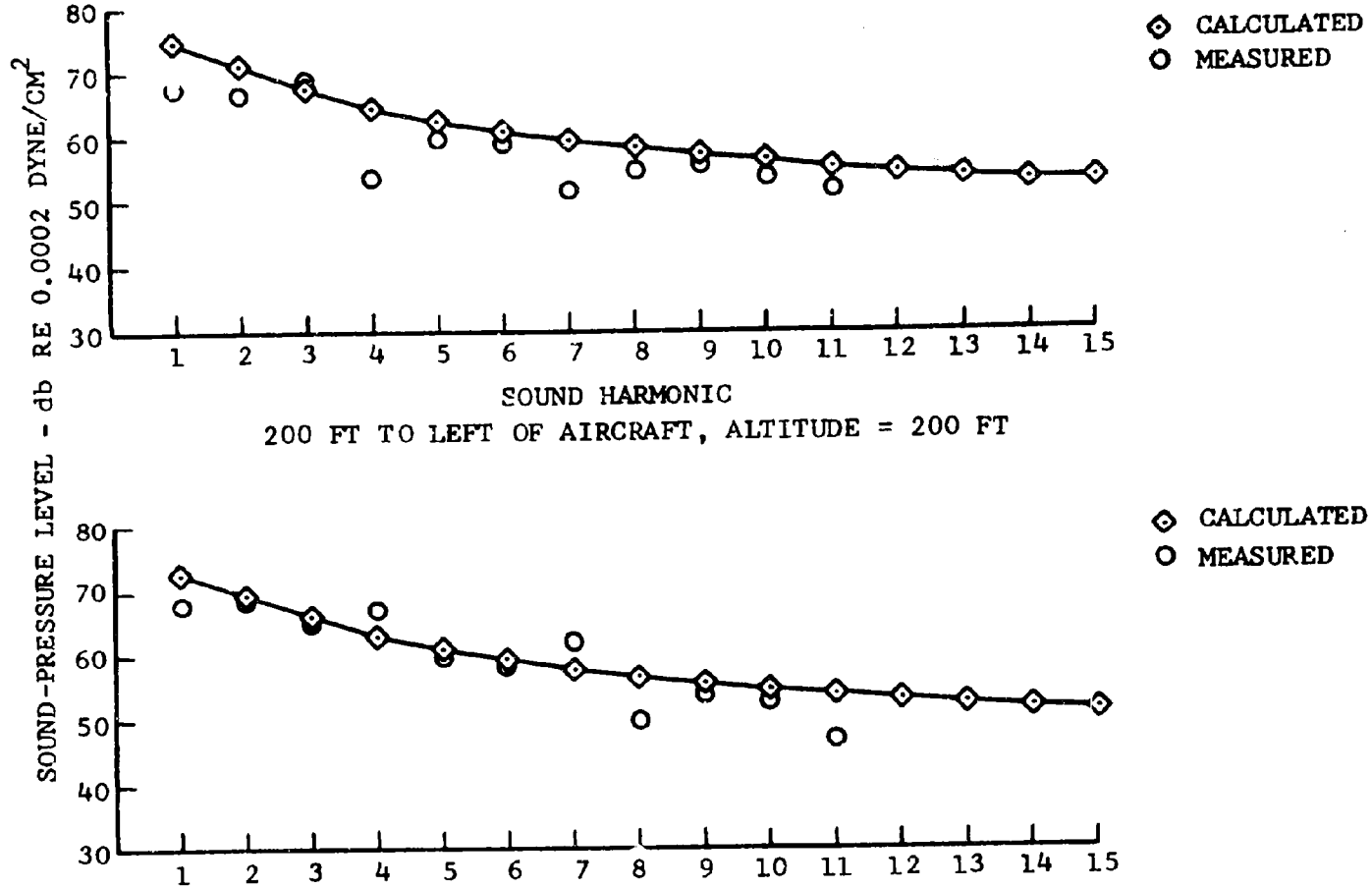

Figure 16. Tail-Rotor Rotational-Noise Correlation to Sides of Hovering OH-58A Helicopter.

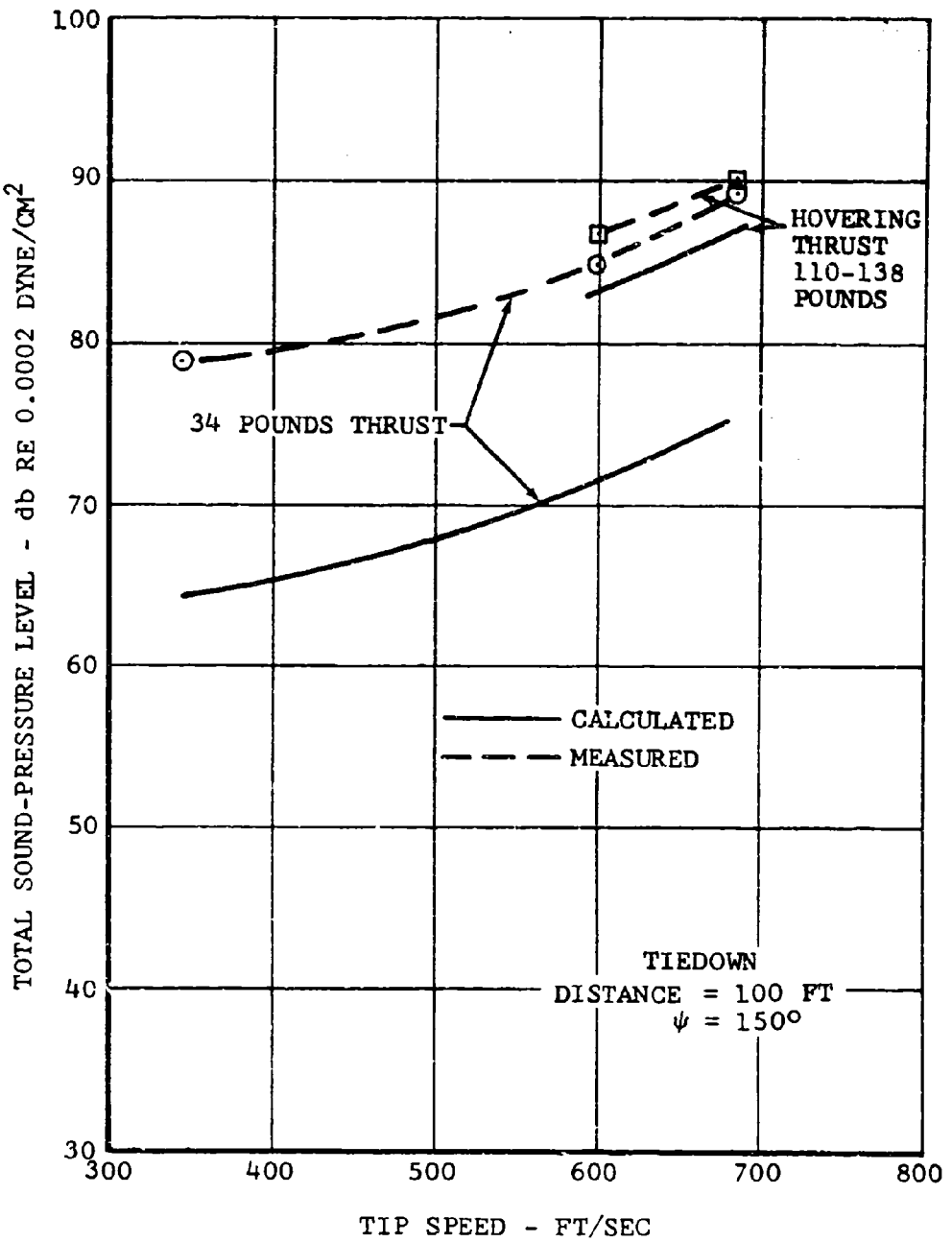

Figure 17. Measured and Predicted Variation of Tail-Rotor Rotational Noise With Tip Speed.

c. Complete Helicopter

Measured octave-band sound-pressure levels of the OH-58A are compared in Figures 18 through 23 with the total calculated levels for the main and tail rotors. Engine noise and empirical corrections are not included. The perceived noise levels calculated from these data are also shown. For hover and ψ = 0 degrees, Figure 18 shows that the calculated levels agree with the measured levels for the fourth through the eighth octaves. Main-rotor noise in the first octave is underestimated by about 5 db. Tail-rotor noise in the second and third octaves is underestimated by 6 to 9 db. However, the measured and calculated perceived noise levels agree within ±1 PNdb, because the perceived noise level at this distance is determined by the noise in the high octaves, where measured and calculated levels correlate well. At ψ = 90 and 270 degrees, Figures 19 and 20, respectively, theory also underestimates the noise of the tail rotor. In addition, it underestimates high-frequency noise at ψ = 90 degrees, but overestimates it at ψ = 270 degrees.

Noise comparisons are given in Figures 21, 22, and 23 for fly-over airspeeds of 45, 102, and 113 knots, respectively. Calculated and measured sound-pressure levels do not compare very well. The noise levels in the octave bands centered at 250, 500, and 1000 Hertz are underestimated by as much as 17 db. Similarly, main-rotor rotational noise in the octave bands centered at 63 and 125 Hertz is underestimated by as much as 9 db. The perceived noise levels reflect this discrepancy to some degree, but they indicate a difference of only about 9 PNdb for the worst case.

3. Empirical Corrections

In establishing correlation of the analytical approach with the measured noise level, it was found that significant adjustments were required. Several factors that are not accounted for in the theory could make these adjustments necessary (Section II.B):

- Inflow disturbances to the tail rotor
- Main-rotor and tail-rotor interference noise at forward speeds
- Rotor-vortex interference from preceding blades
- Increase in engine noise with increase in power

Considerable effort was expended in evaluating this discrepancy and in determining empirical correlation factors.

To obtain analytical correlation with measured data in forward flight at 200 feet, by making corrections to the rotor source

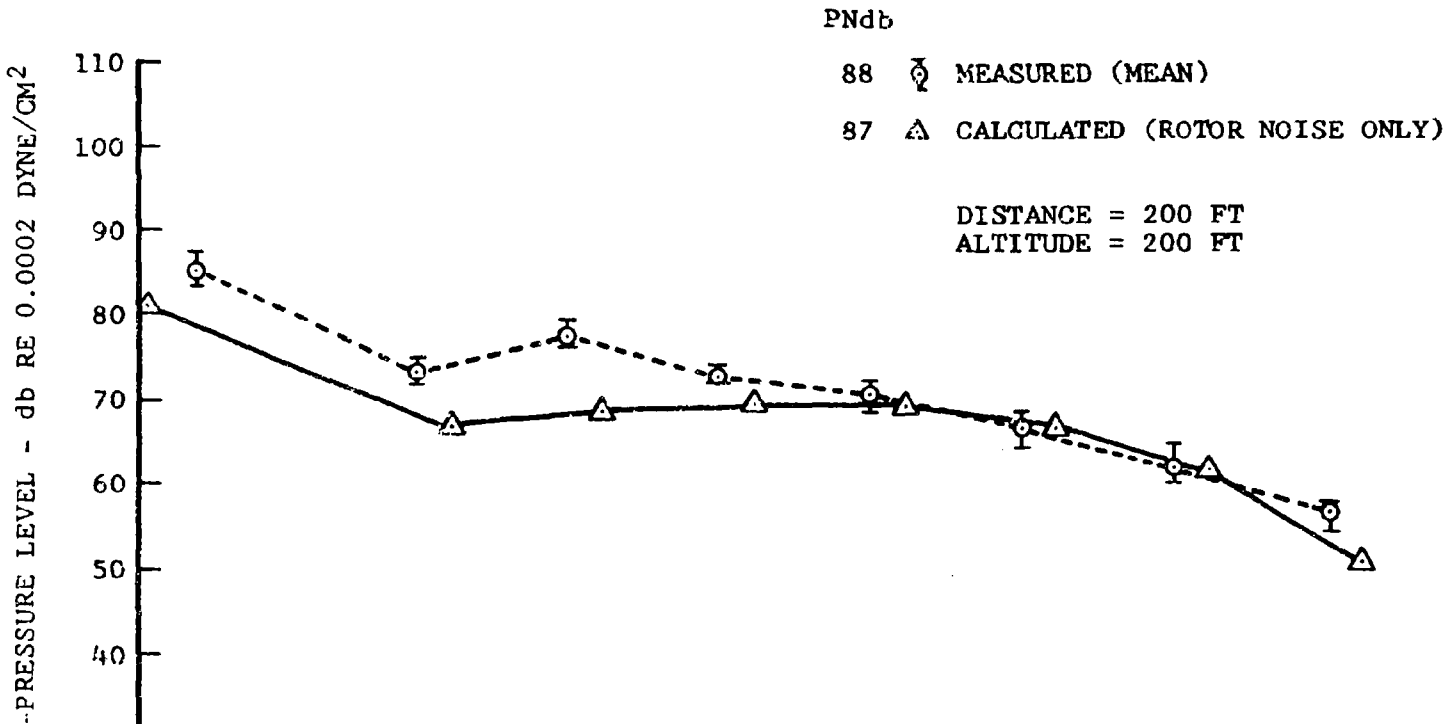

Figure 13. OH-58A Hover Noise Correlation at $\psi = 0^{\circ}$.

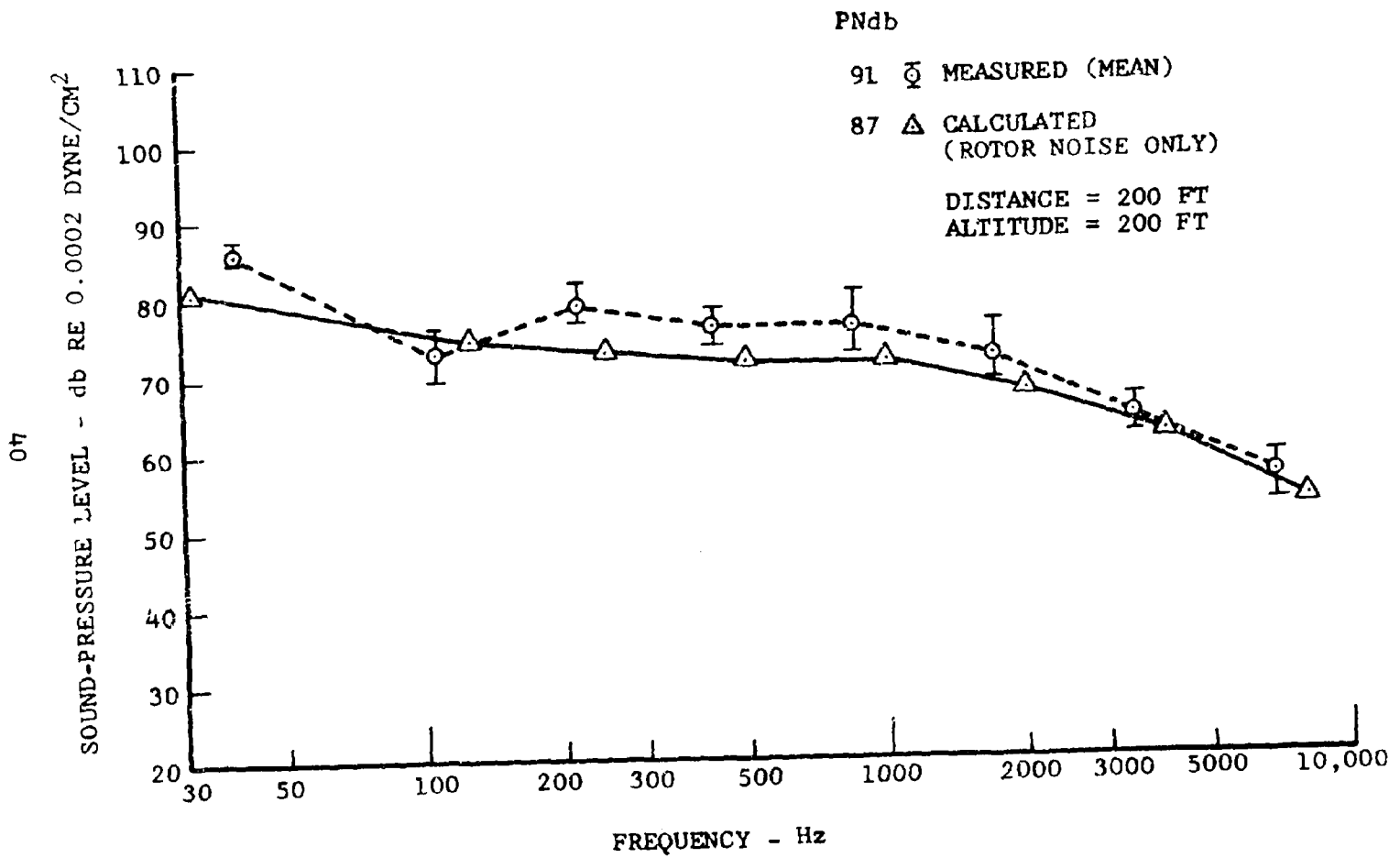

Figure 19. OH-58A Hover Noise Correlation at $\psi = 90^{o}$.

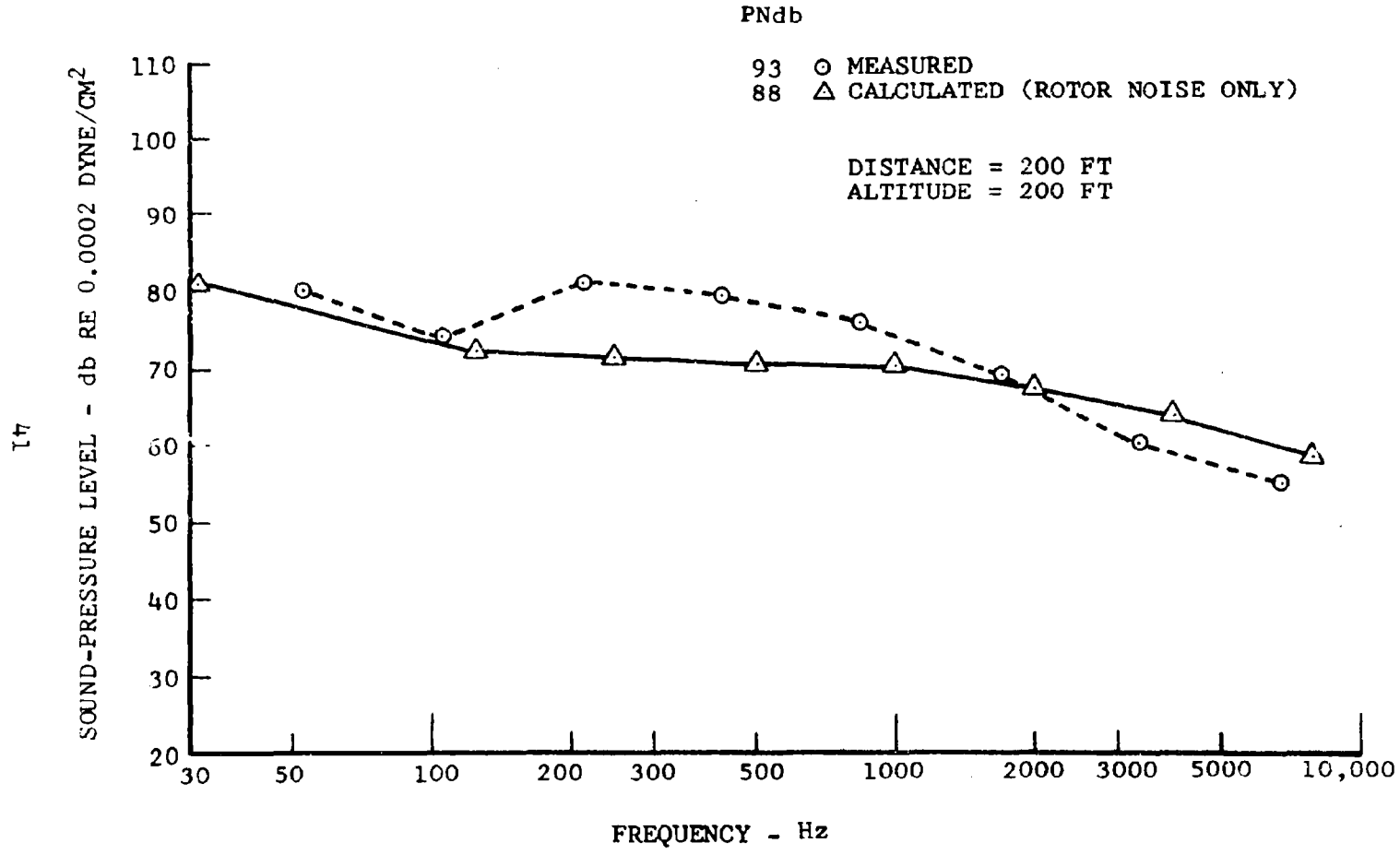

Figure 20. OH-58A Hover Noise Correlation at $\psi = 270^{\circ}$.

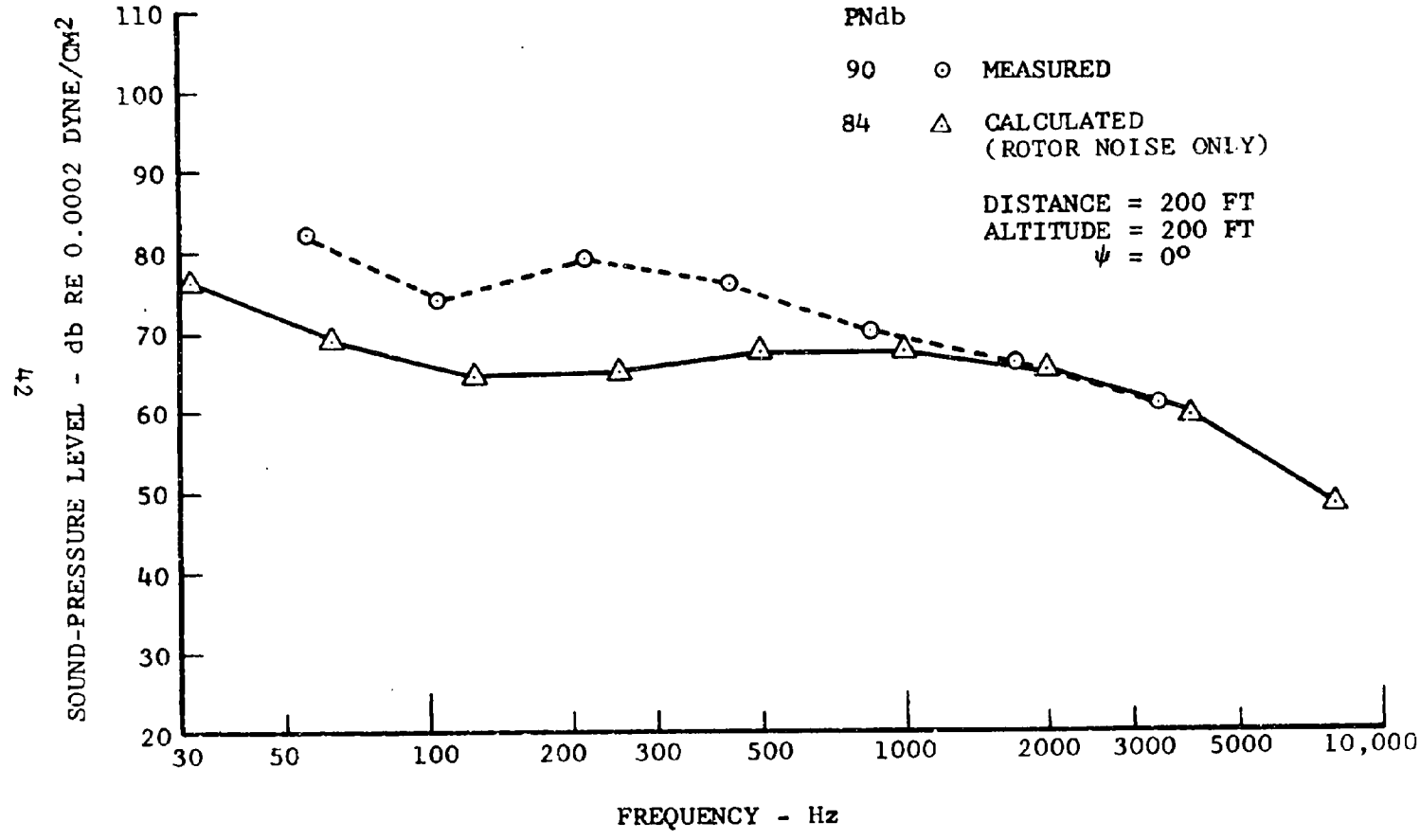

Figure 21. OH-58A Forward-Flight Noise Correlation at 45 Knots.

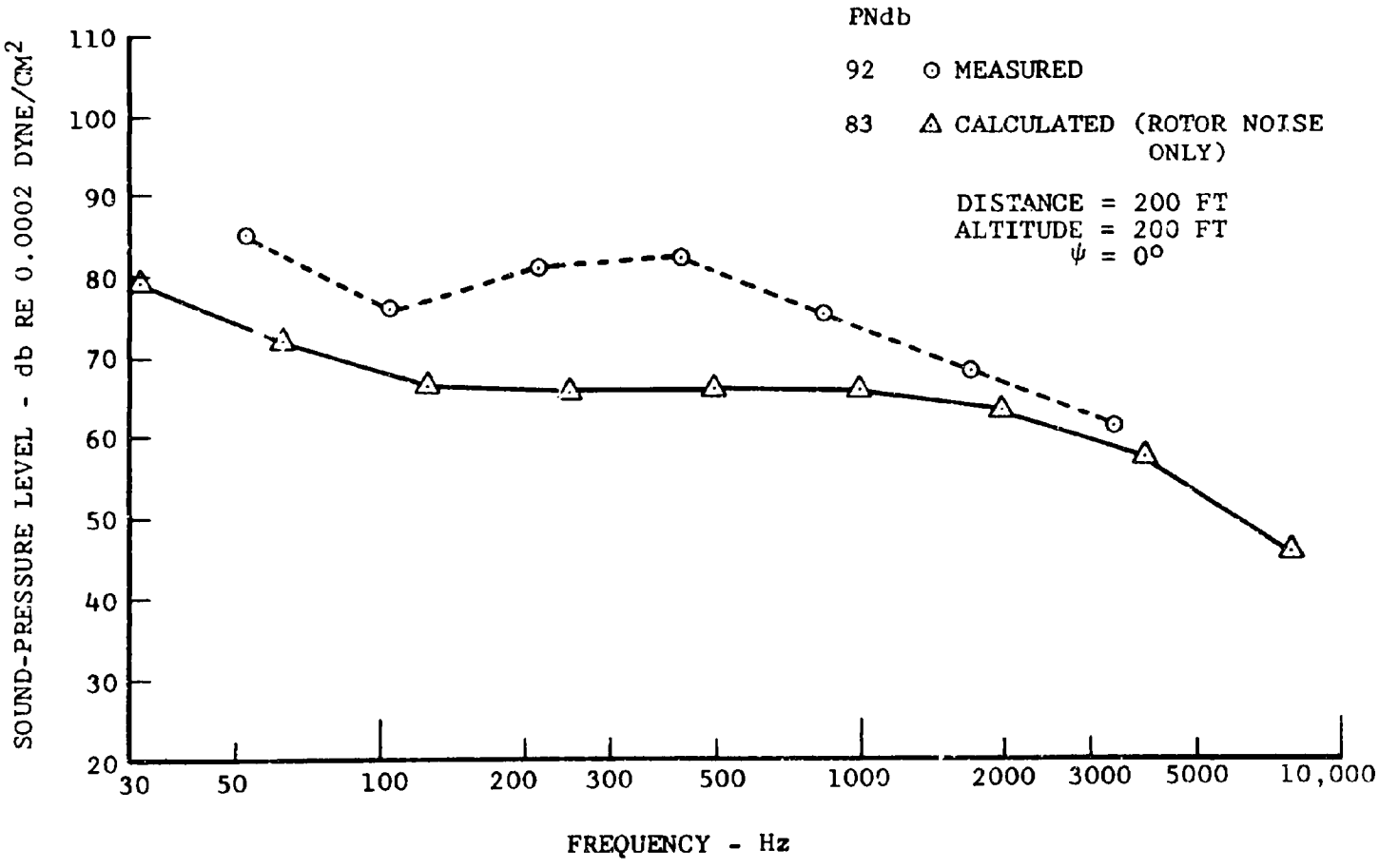

Figure 22. OH-58A Forward-Flight Noise Correlation at 102 Knots.

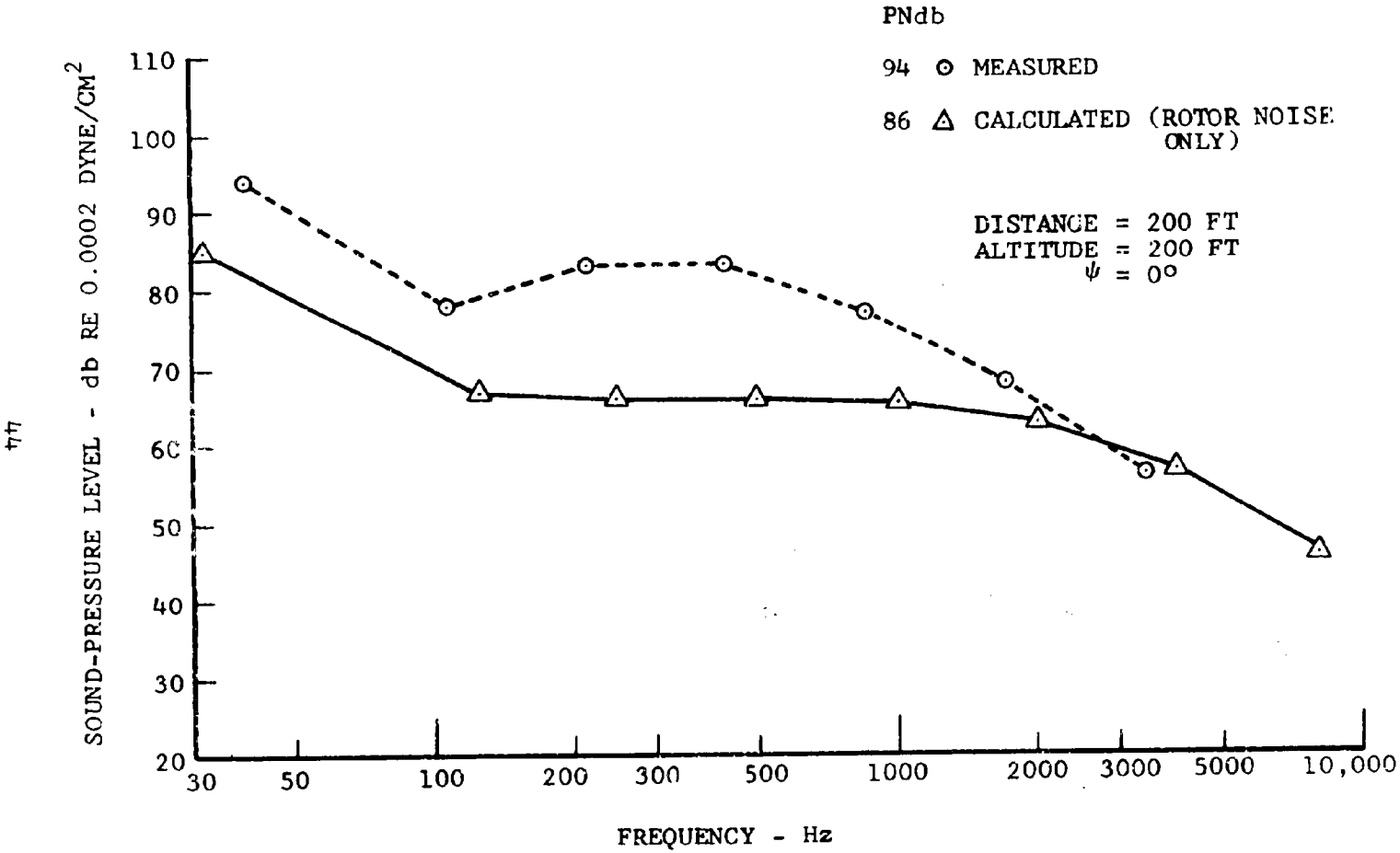

Figure 23. OH-58A Forward-Flight Noise Correlation at 113 Knots.

only, additions to tail-rotor noise on the order of 25 to 35 db are required in the octave bands centered at 250, 500, and 1000 Hertz. Although these bands correspond to those for tail-rotor rotational noise, this magnitude of correction seems unreasonable. The engine noise is also the loudest in the octave bands centered at 250, 500, and 1000 Hertz. It was estimated that in order to obtain correlation, the engine-component-noise test data taken at low power would have to be corrected in these three octaves on the order of 10 db for the horsepowers used in the flight tests. Finally, the approach was evaluated to make empirical corrections to the main and tail rotors limited to the differences between the theory and the rotor-component test data, and the remaining discrepancy was made up with corrections to engine noise.

This gives three different methods for correlating the theory with the measured noise of the complete helicopter:

- Corrections added to main- and tail-rotor rotational noise only, Table V
- Corrections added to engine noise only, Table VI
- Corrections added to both main- and tail-rotor rotational noise and engine noise, Tables VII and VIII

The perceived noise levels calculated for the OH-58A using the three methods are given in Table IX. After analyzing the accuracy of the three methods, the third one (using corrections to rotor noise and engine noise) was determined to be more practical for representing the difference between the theory and the measured data. Therefore, the empirical corrections in Table VII are used in the remainder of the study for predicting the noise levels of the different configurations.

The orders of magnitude of the empirical corrections required for main-rotor noise at angles near the plane of the rotor and for tail-rotor noise, particularly at zero thrust, are much greater than desired. The need for such large corrections points out important areas in which insufficient data are available and in which current theory is inadequate, but these are the best data currently available for this study.

TABLE V. ROTOR CORRECTIONS TO BE ADDED TO ROTOR-ONLY CORRELATION

Distance (ft)	Velocity (kt)	Sound Harmonic (mB)	db to be added at azimuth of:		
			0°, 180°	90°	270°
Main Rotor					
200	Hover	All	0	0	0
	45	2-6	3	3	3
		8-10	5	5	5
		≥ 12	6	6	6
	102	2-6	6	6	6
		8-10	7	7	7
		≥ 12	8	8	8
	113	2-6	8	8	8
		8-10	10	10	10
		≥ 12	12	12	12
4000	All	2-6	12	12	12
		8-10	13	13	13
		≥ 12	14	14	14
Tail Rotor					
200, 4000	Hover	2	6	0	3
		4-8	10	5	10
		10-16	6	5	8
		≥ 18	0	2	4
	45	2	8	5	7
		4-8	14	11	13
		10-16	12	9	10
		≥ 18	10	6	8
	102	2	12	10	15
		4-8	18	18	25
		10-16	15	22	21
		≥ 18	10	15	15
	113	2	17	15	17
		4-8	20	22	27
		10-16	15	24	21
		≥ 18	11	17	15

TABLE VI. ENGINE CORRECTIONS TO BE ADDED TO ENGINE-ONLY CORRELATIONS

Azimuth (deg)	Octave Band (Hz) 16	31	63	125	250	500	1000	2000	4000	8000
0, 90, 270	0	0	5	10	11	10	4	2	0	0
180	0	0	5	8	8	6	0	0	0	0

TABLE VII. ROTOR CORRECTIONS TO BE ADDED TO ROTOR-AND-ENGINE CORRELATION

Distance (ft)	Velocity (kt)	Sound Harmonic (mB)	db to be added at azimuth of: 0°, 180°	90°, 270°
Main Rotor				
200	Hover and forward flight	All	0	0
4000	Hover and forward flight	2-6	12	12
		8-10	13	13
		≥ 12	14	14
Tail Rotor				
200, 4000	Hover	2	10	0
		4	12	6
		6-18	11	5
		≥ 20	7	4
	45, 102, 113 kt	2	17	17
		4	22	22
		6-8	13	13
		10-16	11	11
		≥ 18	7	7

TABLE VIII. ENGINE CORRECTIONS TO BE ADDED TO ROTOR-AND-ENGINE CORRELATION

Azimuth (deg)	Octave Band (Hz) 16	33	67	125	250	500	1000	2000	4000	8000
All	0	0	2	5	5	5	2	0	0	0

TABLE IX. COMPARISON OF OH-58A PERCEIVED NOISE LEVELS (PNdb) FOR DIFFERENT TYPES OF CORRECTIONS

Azimuth (deg)	Velocity (kt)	200 Ft				4000 Ft		
		Measured	Rotor Only	Engine Only	Rotor and Engine	Rotor Only	Engine Only	Rotor and Engine
Hover								
0	-	87.8	86.9	89.4	91.1	50.5	51.6	50.8
90	-	91.5	89.6	90.4	91.8	55.5	53.5	54.2
180	-	92.1	90.0	91.2	91.2	53.0	53.8	53.4
270	-	93.4	91.2	91.4	92.6	60.2	55.6	58.7
Forward Flight								
0	45	89.9	86.5	89.0	90.6	50.5	50.9	50.4
	102	92.5	89.6	88.8	91.3	57.5	51.0	54.3
	113	93.7	92.8	88.8	91.8	60.6	51.2	56.5
90	45	89.3	88.4	89.3	88.6	52.1	50.3	51.1
	102	91.8	89.3	88.9	89.1	49.7	49.4	49.6
	113	93.7	90.7	88.8	91.3	53.1	51.4	50.9
180	45	90.1	89.5	91.0	89.6	46.8	53.3	48.7
	102	92.9	87.8	91.1	90.6	46.8	53.2	48.4
	113	93.4	90.2	91.5	91.3	46.8	53.2	48.4
270	45	88.8	88.6	90.7	87.6	59.6	53.2	54.6
	102	91.5	89.0	90.5	88.7	55.1	52.6	53.9
	113	94.1	89.1	90.5	90.1	56.2	52.6	54.9

III. NOISE-REDUCTION TECHNIQUES

Design techniques for noise reduction other than those that could be examined theoretically were reviewed. The concepts that were reviewed include:

- Reduction of the noise caused by the proximity of airframe structure
- Use of a regenerative engine
- Unloading of the tail rotor
- Use of a wing to permit tilting the rotor forward to reduce blade-wake interactions
- Modifications of the blade tip and planform

The proximity of aircraft structure to rotors may cause an increase in noise. The possibility that the vertical fin of the OH-58A might thus increase tail-rotor noise was considered. The effects of removing the fin were investigated during the Model 206A component-noise tests, and they were found to be insignificant except when thrust was low (Figure 24). Therefore, no attempt was made to relocate the fin or to change the fin-to-rotor distance.

Measurements reported by Prevoznik[9] indicate that the noise reduction to be expected from the Allison 250-B15A regenerative engine is 1 to 3 PNdb. Since a 15-db reduction is needed, and because substantial power and weight penalties are involved, this engine is not considered for the quiet helicopter.

It has been suggested that unloading the tail rotor in forward flight might reduce noise. Since the tail rotor of the OH-58A is normally unloaded, this measure is not applicable, but test data suggest that unloading a tail rotor is not an especially effective noise-reduction technique.

There is some evidence to support the suggestion that oscillatory airloads on a rotor blade, and thus noise, are reduced when the blade does not operate in or near the vortices of the preceding blades. If a wing is used to unload the rotor and the rotor is tilted forward, noise due to blade-vortex interactions might be reduced. NASA has conducted some tests in this area, but no data are yet available.

The ordinary effects of rotor planform taper and twist were examined theoretically using the propeller noise theory of Gutin[10] and conventional helicopter hover theory. Small

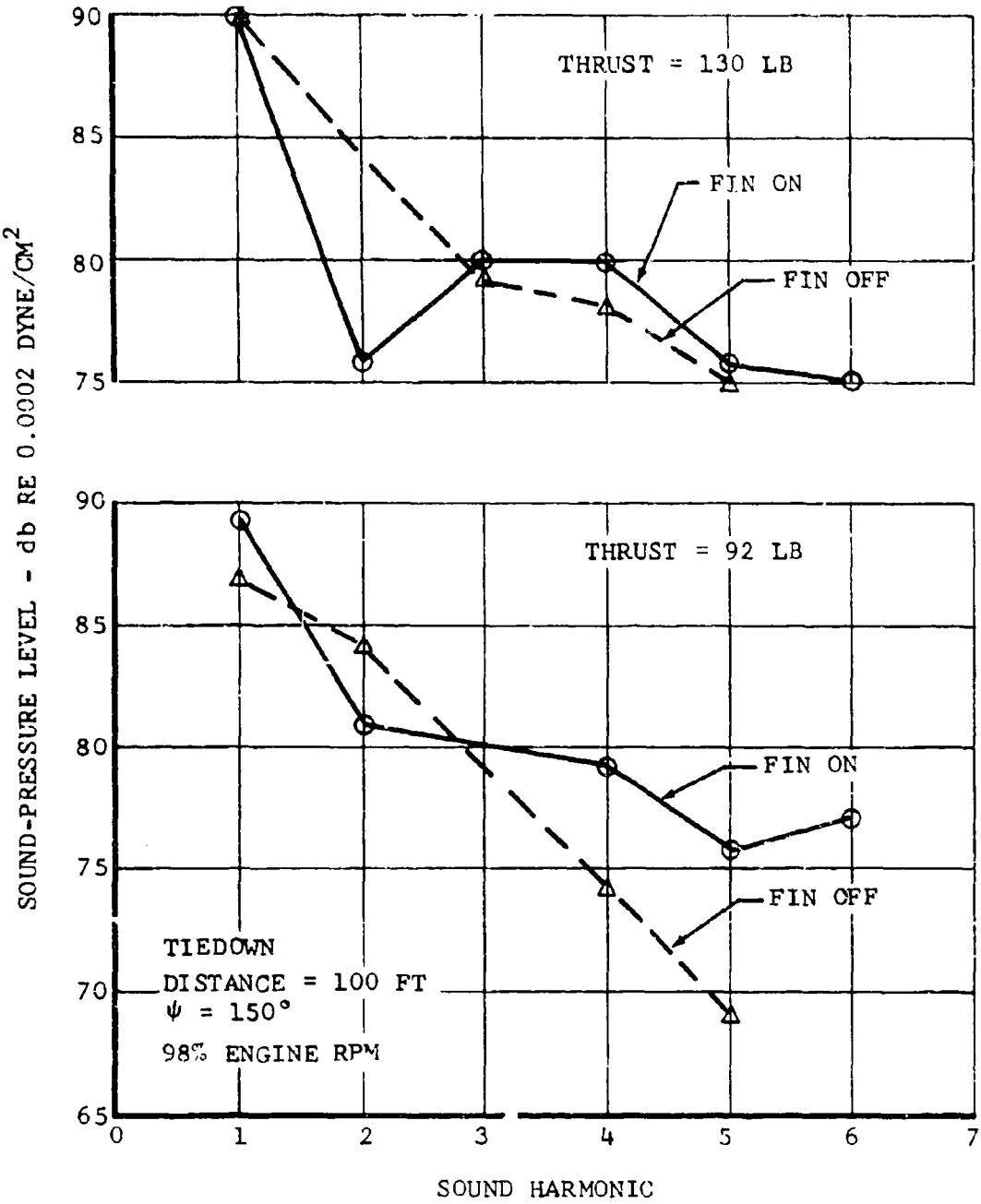

Figure 24. Effects of Vertical Fin on OH-58A Tail-Rotor Noise.

reductions are possible; but for blades that have the same lifting capability, noise reductions over the outer radius are offset by noise increases inboard.

The principal means of reducing rotor noise, other than by changes that can be examined theoretically, appears to be modification of the blade outboard planform or tip. Cox[11, 12] has shown that thin-tip blades reduce the noise of main rotors by approximately 5 db. This is consistent with the noise reductions found by Schlegel et al[4] for trapezoidal tips and by Sp[illegible]r et al[13] for single-swept tips. The various investigations differ somewhat in their explanation of the mechanism by which tip shape reduces noise, but there is enough supporting evidence to justify a tip modification. Figure 25 shows whirl-stand noise data versus frequency for two UH-1 tail-rotor blade configurations. One is a standard square-tip blade, and the other is a double-swept-tip blade, where the outermost leading-edge sweep angle is 45 degrees and the inner sweep angle is 27 degrees. Noise reductions on the order of 2 to 3 db are indicated at low frequencies and 8 to 10 db at high frequencies.

Table X shows the noise reductions that are used in the calculations for effects of blade modifications. In the final configurations, the noise reductions for double-swept-tip shapes are used for tail rotors. The noise reductions for thin-tip airfoils are used for main rotors.

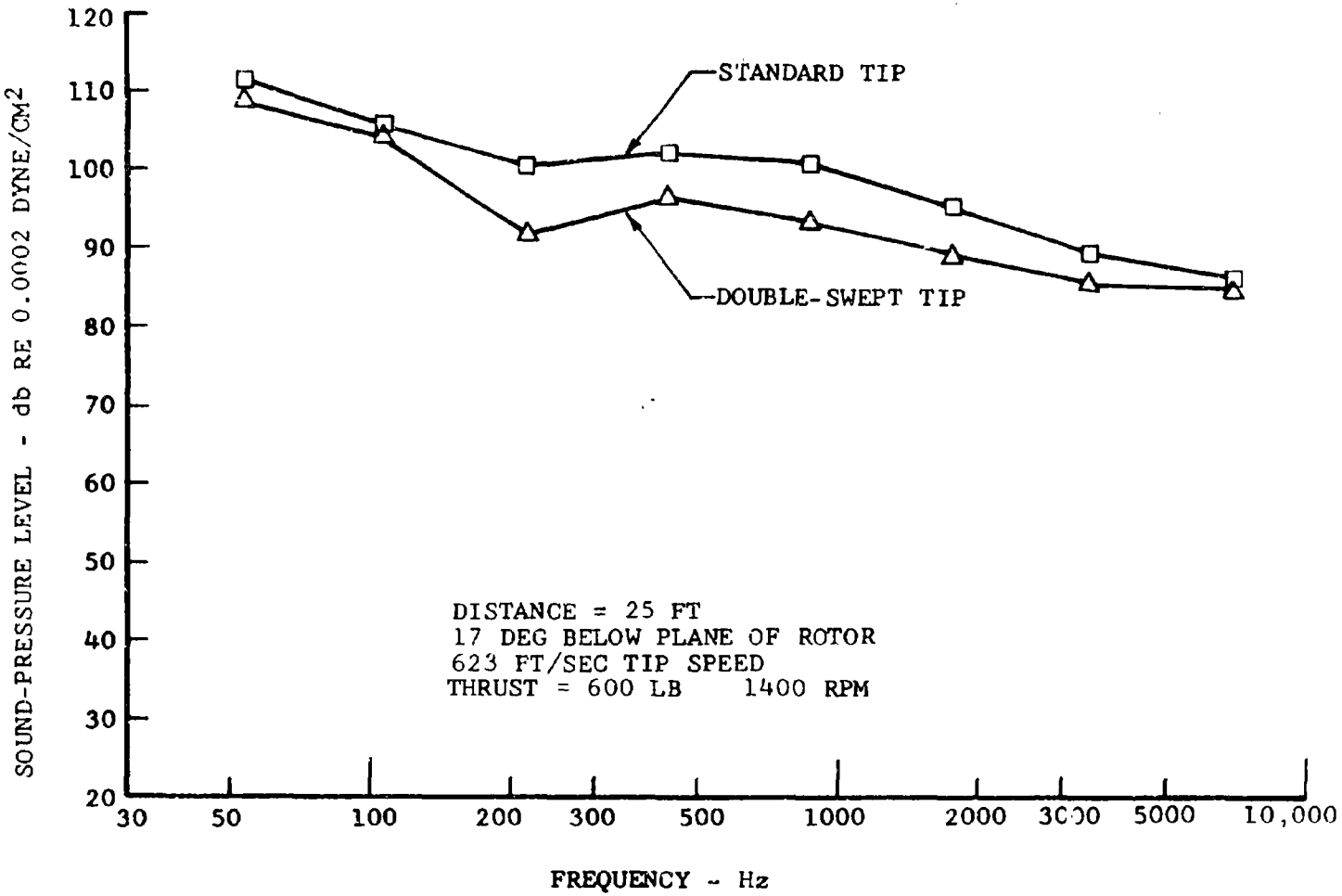

Figure 25. Comparison of UH-1 Square-Tip and Double-Swept-Tip Blades on Tail-Rotor Whirl Stand.

TABLE X. NOISE REDUCTIONS FOR BLADE-PLANFORM MODIFICATIONS

Modification	Sound-Pressure-Level Reduction (db re 0.0002 dyne/cm^2)						
	Harmonics						
	1	2	3	4	5	6-27	≥28
Hover							
Tip Shape (tail rotor only)	2.0	2.0	2.0	8.0	8.0	8.0	5.0
Planform Taper	0.2	0.3	0.3	0.4	0.4	0.4	0.4
Total	2.2	2.3	2.3	8.4	8.4	8.4	5.4
Forward Flight							
Tip Shape (tail rotor only)	2.0	2.0	2.0	8.0	8.0	8.0	5.0
Planform Taper	0.2	0.4	0.5	0.6	0.6	0.7	0.7
Thin Airfoil* (tail rotor only)	2.0	2.0	2.0	2.0	2.0	2.0	2.0
Total	4.2	4.4	4.5	10.6	10.6	10.7	7.7

* For thin-tip main-rotor blades, a 5-db reduction in the broadband noise component is assumed.

IV. EFFECTS OF PARAMETERS

A. INTRODUCTION

Noise was calculated for a range of values of main- and tail-rotor tip speed, number of blades, gross weight, rotor diameter, and blade area. All main-rotor calculations were made for a forward-flight speed of 115 knots, a bearing of 0 degrees (head-on), and ground ranges of 200 and 4000 feet. Tail-rotor calculations were made for hover conditions at a bearing of 30 degrees and for a forward flight speed of 115 knots at a bearing of 10 degrees, at the same ground ranges as those for the main rotor.

A sample output of the computer program, which includes the equations for the rotational and broadband noise components, is shown in Figure 26. The case shown is for the OH-58A main rotor at a tip speed of 655 feet per second at a field point range of 200 feet, a velocity of 115 knots, and an azimuth of 0 degrees.

B. MAIN ROTOR

The effects of tip speed and diameter are shown in Figures 27 and 28 for two- and four-bladed rotors, respectively. Also shown are the effects of diameter for constant hover ceiling and t_c ratio. The figures show the results for two field points, 200 and 4000 feet from the helicopter. For the design conditions of constant hover ceiling and t_c ratio, where blade chord is increased as tip speed is reduced, the rate of noise reduction is about 5 PNdb for a 100-foot-per-second reduction in tip speed.

The effects of diameter are small. Increasing the diameter reduces the perceived noise level about 3.0 PNdb at 200 feet. At 4000 feet, however, this effect is reversed; an increase in diameter increases the perceived noise level slightly.

As can be seen in Figures 27 and 28, increasing the number of blades does not appreciably affect perceived noise level of the main rotor. This is because rotor broadband noise contributes more to the perceived noise level than does rotational noise, even at far distances. As can be seen in Equation 14, the peak level of broadband noise is a function of tip speed, thrust, and blade area. Doubling the blade area reduces the peak level by 3 db.

C. TAIL ROTOR

The effects of tip speed and number of blades on tail-rotor noise are shown in Figure 29. Both a reduction in tip speed and an increase in the number of blades reduce tail-rotor

TITLE ** BELL HELICOPTER
ROTOR PARAMETER STUDY
CASE 1

ROTOR GEOMETRY ...

NO. OF BLADES	2
ROTOR RADIUS - FT	16.670
RPM	276.00
TIP SPEED - FT/SEC	481.807
DISC ANGLE OF ATTACK - DEG	.000
VELOCITY - FT/SEC	.000
SPEED OF SOUND - FT/SEC	1100.000
CHORD - INCHES	13.000

LOADING ...

THRUST - LBS	290.0
TORQUE - LB.FT.	471.0
EFFECTIVE CONING ANGLE - DEG	.513
LOADING STATION	.805
POWER LAW EXPONENT	2.500
NO. OF LOADING HARMONICS	60
CORRELATION LENGTH CONSTANT	.700
HEIGHT - FEET	5.5

*** * *** * *** * *** * *** * *** * *** * *** * *** * *** * *** * *** * *** * *** * *** * *** * *** *

FIELD POINT NUMBER 1

X -	100.000
Y -	.000
Z -	5.540
XI -	100.000
RI -	100.153

HARMONIC NO.	1	2	3	4	5	6	7	8	9	10	11	12	13	14	15	16
FREQUENCY - HZ	9.2	18.4	27.6	36.8	46.0	55.2	64.4	73.6	82.8	92.0	101.2	110.4	119.6	128.8	138.0	147.2
SPL - DB	32.4	45.1	43.0	39.6	37.0	34.2	32.0	30.2	28.6	27.1	25.9	24.6	23.5	22.5	21.6	20.6
MBL. ABS. - DB	.0	.0	.0	.0	.0	.0	.0	.0	.0	.0	.0	.0	.0	.0	.0	.0
GRND ABS. - DB	.0	.0	.0	.0	.0	.0	.0	.0	.0	.0	.0	.0	.0	.0	.0	.0
CORR. SPL - DB	32.4	45.1	43.0	39.6	36.9	34.2	32.0	30.2	28.6	27.1	25.9	24.6	23.5	22.5	21.5	20.6

HARMONIC NO.	17	18	19	20	21	22	23	24	25	26	27	28	29	30	31	32
FREQUENCY - HZ	156.4	165.6	174.8	184.0	193.2	202.4	211.6	220.8	230.0	239.2	248.4	257.6	266.8	276.0	285.2	294.4
SPL - DB	19.8	19.0	18.3	17.5	16.8	16.2	15.6	15.0	14.5	14.0	13.5	13.0	12.5	12.1	11.6	11.2
MBL. ABS. - DB	.0	.0	.0	.0	.0	.0	.0	.0	.0	.0	.0	.0	.0	.0	.0	.0
GRND ABS. - DB	.0	.0	.0	.0	.0	.0	.0	.0	.0	.0	.0	.0	.0	.0	.0	.0
CORR. SPL - DB	19.8	19.0	18.2	17.5	16.8	16.2	15.6	15.0	14.5	13.9	13.4	12.9	12.5	12.0	11.6	11.1

OCTAVE BAND CENTER FREQUENCY	16	31.5	63	125	250	500	1000	2000	4000	8000	*BASPL*	*PNDB*
ROTATIONAL WITH ABSORPTION	49.4	47.2	40.4	33.7	27.3	21.0	14.4	7.5	.0	.0	51.8	23.2*
ROTATIONAL WITHOUT ABSORPTION	49.4	47.2	40.5	33.7	27.3	21.1	14.6	7.8	.8	.0	51.8	23.2*
VORTEX WITH ABSORPTION	12.4	24.8	32.4	37.9	41.9	43.9	42.7	38.3	31.6	23.5	48.8	55.6
VORTEX WITHOUT ABSORPTION	12.4	24.8	32.4	37.9	42.0	44.0	42.8	38.7	32.5	26.7	48.9	56.4
TOTAL WITH ABSORPTION	49.4	47.2	41.1	39.3	42.1	43.9	42.7	38.3	31.6	23.5	53.6	55.7
TOTAL WITHOUT ABSORPTION	49.4	47.2	41.1	39.3	42.1	44.0	42.8	38.7	32.5	26.7	53.6	56.6

Figure 26. Sample Computer Program Output.

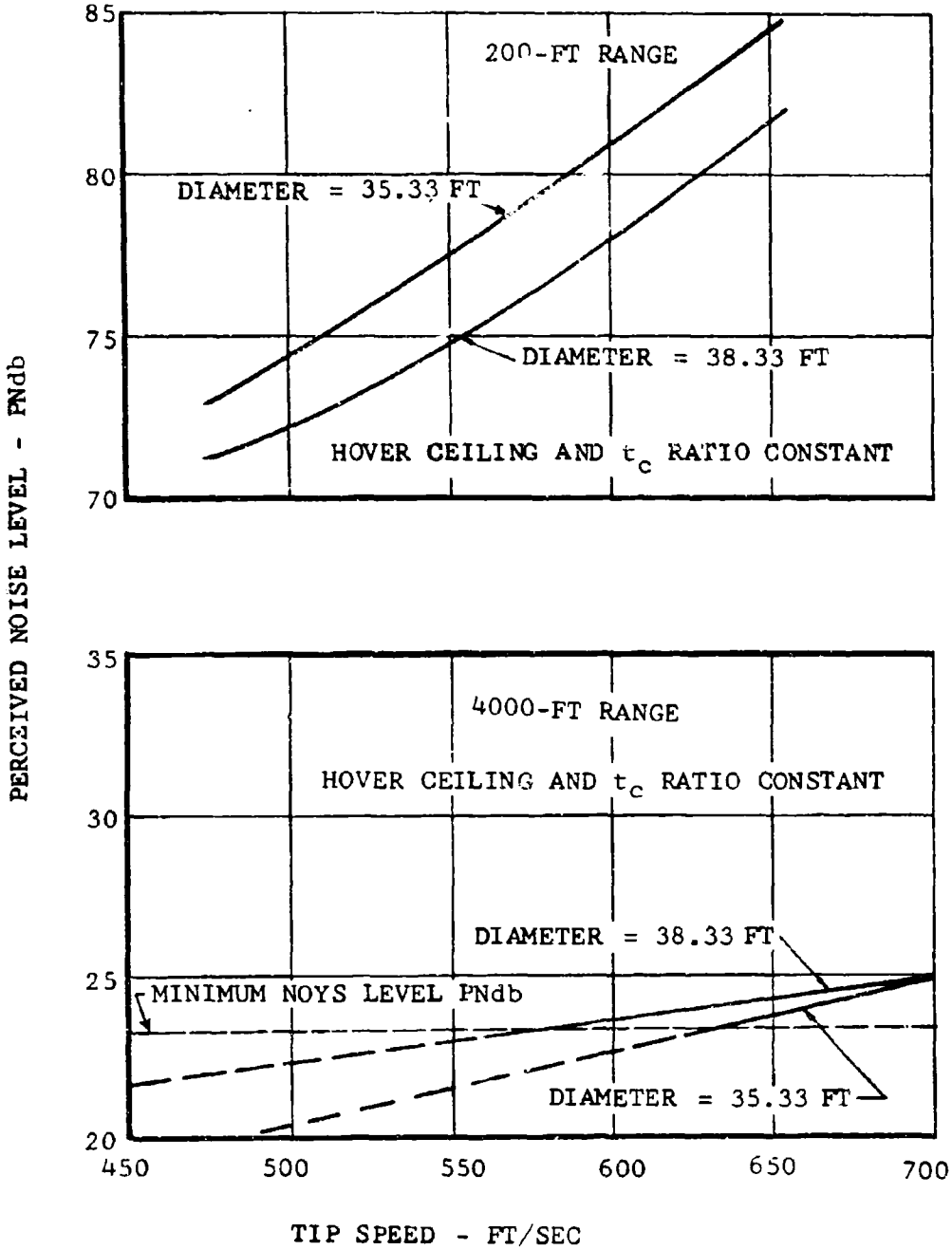

Figure 27. Effects of Tip Speed and Diameter on Two-Bladed Main-Rotor Noise.

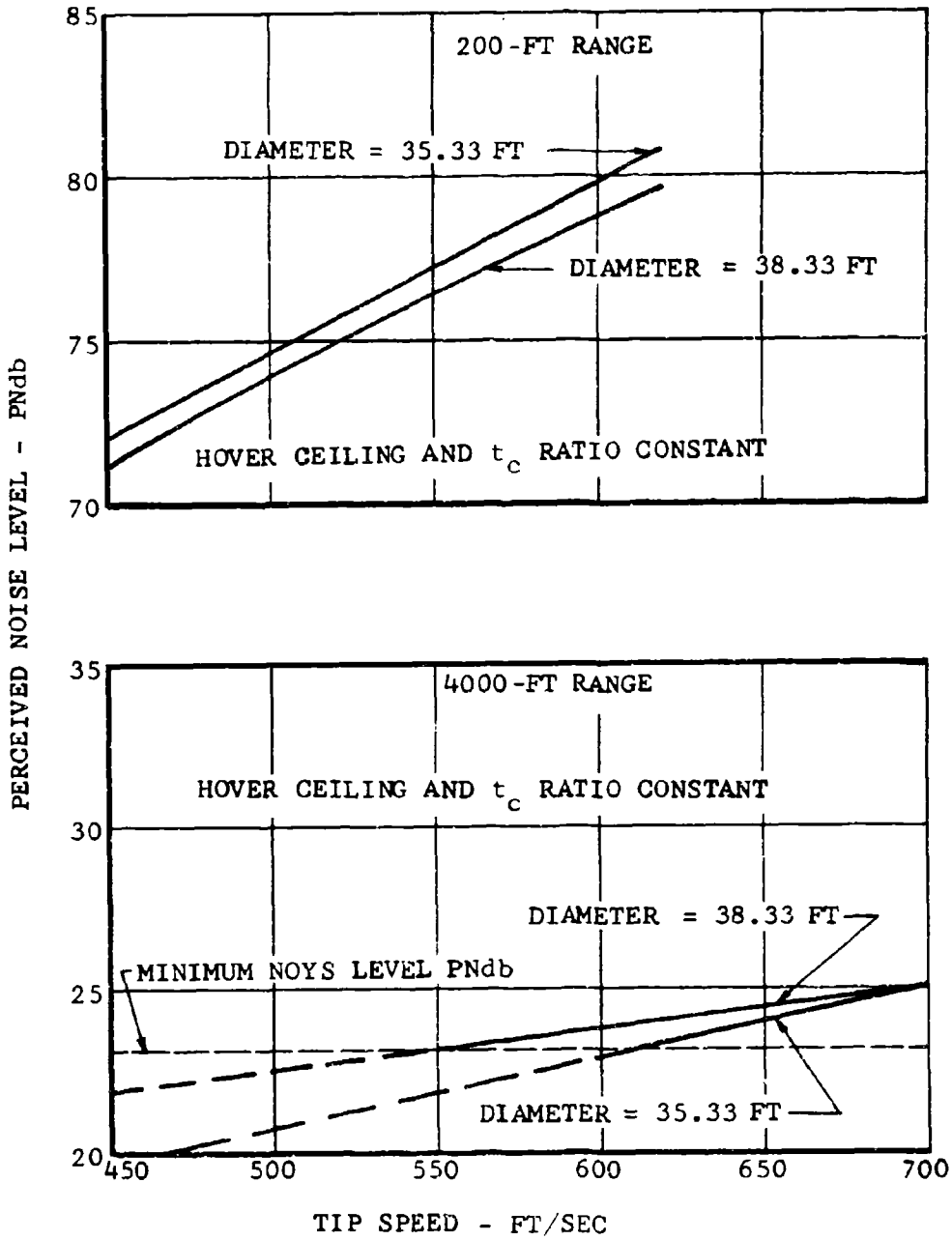

Figure 28. Effects of Tip Speed and Diameter on Four-Bladed Main-Rotor Noise.

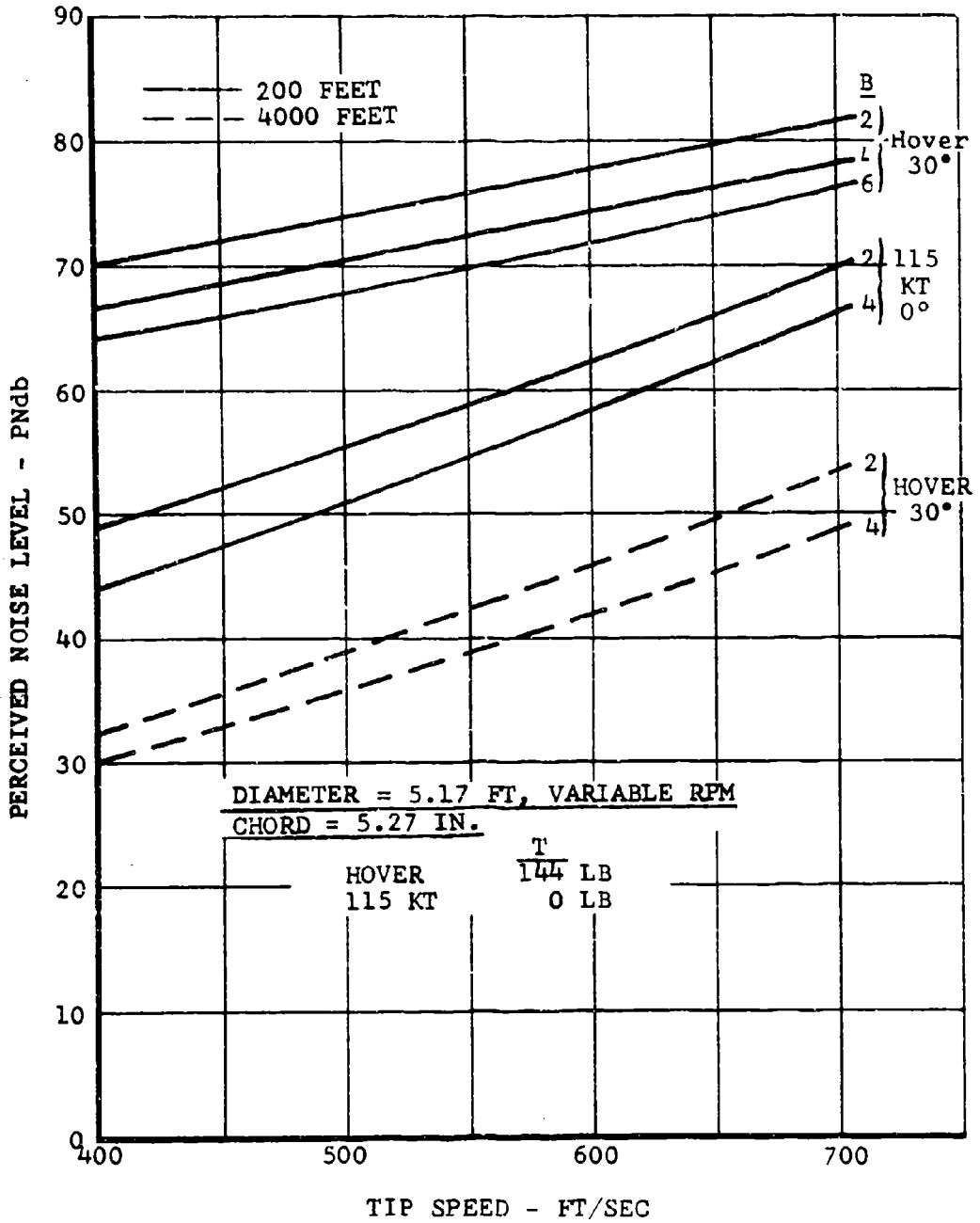

Figure 29. Effects of Tip Speed and Number of Blades on Tail-Rotor Noise.

noise. For the tip-speed range shown and for constant thrust, power, and diameter, the hovering perceived noise levels decrease at a rate of 3 PNdb for a 100-foot-per-second reduction in tip speed. At 4000 feet, this rate is 6.5 PNdb for a 100-foot-per-second reduction in tip speed.

Tip-speed reduction is also significant in reducing tail-rotor noise in forward flight. The perceived noise level for a 115-knot head-on approach decreases 6.5 PNdb per 100-foot-per-second reduction in tip speed.

Increasing the number of tail-rotor blades from two to four reduces the perceived noise level by 4 PNdb for hover and in forward flight. A six-bladed tail rotor is 6 PNdb quieter than a two-bladed one.

The effects of thrust for a tip speed of 550 feet per second are shown in Figure 30. At a distance of 4000 feet in hover, the theory predicts that the perceived noise level is decreased approximately 4 to 6 PNdb by decreasing the thrust by 100 pounds. Although not shown in the figure, this effect is not realized when the azimuth position is near the plane of the rotor.

The theoretical effects of torque and diameter on tail-rotor perceived noise are shown in Figure 31 for a 115-knot forward speed and zero thrust. At a constant tip speed of 550 feet per second, both a decrease in torque and an increase in diameter reduce the perceived noise levels. Increasing the diameter from 5.17 to 7.17 feet reduces tail-rotor noise about 8 PNdb at constant torque because of the reduction of drag by 28 percent. The rate of noise reduction for torque decrease is about 0.5 PNdb per foot-pound for constant diameter.

The theory shows that tail-rotor noise varies significantly for various headings. This is illustrated in Figure 32, which compares the theory to the test data at a tip speed of 711 feet per second and for thrusts of 92 to 144 pounds. The theory predicts accurately the maximum noise generated at Ψ = 30 and 150 degrees, but it overestimates the noise by about 4 PNdb at Ψ = 90 degrees. It underestimates the noise by as much as 10 PNdb in the rotor plane at Ψ = 0 and 180 degrees, where minimum noise is predicted.

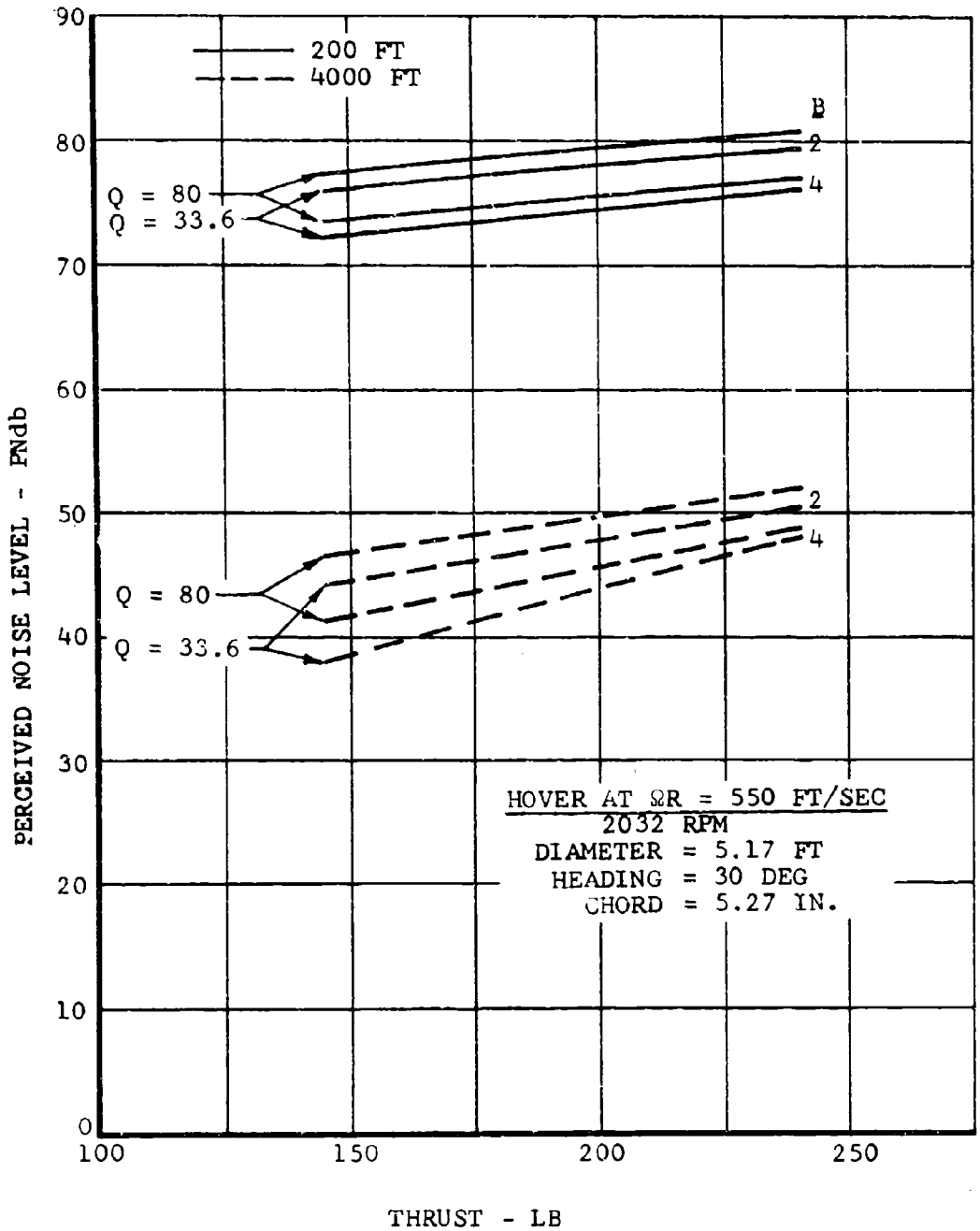

Figure 30. Effects of Thrust and Torque on Tail-Rotor Noise.

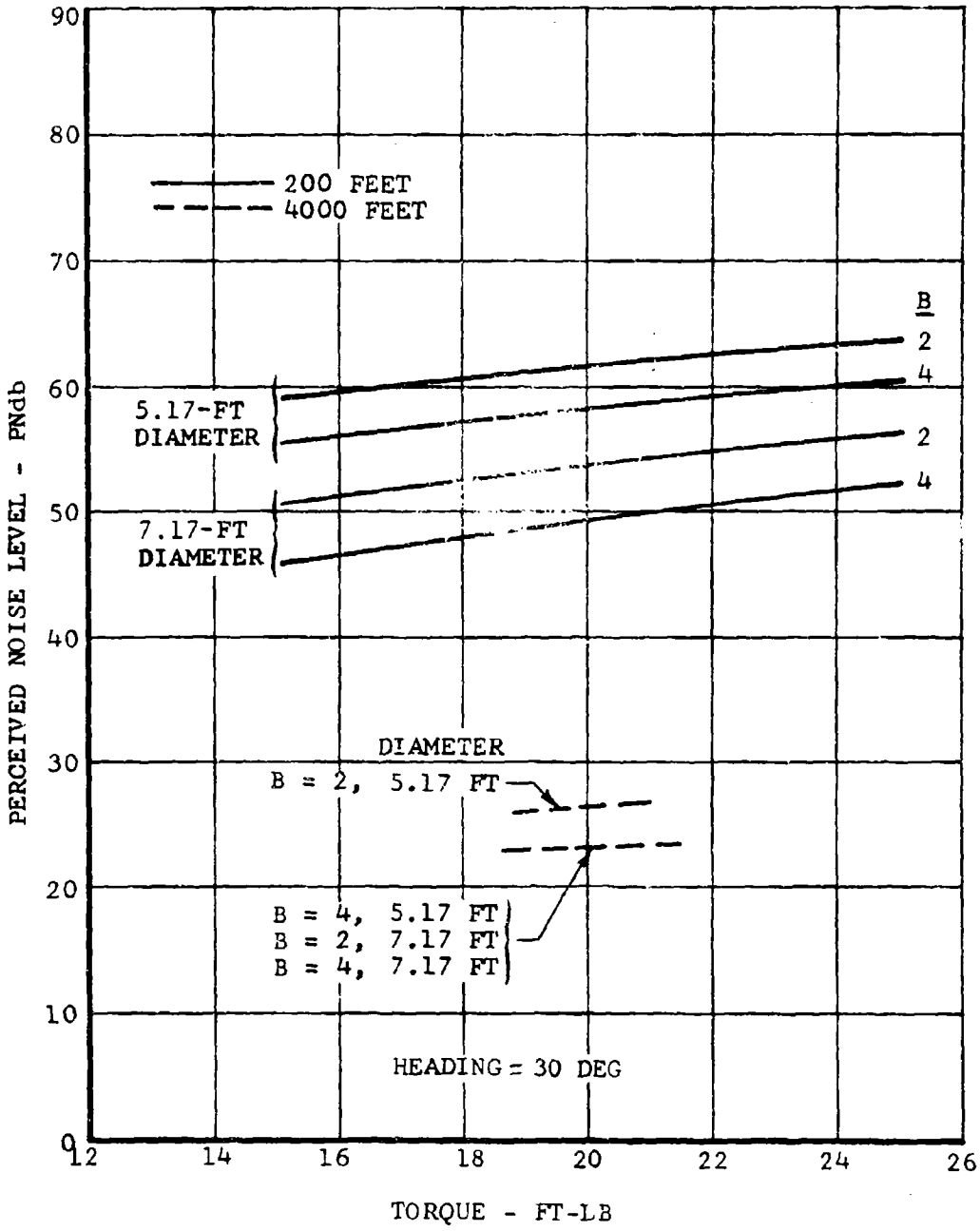

Figure 31. Effects of Torque and Diameter on Tail-Rotor Noise.

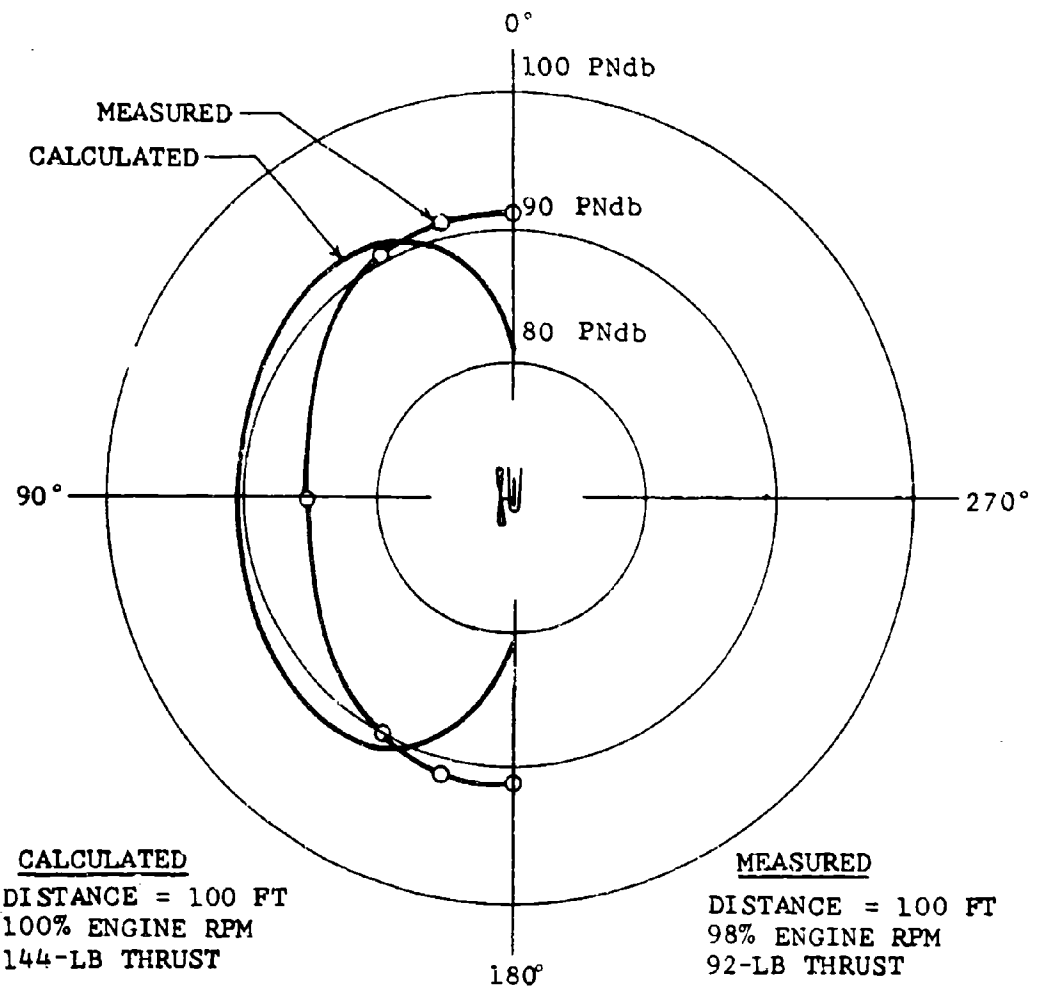

Figure 32. Variation of Tail-Rotor Noise for Different Headings.

V. DESIGN ALTERNATIVES AND SELECTION OF COMPONENT PARAMETERS AND CONFIGURATIONS

The previous section shows the variation of noise with changes in parameters of the main rotor and tail rotor, separately. In this section, the variation of noise is shown for the complete helicopter, for various combinations of main- and tail-rotor tip speeds, and for several degrees of engine and drive-system noise reductions. The purpose of the calculations was to determine the importance of main-rotor tip-speed reductions relative to tail-rotor tip speed and engine/drive-system noise reductions. The calculations also include the effect of noise reductions due to main-rotor-blade thin-tip modifications and the effect of tail-rotor-blade double-swept-tip modifications.

Final results are shown in Table XI. In the table, values are given for PNdb of the OH-58A (in the first column) and for three alternate combinations of parameters (in the last three columns). The data show that significant reductions in noise of the OH-58A are possible at a range of 4000 feet. Much of the noise reduction relative to the OH-58A is realized when main-rotor tip speed is reduced to 600 feet per second and tail-rotor tip speed to 530 feet per second--if blade-tip modifications are used on the tail rotor and if engine noise is reduced at least 15 db. This combination of parameters is feasible for a modified OH-58A using production main-rotor blades and four modified OH-58A tail-rotor blades. A summary of the calculation of PNdb for the combination is shown in Table XII. Noise in three octave bands contributes to the value of PNdb. In the 125-Hertz band, the total sound-pressure level is determined by tail-rotor noise and, to some extent, main-rotor noise. In the 250- and 500-Hertz bands, the total level is determined by all three noise sources.

PNdb levels were calculated for one other combination of parameters (not shown in the table). A main-rotor tip speed of 530 feet per second and a tail-rotor tip speed of 431 feet per second were combined with engine silencing and tail-rotor-blade modifications. PNdb was reduced to 28.5 for a four-bladed tail rotor and to 26.3 for a six-bladed tail rotor. The tail rotor for this configuration requires a high solidity (0.31 to 0.394). Further research and development will be required.

Several important factors that cannot be quantified at present are not included in the calculation. They are: the effects of impulsive noise, the effect of main-rotor-planform modifications, and/or the effect of reductions in blade-tip-vortex strength on main-rotor noise. The effects of impulsive noise are not included because the rotor theory calculates only the long-time root-mean-square magnitudes of sound-pressure levels. A conclusive method of accounting for impulsive noise was not

TABLE XI. PERCEIVED NOISE LEVELS FOR ALTERNATE COMBINATIONS OF PARAMETERS

Variant	Perceived Noise Level at 4000 Feet* (PNdb)				
	Main Rotor Tip Speed, ft/sec	655	600	600	530
	Main Rotor Number of Blades	2	2	2	2
	Tail Rotor Tip Speed, ft/sec	711	600	530	530
	Tail Rotor Number of Blades	2	3	4	4
No Blade Planform Modifications					
No Engine-Noise Reduction		56.5	48.2	45.7	45.5
15-db Engine-Noise Reduction		56.1	45.6	37.3	36.9
Engine Noise Reduced to 0		56.1	45.5	36.6	36.2
Double-Swept-Tip Tail-Rotor Blades					
No Engine-Noise Reduction		53.7	46.7	44.6	43.8
15-db Engine-Noise Reduction		52.7	42.2	32.0	30.8
Engine Noise Reduced to 0		52.7	41.7	30.8	30.0
Double-Swept-Tip Tail-Rotor Blades and Thin-Tip Main-Rotor Blades					
No Engine-Noise Reduction		53.7	46.7	44.5	43.8
15-db Engine-Noise Reduction		52.7	42.2	31.9	30.7
Engine Noise Reduced to 0		52.7	41.7	30.8	29.8

* ψ = 0 deg, V = 115 kt

TABLE XII. COMBINED NOISE OF COMPLETE HELICOPTER*

	Sound-Pressure Level (db) Center Frequency of Octave Band (Hz)									
	16	31.5	63	125	250	500	1000	2000	4000	8000
Main-Rotor Rotational Noise	48.4	47.5	43.1	34.2	25.2	15.9	5.3	<0	<0	<0
Main-Rotor Vortex Noise	<0	4.7	10.4	15.1	18.1	18.2	16.6	1.7	<0	<0
Total Main-Rotor Noise	48.4	47.5	43.1	34.2	25.9	20.0	16.9	1.7	<0	<0
Total Tail-Rotor Noise	<0	<0	4.5	40.5	29.7	19.0	5.5	<0	<0	<0
Engine/Drive-System Noise	-	-	12.4	25.1	27.0	22.5	10.8	<0	<0	<0
Total	48.4	47.5	43.1	41.5	32.6	25.5	18.1	1.7	<0	<0
Noy	0	0	0	0.4	0.3	0.1	0	0	0	0

Overall Sound-Pressure Level	52.0 db
Maximum Noys	0.4
Total Noys	0.5
Perceived Noise Level	32.0 PNdb

* Main-rotor tip speed, 600 ft/sec; double-swept tail-rotor tip; tail-rotor tip speed, 530 ft/sec; engine noise reduced 15 db; field point range, 4000 ft; V = 115 kt; helicopter bearing, 0 deg head-on.

found in the literature. Some evidence of the possible effect is found in Kryter and Pearsons.[1] Listening tests show that there is a distinct subjective impression of a tone modulated at a very low frequency. A 500-Hertz tone modulated in amplitude at a frequency of 5 Hertz is judged to be noisier by approximately 6 PNdb than an unmodulated tone. If this applies to main-rotor noise modulated in amplitude at blade-passage frequency, then a correction factor of 6 PNdb may be required. A reduction in impulsive noise of the main rotor may be obtained by further reductions in tip speed. The combination of parameters shown in the last column in Table XI shows main-rotor noise levels which are 6 to 10 db lower than those of the other two noise sources, in the bands that have the highest values of noisiness.

The effects of main-rotor tip-planform modifications are not included because of lack of theory and/or test data. Significant reductions in the tip-vortex strength of model blades have been observed in schlieren photographs made in the Bell Helicopter Company Research Laboratory. Since Lowson[3] has reported that the largest component of rotor vortex noise is that due to interaction of the following blade with the tip vortex of the preceding blade, it is likely that reductions in main-rotor noise will be realized by blade-tip-planform modifications. The modifications used are related to the blade aspect ratio. Tests of double-swept-tip tail-rotor blades with low aspect ratios show substantial reductions in noise levels. The reductions at low tip speeds are believed to result from the larger span of the tip modification and perhaps from the leading-edge sweep. Therefore, double-swept tips are used on low-aspect-ratio blades (such as the tail-rotor and wide-chord main-rotor blades). For high-aspect-ratio blades (such as those of the CH-58A), the double-swept-tip modification is relatively small in span, so tapered tips are used to increase the span of the modification. The taper begins farther inboard, but the taper ratio is less than that obtainable with the double-swept-tip modification.

In conclusion, it was found that most of the noise reduction shown by the various combinations of parameters could be achieved with a main-rotor tip speed of 600 feet per second and a tail-rotor tip speed of 530 feet per second; a four-bladed tail rotor is required for maximum noise reduction. Tip modifications should be used on the tail rotor. Engine/drive-system noise should be reduced by 15 db. These are the parameters selected for the primary configurations. Tip modifications to the main rotor may reduce noise. Reductions in main-rotor noise and impulsive noise may be realized by reducing tip speed to 530 feet per second--the main-rotor tip speed of the alternate configurations.

VI. DESIGN DESCRIPTIONS

This section describes two test and two operational configurations of the quiet OH-58A. The primary configurations are designed to reduce the overall noise level, and the alternate configurations, to further reduce the impulsive noise of the main rotor. The test/demonstrator designs have been developed to show practicable modifications that may be used to verify the theoretical approach to the development of a quiet helicopter. The operational versions include the quieting features of the corresponding test versions, but they are extensively modified to have capabilities comparable to those of the OH-58A. The rotor tip speeds of the primary configurations are reduced, and measures to quiet their powerplants and drive systems are employed. For the alternate configurations, the main-rotor tip speeds are further reduced. Table XIII gives design data for all five aircraft.

A. TEST VERSION--PRIMARY CONFIGURATION

The primary test configuration has modified OH-58A main- and tail-rotor blades and a new hub for the four-bladed tail rotor. It uses the same engine as the production OH-58A, but with speed reduced from 6180 to 5660 rpm in order to lower the tip speeds of the rotors. Engine power is reduced from 317 to 290 horsepower, for the same maximum torque on the drive system. No changes are required in the main transmission or the drive system. The tip speed of the tail rotor is further reduced by changing the gear ratio in a redesigned tail-rotor gearbox. The changes in the control system for the four-bladed tail rotor are minimal, and the airframe is unchanged. Sound-absorbing material is added to engine cowlings and firewalls, and absorptive silencers are installed on the engine exhaust.

1. Rotor System

a. Main Rotor

The 35-foot-4-inch main rotor is the same as that on the OH-58A, except that in the outboard 15 percent of its span, the chord tapers from 13 to 4.3 inches. This taper is expected to result in a noise reduction comparable to that which has been achieved on tail-rotor blades. The tip inertia weight is reduced from 12 to 5 pounds, and 10 pounds are added at 85 percent of the radius. The outboard 15 percent of the blade, with its attachment to the basic 13-inch-chord OH-58A blade, is shown in Figure 49 (Appendix).

The main rotor's natural frequencies are shown in Figure 33. They differ slightly from those of the OH-58A because of the altered stiffness and mass distribution of the outboard 15 percent of the span, but the curves show that they are well placed

TABLE XIII. DESIGN DATA

		OH-58A	Test Version		Operational Version	
			Primary	Alternate	Primary	Alternate
Design Gross Weight	lb	3000	3000	3000	3220	3400
Empty Weight	lb	1583	1679	1811	1831	2013
Powerplant		T63-A-700	T63-A-700	T63-A-700	Allison 250-C20	Allison 250-C20
Power						
Military Rated	hp	317	290	279	317	317
Normal Rated	hp	270	247	237	270	270
Engine Output	rpm	6180	5660	5000	6000	6000
Main Rotor						
Diameter	ft	35.33	35.33	35.33	35.33	35.33
Tip Speed	fps	655	600	530	600	530
RPM		354	324	287	324	287
Number of Blades		2	2	2	2	2
Blade-Root Chord	in.	13	13	21	20.7	30.5
Tip Modification		Swept-Tip	Tapered	Double-Swept	Tapered	Double-Swept
Equivalent Chord	in.	13	11.2	18.8	17.7	25.9
Equivalent Solidity		0.0391	0.0338	0.0562	0.0530	0.0776
Tail Rotor						
Diameter	in.	62	62	69	62	69
Tip Speed	fps	711	530	521	530	530
RPM		2627	1960	1760	1960	1730
Number of Blades		2	4	4	4	4
Blade-Root Chord	in.	5.27	5.27	5.27	6.21	6.33
Tip Modification		None	Double-Swept	Double-Swept	Double-Swept	Double-Swept
Equivalent Chord	in.	5.27	4.33	4.44	5.06	5.09
Equivalent Solidity		0.108	0.178	0.164	0.208	0.188

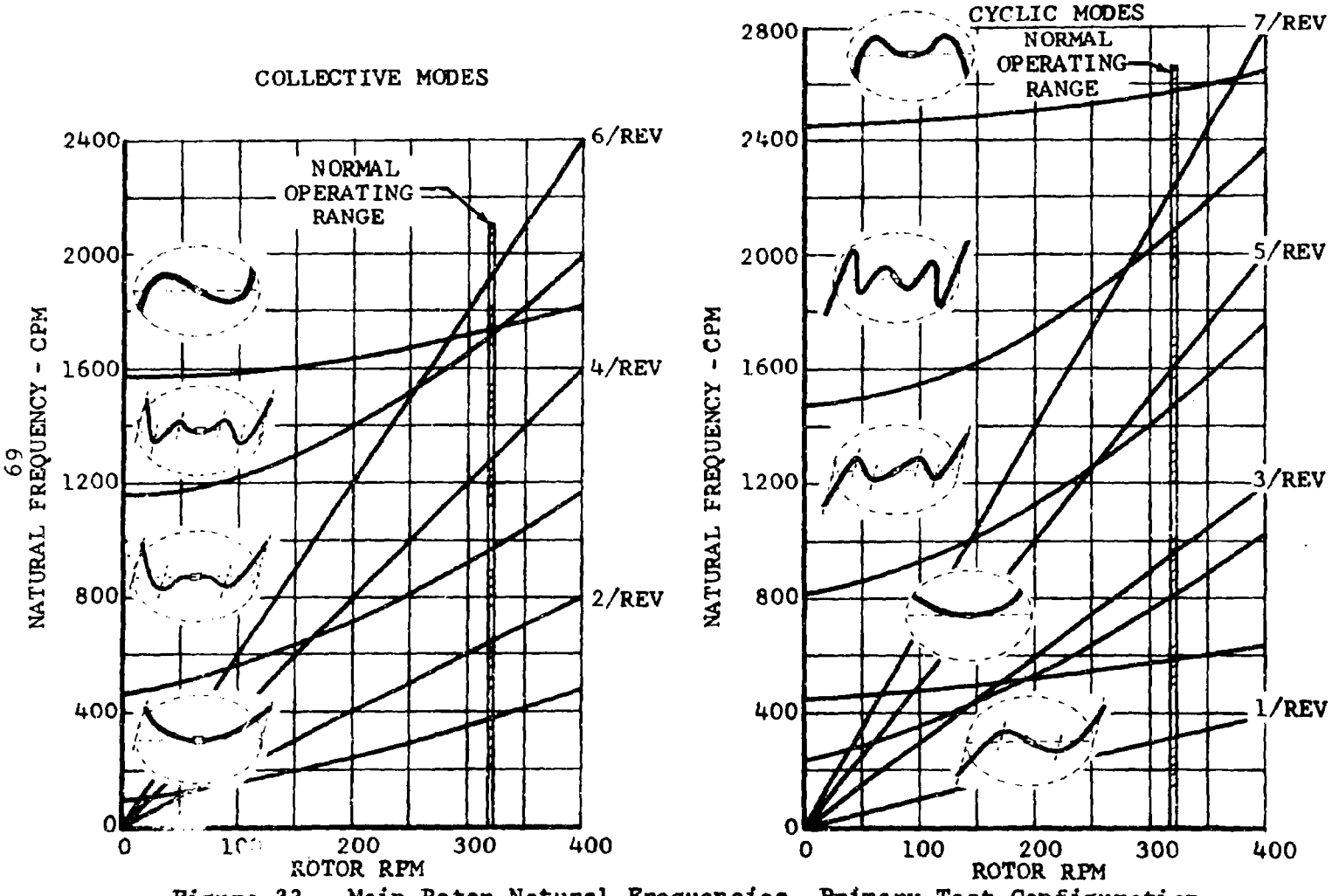

Figure 33. Main-Rotor Natural Frequencies, Primary Test Configuration.

in relation to rotor rpm. Because of the increased thrust coefficients at which the rotor will operate, the blade and hub stresses will differ from those on the OH-58A. They will therefore be monitored during the flight-test program.

b. Tail Rotor

The four-bladed, semirigid tail rotor (Figure 51, Appendix) has a gimbaled hub. Delta-three is 45 degrees, the same as that of the OH-58A. The rotor's diameter is 62 inches.

The blades have a constant 5.27-inch chord and an NACA 0012.5 airfoil, except for the double-swept tip fairings. Each blade has a shell of 2024-T3 aluminum alloy, with a bonded aluminum-honeycomb core strip. The leading edge is reinforced with a stainless-steel abrasion strip. The double-swept tip fairing is welded 6061 aluminum alloy, with provisions for mounting a balance weight.

Each blade is attached to two aluminum-alloy yoke plates through Teflon-fabric-lined pitch-change bearings. A gimbaled hub permits angular movement of the plane of rotation. The assembly is attached to the mast through a splined steel shaft.

2. Drive System

All components of the drive system except the tail-rotor gearbox are standard OH-58 units. The system is rated for engine output at 5660 rpm of 290 horsepower for takeoff and 247 horsepower for continuous operation. At these ratings, the torques are the same as those at the 317 (takeoff) and 270 (continuous) horsepower at 6180 rpm for which the OH-58A is qualified. At 5660 engine rpm, the standard OH-58A tail-rotor drive shafting can transmit 55 horsepower continuously at the same torque level as the OH-58A system; only 30 horsepower is required by the tail rotor at maximum pitch (220 pounds' thrust).

A centrifugal fan driven by the tail-rotor drive shaft cools the engine oil. It has sufficient cooling capacity when operating at the reduced speeds used in the test configurations.

With the engine operating at 5660 rpm, the capacity of the OH-58A transmission-cooling system is more than ample for the primary test configuration. In tests with the helicopter hovering in ground effect at 3000 pounds' gross weight, and with the engine at 6180 rpm and 235 shaft horsepower, the transmission-oil temperature, corrected to a 125°F day, was 214°F--16 degrees below the allowable limit. When the engine speed is reduced to 5660 rpm, airflow and oil flow are reduced proportionally. The result is a 7-degree rise in the oil temperature--to 221°F on a 125°F hot day.

A tail-rotor gearbox with a higher reduction ratio replaces the OH-58A gearbox. Its 90-degree spiral bevel gears have a reduction ratio of 2.89 to 1. It uses the bearings, retainers, and rotor shaft of the OH-58A unit, and the new bevel gears are designed to utilize the OH-58A tooling. The housing is modified to accept the larger gears. The mounting arrangement and support for the tail-rotor controls are unchanged.

3. Powerplant

The conventional OH-58A powerplant installation is modified by the addition of exhaust silencers and baffles, and sound-absorbing coatings on the cowling and firewalls (Figure 52, Appendix). The engine mounting is unchanged. The Allison Model 250-C10D (T63-A-700) engine is operated at 5660 rpm, and it is derated to 290 horsepower for takeoff and 247 horsepower for continuous operation. These ratings keep torque below the engine and main-transmission limit. Allison has approved operation at the reduced speed.[15]

a. Firewall and Cowl Modifications

Two vertical firewalls and the deck isolate the engine compartment from the remainder of the helicopter. The forward firewall is also the aft wall of the engine air plenum. The aft firewall isolates the oil tank, cooler, and blower from the engine. Both are treated with a spray-on acoustical attenuation material such as Lord Manufacturing Company Type 1011.

The forward fairing, which encloses the flight-control servo-actuators, the hydraulic system, and the forward portion of the transmission, is constructed of honeycomb sandwich and an aluminum core and fiberglass facing. No additional soundproofing is used. The inner surface of the air-inlet section and the engine cowl are coated with a spray-on acoustical attenuation material such as Lord Manufacturing Company Type 1011, 1/16 inch thick. External baffles on the engine-cowl ventilation louvers provide a labyrinth for noise attenuation. The aft fairing, which encloses the oil tank, cooler, and blower, is constructed of aluminum honeycomb with fiberglass facing. The interior is treated with acoustical attenuation material.

b. Air Induction

Engine air enters through inlets on each side of the cowling. The inertial dust separator, which is standard equipment on the OH-58, attenuates noise emanating from the compressor.

c. Exhausts

The basic requirement for exhaust silencing was a 15-db reduction in the octave band centered on 250 Hertz. The exhaust

system (Figure 52, Appendix) has two absorptive silencers, one on each exhaust pipe. Each diverted-vane absorption silencer has three modules, with eight vanes in each module. The modules are rotated approximately 15 degrees with respect to each other. Calculations show that the back pressure on the exhaust, approximately 4.5 inches of water, causes a power loss of about 4.5 horsepower. This loss is considered in computing the performance of the helicopter. Additional detailed design and noise tests will be required to determine the optimum configuration.

d. Cooling and Lubrication

The baffles over the engine-compartment cooling-air inlet have forward-and-aft openings to permit convective circulation. The transmission compartment is cooled by forced circulation of the exit air from the transmission-oil cooler. The adequacy of transmission-compartment cooling has been demonstrated in the commercial version (Bell Model 206A) at 5700 engine rpm.

4. Control System

The OH-58A flight-control system is used without modification, except for the crosshead and pitch links for the four-bladed tail rotor. The hydraulic system is powered by a single variable-displacement pump mounted on and driven by the main transmission. The system was examined to determine if it would supply sufficient power at the reduced rpm. At the 6180 engine rpm of the OH-58A, the pump delivers 2.05 gpm at 600 psi. For this test configuration, with its engine speed of 5660 rpm, the maximum capacity of the pump is 1.9 gpm. Since the flow rate on the Bell Model 206A, which uses the same flight-control components, is only 1.75 gpm, the system will provide acceptable control rates for the test aircraft.

5. Airframe

The airframe is identical to that of the OH-58A.

6. Weight and Balance

The weight and the center of gravity were estimated by adjusting weight data for the OH-58A in current production. The effects of these changes on the weight and moments of the helicopter are shown in Table XIV. Except for the exhaust-silencer weight which was furnished by the vendor, the weight changes were estimated from preliminary layout drawings. Table XV compares the group weights of the OH-58A and the primary test configuration. The derivation of the center of gravity is summarized in Table XVI. Nose ballast required to offset the increased tail-rotor weight is 17 pounds.

TABLE XIV. WEIGHT AND MOMENT CHANGES, PRIMARY TEST CONFIGURATION

Group	Change	Weight (lb)	Moment (in.-lb)
Rotor	Taper chord and thickness of outboard 15 pct of span	-	-
	Add inertia weight for reduced rpm	+ 6	+ 642
Tail	Add four-bladed tail rotor	+ 9	+ 3,168
Engine Section	Add spray-on sound-absorption material to cowl	+20	+ 2,640
	Add sound baffles	+ 1	+ 132
Propulsion	Add exhaust silencers	+40	+ 6,200
	Change tail-rotor gearbox to reduce rpm	+ 3	+ 1,056
Electrical	Relocate battery to nose	-	- 3,250
Equipment	Add required nose ballast	+17	+ 272
	Total Change	+96	+10,860

TABLE XV. GROUP WEIGHT STATEMENT, PRIMARY TEST CONFIGURATION

Group	Weight, OH-58A (lb)		Weight, Primary Test Configuration (lb)	
Rotor		280		286
Tail		31		40
Body		326		326
Alighting Gear		34		34
Flight Controls		123		123
Engine Section		35		56
Propulsion		423		466
Engine Installation	136		136	
Air Induction	11		11	
Exhaust	4		44	
Fuel	39		39	
Lubricating	27		27	
Controls	10		10	
Starting	18		18	
Drive	178		181	
Instruments		54		54
Electrical		81		81
Avionics		97		97
Furnishings and Equipment		42		59
Air Conditioning		24		24
Unusable Fuel		6		6
Undrainable Fuel		3		3
Undrainable Oil		1		1
Weight Record Adjustment		23		23
Empty Weight		1583		1679

TABLE XVI. WEIGHT AND BALANCE, PRIMARY TEST CONFIGURATION

	Weight (lb)	Arm (in.)	Moment (in.-lb)
Empty Weight, OH-58A	1583	118.2	187,110
Changes	+ 96		+ 10,860
Empty Weight, Primary Test Configuration	1679	117.9	197,970
Add Crew	+ 170	65.0	+ 11,050
Add Engine Oil	+ 11	180.0	+ 1,980
Gross Weight, Minimum	1860	113.4	211,000
Add Crew to 400 Lb	+ 230	65.0	+ 14,950
Add Mission Equipment	+ 455	107.0	+ 48,685
Add Fuel	+ 455	116.6	+ 53,053
Gross Weight, Maximum	3000	109.2	327,688
CG Limits: Fuselage Stations 105.2 to 114.2			

7. Performance

The performance of the primary test configuration in observation and scout missions is summarized in Table XVII. The comparisons with the OH-58A in this table are based not on equal gross weight and range but on equal payload and fuel. The computer programs used to calculate the performance have been found to give results that agree quite well with OH-58A flight-test data. Payload for the observation mission includes 200 pounds of mission equipment and 111 pounds of removable armor. For the scout mission, an additional 237 pounds of armament is carried. At the observation-mission weight of 2856 pounds, the hovering ceiling is 6900 feet on a standard day and 800 feet at 95°F. Maximum speed is 113 knots.

The tapered planform of the main-rotor blades is accounted for in the calculations of power required. The parasite drag of the OH-58A is increased by 1.0 square foot of equivalent drag area to account for the addition of the exhaust silencers and their supporting structure. For the scout configuration (armed), an additional 1.5 square feet of equivalent drag area is added for the faired weapon installation.

Power available and fuel flow for the T63-A-700 engine at 5660 rpm are calculated using the Allison-supplied engine-performance program. The installation losses employed (Table XVIII) are those of the OH-58A, except for the exhaust-pressure rise, which is increased by 3.3 inches of water to account for the exhaust silencer.

The rotor-thrust coefficients (Table XVII) are for the mission weight and for unaccelerated flight conditions on a sea-level-standard day. Because the main rotor's chord is not constant, an equivalent aerodynamic chord based on thrust must be used in the calculation of t_c.[14] For this configuration, it is 11.24 inches. Since there is a relationship between the thrust coefficient and blade stall, t_c is a measure of g-capability; an increase in t_c indicates a decrease in g-capability.

B. TEST VERSION--ALTERNATE CONFIGURATION

The lower main-rotor tip speed reduces impulsive noise, but it makes necessary an increase in blade chord to maintain thrust capacity. Modified UH-1D thin-tip blades are adapted to the OH-58A hub. The tail-rotor gearbox is the same as that on the primary configuration. The four-bladed tail rotor is also the same except that its diameter is increased from 62 to 69 inches. The engine is the same as that in the production OH-58A, but its speed is reduced from 6180 to 5000 rpm, to reduce the tip speeds of both rotors. To keep the engine operating within its specified torque limits at 5000 rpm, its power is reduced from 317 to 279 horsepower. The maximum

TABLE XVII. PERFORMANCE SUMMARY, PRIMARY TEST CONFIGURATION

		OH-58A		Primary Test Configuration	
		Observation Mission	Scout Mission	Observation Mission	Scout Mission
Gross Weight	lb	2760	2970	2856	3039
Crew	lb	400	400	400	400
Payload	lb	311	548	311	548
Fuel	lb	455	428	455	428
Hovering Ceiling, OGE					
Standard Day	ft	8400	5800	6900	4750
95°F	ft	1700	100	800	-
Maximum Speed, SLS Day					
Military Rated Power	kt	120(V_{ne})	120(V_{ne})	113	108
Normal Rated Power	kt	113	109	107	103
Maximum Rate of Climb, Maximum Power	fpm	1680	1490	1670	1485
Maximum Endurance, SLS Day*	hr	3.49	3.13	3.45	3.18
Speed for Maximum Endurance, SLS Day	kt	50	50	53	54
Range, SLS Day*					
Normal Rated Power	nm	241	224	237	218
Long-Range Cruise	nm	245	226	245	226
Long-Range Cruise Speed, SLS Day	kt	109	109	96	96
Rotor-Thrust Coefficient, SLS Day		0.142	0.153	0.202	0.215

*10-pct fuel reserve, 5-pct increase in specification fuel flow

TABLE XVIII. INSTALLATION LOSSES, PRIMARY TEST CONFIGURATION	
Inlet-Pressure Loss (including particle separator)	4.0 in. of water
Inlet-Temperature Rise	2.5°F
Exhaust-Pressure Rise	4.8 in. of water
Power Extraction (generator)	2.0 hp

transmission torque is 10 percent greater than for the OH-58A, but this increase has been found to be acceptable for a 10-hour test program; no change is required in the main transmission. Loads in the main-rotor hub may limit airspeeds to 105 knots. Loads in the control system will have to be monitored and may result in the mandatory retirement of some Government-furnished components. The changes in the tail-rotor control system are minimal. To maintain clearance between the main and tail rotors, the tail boom is extended; this change necessitates an increase in the length of the tail-rotor drive shaft. Sound-absorbing material is added to engine cowlings and firewalls, and absorptive silencers are installed on the engine exhaust.

1. Rotor System

The modified thin-tip UH-1D main-rotor blade is adapted to fit a standard OH-58A hub (Figure 50, Appendix). The rotor is 35 feet, 4 inches in diameter. The 21-inch-chord blade has 8 degrees of twist. The airfoil is 12-percent thick and symmetrical to 72.6 percent of the radius, and from that point it tapers to a thin tip. The tip planform is double-swept. Inboard from 27.6 percent of the radius, it tapers to match an aluminum-alloy grip adapter that fits the UH-1 blade to the OH-58A hub. Because of this taper, the skin doublers are slightly modified. Thirty pounds of midspan weight is used in the spar for proper placement of the rotor's natural frequencies. Except for the fiberglass tip modification, the bonded blade is all metal. It is made up of a two-piece spar, a trailing-edge extrusion, a moisture-sealed honeycomb core, and an outboard leading-edge abrasion strip.

The rotor's natural frequencies, shown in Figure 34, are satisfactorily placed in relation to its rpm. The structural loads on the blades are less than those on the UH-1 rotor. However, the OH-58A hub was designed for the structural loads imposed on it by a smaller (13-inch-chord) blade, and analysis shows that for comparable flight conditions the 21-inch-chord blade applies

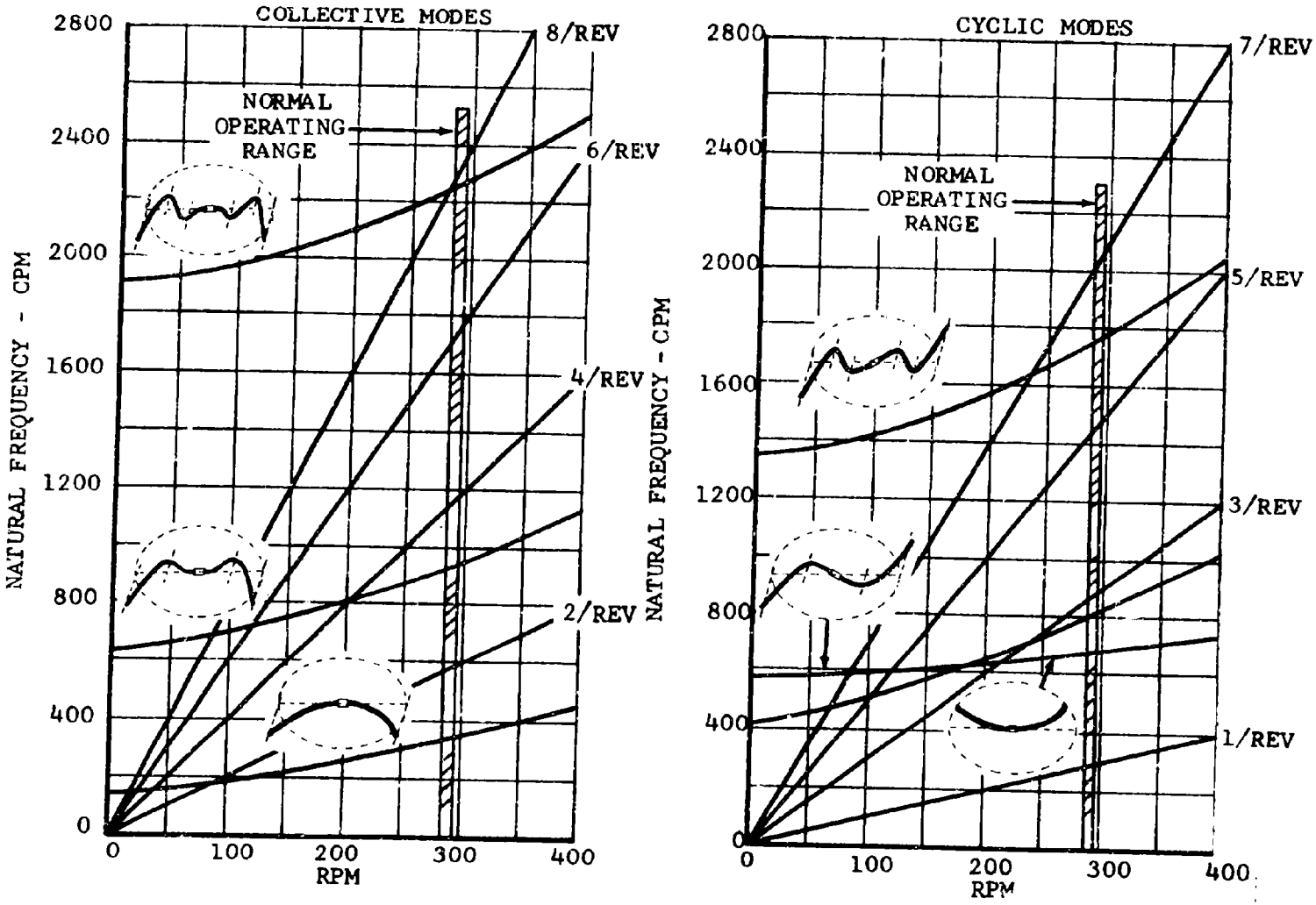

Figure 34. Main-Rotor Natural Frequencies, Alternate Test Configuration

higher loads. The critical piece of structure is the blade grip (Figure 50, Appendix).

Instead of a full spectral fatigue analysis, a "life at high speed" was established for this part. Figure 35 shows this life as a function of aircraft speed. To develop the curve, we assumed the aircraft to be in continuous operation at the specified speed, at 3000 pounds' gross weight. To be conservative for the test program, the high speed was restricted to that which results in slightly more than 500 hours of life. This figure will permit a nominal series of maneuvers which will produce local loads for short periods that will be higher than those of the 1-g high-speed condition. On this criterion, a speed restriction of 105 knots is recommended for the test program with this rotor.

The tail rotor is identical to that on the primary configuration except that its diameter is increased from 62 to 69 inches. Because of this increase, the tail boom is lengthened by 3.5 inches to maintain clearance between the main and tail rotors.

2. Drive System

Except for the mast and the lengthened tail-rotor drive shaft, the drive system of the primary test configuration is used without change. Torque to the main transmission is increased by approximately 10 percent to match the maximum operating power planned for the test program. The transmission has been bench-tested at this higher torque level for approximately 30 hours at an engine power rating of 350 horsepower and an engine speed of 6180 rpm. This power and this speed produce a torque equivalent to that at 287 horsepower at 5000 engine rpm. For this configuration, the drive system is rated to the engine limits--279 horsepower for takeoff and 237 horsepower for continuous operation--at 5000 rpm.

A main-rotor mast with an ultimate tensile strength in the high end of the allowable heat-treat range (180-200 ksi) will be selected. It will have a 5-percent margin of safety at 190 ksi under the ultimate design conditions.

The tail-rotor drive shafting is limited to the same torque rating as that qualified for the OH-58A. At the engine speed of 5000 rpm, the drive system can transmit 48 horsepower continuously. At the tail rotor's maximum pitch it can develop 220 pounds of thrust, for a requirement of 30 horsepower. Thus, the OH-58A drive shafting has an ample power margin.

The OH-58A transmission-cooling tests (VI.A.2) indicate that the transmission-oil temperature will not exceed the OH-58A limits

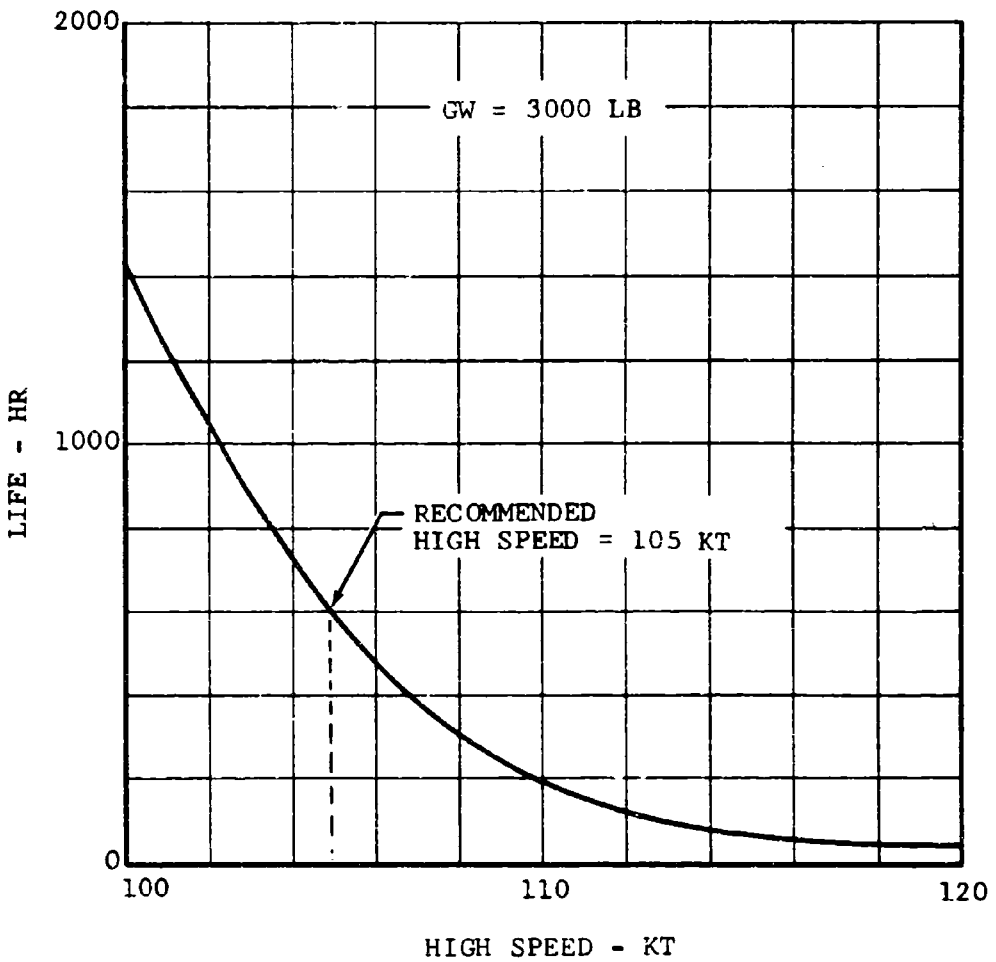

Figure 35. Fatigue Life of Blade Grip, Alternate Test Configuration.

when the alternate test vehicle operates at 3000 pounds' gross weight at sea level and a temperature of 125°F. The temperature will rise 16°F above that in the OH-58A, resulting in an oil temperature of 230°F--the maximum allowable operating temperature.

3. Powerplant

The powerplant installation is the same as that of the primary test configuration. Power-turbine speed is reduced to 5000 rpm to allow the main rotor to operate at a tip speed of 530 fps. Maximum power is 279 horsepower for 5 minutes and 237 horsepower continuous; it is within the thermodynamic capability of the engine, and within the maximum and continuous torque limits at 5000 rpm. Allison has approved operation at the reduced speed. The power-turbine governor may easily be readjusted to maintain the reduced speed setting.

4. Control System

The control system is identical to that of the primary test configuration except that the operating hydraulic pressure is higher and the tail-rotor controls are lengthened because of the extension of the tail boom. The control loads estimated for the wider-chord main rotor are nearly twice those on the OH-58A. To accommodate these loads, the hydraulic pressure is increased from 600 to 1200 psi. The increased loads will reduce the life of the components between the hydraulic servo-actuators and the rotor-pitch controls, but the life margins will be adequate for the flight-test program. These components would have to be retired, however, after the test program.

At the 5000-rpm engine speed, the OH-58A hydraulic pump will have a flow rate of 1.66 gpm. This rate is 95 percent of the 1.75-gpm rate that has been found to be acceptable for identical servo-actuators on the Bell Model 206A. This rate will suffice for the test program.

5. Airframe

The airframe for the alternate test configuration is identical to that of the OH-58A except that the tail boom is lengthened by 3.5 inches in order to maintain the clearance between the main rotor and the enlarged tail rotor. The length is increased by splicing in a section at the aft end of the boom.

6. Weight and Balance

Weight and balance were estimated from OH-58A data with allowances for the design changes shown in Table XIX. The weight of the new main-rotor blades was estimated from the

weight of the outboard portion of the UH-1D blade. A double-swept-tip blade has been built and flown; the actual weight was used. The weight of the hub adapters was estimated from layout drawings. Table XX summarizes the derivation of empty and gross weights, and the balance calculation. Ballast required to offset the increased tail-rotor weight is 15 pounds.

TABLE XIX. WEIGHT AND MOMENT CHANGES, ALTERNATE TEST CONFIGURATION

Group	Change	Weight (lb)	Moment (in.-lb)
Rotor	Substitute 21-in.-chord blades with hub adapters	+137	+14,659
Tail	Substitute 69-in. four-bladed rotor	+ 11	+ 3,872
Body	Extend tail boom 3.5 in.	+ 1	+ 338
Engine Section	Add spray-on sound-absorption material to cowl	+ 20	+ 2,640
	Add sound baffles	+ 1	+ 132
Propulsion	Add exhaust silencers	+ 40	+ 6,200
	Change tail-rotor gearbox and lengthen drive shaft	+ 3	+ 1,056
Electrical	Relocate battery to nose	-	- 3,250
Furnishings and Equipment	Add required nose ballast	+ 15	+ 240
Miscellaneous	Relocate tail rotor, gearbox, cover, and fin 3 in. aft	-	- 135
	Total Change	+228	+ 26,022

TABLE XX. WEIGHT AND BALANCE, ALTERNATE TEST CONFIGURATION			
	Weight (lb)	Arm (in.)	Moment (in.-lb)
Empty Weight, OH-58A	1583	118.2	187,110
Changes	+ 228		+ 26,022
Empty Weight, Alternate Test Configuration	1811	117.7	213,132
Add Crew	+ 170	65.0	+ 11,050
Add Engine Oil	+ 11	180.0	+ 1,980
Gross Weight, Minimum	1992	113.5	226,162
Add Crew to 400 Lb	+ 230	65.0	+ 14,950
Add Mission Equipment	+ 323	107.0	+ 34,561
Add Fuel	+ 455	116.6	+ 53,053
Gross Weight, Maximum	3000	109.6	328,726
CG Limits: Fuselage Stations 105.2 to 114.2			

7. Performance

The performance of the alternate test helicopter in observation and scout missions is summarized in Table XXI. The comparisons with the OH-58A are based not on equal gross weight and range but on equal payload and fuel. The methods used in computing these data have given results that correlate well with measured data on the OH-58A and the Model 206A. Payload for the observation mission includes 200 pounds of mission equipment and 111 pounds of removable armor. For the scout mission, an additional 237 pounds of armament is carried. At the observation-mission weight of 2987 pounds, the hovering ceiling is 5300 feet on a standard day. Speed is V_{ne}-limited to 105 knots.

The effects of the double-swept-tip planform of the main-rotor blades are accounted for in the calculations of power required. The parasite drag of the OH-58A is increased by 1.0 square foot of equivalent drag area to account for the addition of the exhaust silencers and their supporting structure. For the scout configuration (armed), an additional 1.5 square feet of equivalent drag area is added for the faired weapon installation.

Power available and fuel flow for the T63-A-700 engine at 5000 rpm are computed using the Allison-supplied engine-performance program. The installation losses employed (Table XXII) are those of the OH-58A, except for the exhaust-pressure rise, which is increased by 3.3 inches of water to account for the exhaust silencer.

TABLE XXI. PERFORMANCE SUMMARY, ALTERNATE TEST CONFIGURATION

		Observation Mission	Scout Mission
Gross Weight	lb	2989	3170
Crew	lb	400	400
Payload	lb	311	548
Fuel	lb	455	428
Hovering Ceiling, OGE			
Standard Day	ft	5300	3400
95°F	ft	-	-
Maximum Speed, SLS			
Military Rated Power	kt	105(V_{ne})	105(V_{ne})
Normal Rated Power	kt	105	101
Maximum Rate of Climb, Maximum Power	fpm	1330	1095
Maximum Endurance, SLS Day*	hr	3.55	3.30
Speed for Maximum Endurance, SLS Day	kt	50	52
Range, SLS*			
Normal Rated Power	nm	223	207
Long-Range Cruise	nm	235	218
Long-Range Cruise Speed, SLS Day	kt	95	97
Rotor-Thrust Coefficient, SLS Day		0.163	0.172

* 10-pct fuel reserve, 5-pct increase in specification fuel flow

TABLE XXII. INSTALLATION LOSSES, ALTERNATE TEST CONFIGURATION	
Inlet-Pressure Loss (including particle separator)	4.0 in. of water
Inlet-Temperature Rise	2.5°F
Exhaust-Pressure Rise	4.8 in. of water
Power Extraction (generator)	2.0 hp

The rotor-thrust coefficients t_c (Table XXI) are for the mission weight and for unaccelerated flight conditions on a sea-level-standard day. Because the main rotor's chord is not constant, an equivalent aerodynamic chord based on thrust must be used in calculating t_c.[15] For this configuration, it is 18.75 inches. Since thrust coefficient and blade stall are related, t_c is a measure of g-capability: an increase in t_c indicates a decrease in g-capability.

C. OPERATIONAL VERSION--PRIMARY CONFIGURATION

The operational versions are designed to have performance, payload, and maneuverability comparable to those of the OH-58A, with noise levels comparable to those of the corresponding test versions. Design gross weight is increased to accommodate the payload and fuel required for the LOH scout mission. To get the performance of the OH-58A in the modified aircraft while minimizing changes in the airframe, transmission, and drive system, a larger engine is used, rather than an increased-diameter main rotor.

The tip speeds of both the main and tail rotors of the primary operational configuration are the same as those of the primary test configuration, but the blade chords are increased to regain the rotor lift capability that is lost by reducing the tip speeds. Changes in the gear ratio and the output-torque capability of the main transmission are required, and the tail-rotor gearbox is new. Only minor changes in the powerplant installation and the airframe are necessary, although ballast is required to maintain the center-of-gravity range. Sound-absorbing material is added to engine cowlings and firewalls, and silencers are installed on the engine exhaust.

1. Rotor System

a. Main Rotor

The two blades of the 35.33-foot-diameter main rotor have a 20.65-inch chord to 85 percent of the radius and a linear taper

to a 6.88-inch chord at the tip. The rotor is designed to operate at a tip speed of 600 feet per second. The construction of the blade is similar to that of the 21-inch-chord UH-1 blade (VI.B.1). Its mass and stiffness distributions are so arranged as to obviate excessive hub and control loads. Inertia weights are used to tune the rotor, but the weight is less than in the alternate test configuration.

Because of its lower rotational speed at the same input power, this rotor's static torque input is approximately 9 percent greater than that of the OH-58A. As a result, the in-flight oscillatory loads on the hub and the mast are increased, and some local strengthening is required. Although the rotor is capable of a thrust of 7700 pounds--an increase of 3 percent over that to which the OH-58A was designed--the effects of this increase are minor and local.

b. Tail Rotor

The tail rotor is identical to that on the primary test configuration (VI.A.1.b) except that the chord is increased from 5.27 to 6.21 inches.

2. Drive System

The drive system is rated at 317 horsepower for takeoff and 270 horsepower for continuous operation at an engine speed of 6000 rpm. Its general configuration is identical to that of the OH-58A, and it uses many of the same parts, but the main transmission is redesigned, the tail-rotor gearbox and the mast are new, and the drive shafting is modified.

a. Main Transmission, Drive Shaft, and Mast

The redesigned main transmission has a reduction ratio of 18.5 to 1 (6000 to 324 rpm) in two stages. The spiral-bevel first stage has a 3.96-to-1 ratio; the planetary second stage is a standard OH-58A unit with a ratio of 4.667 to 1. The altered dimensions of the higher-ratio bevel gears make it necessary to use a new housing and a different arrangement of the bevel-gear support bearings. Because of this change, the main drive shaft and the rotor mast must be shortened by 1/2 inch. The mast must also be strengthened by increasing the thickness of its wall, to accommodate the 9-percent increase in torque.

b. Tail-Rotor Drive System

The tail-rotor drive system is similar to that of the OH-58A, but the gearbox is new, and design power is increased to 80 horsepower at 6000 engine rpm because of the higher power available at altitude and the increased main-rotor torque. The reduction ratio of the new gearbox is increased to 3.06 to 1.

This change alters the dimensions and thus necessitates a different mounting attachment to the tail boom. Since the output torque of this gearbox is 82 percent higher than that of the OH-58A, the tail-rotor shaft is also redesigned for the increased torque.

3. Powerplant

The powerplant installation is essentially the same as that of the test versions, but it will incorporate any refinements that the tests show to be necessary. The envelope of the 400-horsepower Allison Model 250-C20 engine is almost identical to that of the T63-A-700. The necessary changes--such as increasing the size of the oil cooler and blower to accommodate increased heat rejection--are minor. The engine is derated to 317 horsepower for takeoff and 270 horsepower for continuous operation, and it operates at 6000 rpm.

4. Control System

The flight-control system is functionally identical to that of the OH-58A. The hydraulic system and the control linkages between the servo-actuators and the main rotor are modified to accommodate the new, wide-chord blades. The operating pressure of the hydraulic system is increased to accommodate the increased control loads estimated for the new main rotor.

5. Airframe

Minor changes in the OH-58A airframe accommodate the increase in the gross weight (from 3000 to 3220 pounds) and the thrust capability of the main and tail rotors: The gauges of the landing-gear crosstubes and the monocoque tail-boom skins are increased. Symmetrical structural flight loads are limited by the main rotor's thrust capability, which is approximately 3 percent more than that of the OH-58A. The effect is negligible; it does not affect the airframe.

6. Weight and Balance

Weight and balance of the operational versions of the quiet helicopter are derived from current data on the production Model OH-58A. Changes in the weight and center of gravity of the primary operational configuration are summarized in Table XXIII and in the group weight statement in Table XXIV. All the changes except those for the main rotor and the silencer are estimated from OH-58A parts. The silencer weight was supplied by the vendor. Nose ballast required to offset the increased weight of the tail rotor is 45 pounds.

TABLE XXIII. WEIGHT AND MOMENT CHANGES, PRIMARY OPERATIONAL CONFIGURATION

Group	Change	Weight (lb)	Moment (in.-lb)
Rotor	Substitute 20.65-in.-chord main rotor	+ 79	+8,453
Tail	Substitute four-bladed, 62-in.-diameter tail rotor	+ 9	+3,520
	Increase fin area for increased main-rotor torque	+ 2	+ 712
Body	Increase tail-boom skin gauge from 0.040 to 0.050 for increased tail-rotor thrust	+ 5	+1,365
Alighting Gear	Add strength to accommodate increased gross weight	+ 5	+ 500
Flight Controls	Increase strength of rotating controls to accommodate increased gross weight	+ 2	+ 218
	Modify boost cylinders and supports to accommodate increased control loads	+ 1	+ 82
Engine Section	Add spray-on sound-absorption material to cowl	+ 20	+2,640
	Add sound baffles	+ 1	+ 132
Propulsion	Change to 400-hp Allison 250-C20 engine	+ 20	+2,840
	Add exhaust silencers	+ 40	+6,200
	Increase engine-oil-cooler size	+ 2	+ 344
	Modify drive train to reduce rotor rpm and to accommodate increased torque:		
	Main transmission	+ 8	+ 904
	Rotor mast	+ 2	+ 216
	Tail-rotor drive shaft	+ 2	+ 456
	Tail-rotor gearbox	+ 5	+1,760
Electrical	Relocate battery to nose	-	-3,250
Furnishings and Equipment	Add required nose ballast	+ 45	720
	Total Change	248	27,812

TABLE XXIV. GROUP WEIGHT STATEMENT, PRIMARY OPERATIONAL CONFIGURATION

Group	Weight (lb)	
Rotor		359
Tail		42
Body		331
Alighting Gear		39
Flight Controls		126
Engine Section		56
Propulsion		502
Engine Installation	156	
Air Induction	11	
Exhaust	44	
Fuel	39	
Lubricating	29	
Controls	10	
Starting	18	
Drive	195	
Instruments		54
Electrical		81
Avionics		97
Furnishings and Equipment		87
Air Conditioning		24
Unusable Fuel		6
Undrainable Fuel		3
Undrainable Oil		1
Weight Record Adjustment		23
Empty Weight		1831

The weight of the main-rotor assembly was derived by two methods. The weight W_{MR} shown in the statement is derived by the first method, using the general equation:

$$W_{MR} = K_T K_M \left(\frac{W N_F}{1000} \right)^{0.43} R^{0.83} c^{0.69} N_B^{0.58} \qquad (25)$$

where K_T, the rotor constant, = 6.94 for a teetering rotor

K_M, the hub-material constant, = 1.0 for steel

W, the design gross weight in pounds, = 3200

N_F, the limit flight-load factor, = 2.5

R, the radius in feet, = 17.67

c, the chord in feet, = 1.471

N_B, the number of blades, = 2

Because of the tapered planform of the blades, an equivalent aerodynamic chord of 17.65 inches, rather than the 20.65-inch maximum chord, was used. In the second method, separate expressions are used for the basic blade structure, inertia and vibration-control weights, and the structure of the hub and the grip. The weights calculated by this method verify those found by using the general equation.

Mission gross weights and centers of gravity are presented in Table XXV.

7. Performance

The performance of the primary operational configuration in observation and scout missions is summarized in Table XXVI. Payload for the observation mission includes 200 pounds of mission equipment and 111 pounds of removable armor. For the scout mission, an additional 237 pounds of armament is carried. The comparisons with the OH-58A are based not on equal gross weight and range but on equal payload and fuel. At the observation-mission weight of 3008 pounds, the hovering ceiling is 12,600 feet on a standard day and 4700 feet at 95°F. Maximum speed is 123 knots.

The effects of the tapered planform of the main-rotor blades are accounted for in the calculations of power required. The parasite drag of the OH-58A is increased by 1.0 square foot of equivalent drag area to account for the addition of the exhaust silencers and their supporting structure. For the scout

TABLE XXV. WEIGHT AND BALANCE, PRIMARY OPERATIONAL CONFIGURATION

	Weight (lb)	Arm (in.)	Moment (in.-lb)
Empty Weight, OH-58A	1583	118.2	187,110
Changes	+ 248		+ 27,812
Empty Weight, Primary Operational Configuration	+1831	117.4	214,922
Add Crew	+ 400	65.0	+ 26,000
Add Mission Equipment	+ 200	107.0	+ 21,400
Add Removable Armor	+ 111	75.7	+ 8,403
Add Engine Oil	+ 11	180.0	+ 1,980
Add Fuel	+ 455	116.6	+ 53,053
Gross Weight, Observation Mission	3008	108.3	325,758
Add Armament	+ 237	107.2	+ 25,413
Remove Fuel to 428 Lb	- 27	124.5	- 3,362
Gross Weight, Scout Mission	3218	108.1	347,809
CG Limits: Fuselage Stations 105.2 to 114.2			

TABLE XVI. PERFORMANCE SUMMARY, PRIMARY OPERATIONAL CONFIGURATION

		Observation Mission	Scout Mission
Gross Weight	lb	3008	3218
Crew	lb	400	400
Payload	lb	311	548
Fuel	lb	455	438
Hovering Ceiling, OGE			
Standard Day	ft	12,600	10,450
95°F	ft	4700	3100
Maximum Speed, SLS Day			
Military Rated Power	kt	123	119
Normal Rated Power	kt	115	111
Maximum Rate of Climb, Maximum Power	fpm	1775	1560
Maximum Endurance, SLS Day*	hr	3.4	3.1
Speed for Maximum Endurance	kt	50	51
Range, SLS Day*			
Normal Rated Power	nm	227	212
Long-Range Cruise	nm	241	223
Cruise Speed, SLS Day	kt	102	102
Rotor-Thrust Coefficient, SLS Day	-	0.136	0.145

* 10-pct fuel reserve, 5-pct increase in specification fuel flow

configuration (armed), an additional 1.5 square feet of equivalent drag area is added for the faired weapon installation.

Power available and fuel flow for the 250-C20 engine are based on data for the T63-A-700 engine, computed with the Allison-supplied engine-performance program. The power of the T63-A-700 at 6000 rpm is increased by the ratio of the military rated power of the 250-C20 to that of the T63-A-700. At the same power, fuel flow is the same for both engines. The installation losses employed (Table XXVII) are those of the OH-58A, except for the exhaust-pressure rise which is increased by 3.3 inches of water to account for the exhaust silencer.

The rotor-thrust coefficients t_c (Table XXVI) are for the mission weight and for unaccelerated flight conditions, on a sea-level-standard day. Because the main rotor's chord is not constant, an equivalent aerodynamic chord based on thrust must be used in calculating t_c.[15] For this configuration, it is 17.65 inches. Since thrust coefficient and blade stall are related, t_c is a measure of g-capability.

TABLE XVII. INSTALLATION LOSSES, PRIMARY OPERATIONAL CONFIGURATION

Inlet-Pressure Loss (including particle separator)	4.0 in. of water
Inlet-Temperature Rise	2.5°F
Exhaust-Pressure Rise	4.8 in. of water
Power Extraction (generator)	2.0 hp

D. OPERATIONAL VERSION--ALTERNATE CONFIGURATION

The lower main-rotor tip speed reduces impulsive noise, but it makes an increase in blade chord necessary to maintain thrust capacity. The engine is also larger than that in the test configuration, and the transmission and drive system are extensively redesigned. The length of the tail boom is increased to provide clearance between the main rotor and the increased-diameter tail rotor, and the gauges of the tail-boom skins are increased to withstand the higher tail-rotor thrust. Some local strengthening of the airframe is required, and ballast is used to keep the center of gravity within the allowable range. A number of control-system changes are also required. Sound-absorbing material is added to cowlings, and silencers are installed on the engine exhaust.

1. Rotor System

The two-bladed main rotor is designed to operate at a tip speed of 530 feet per second. Its blades have a 30.95-inch chord and double-swept tips. They are of aluminum alloy, with stainless-steel abrasion strips on the leading edges and with double-swept molded-fiberglass tips. A lightweight spar forms the forward 25 percent of each blade. The portion aft of the spar is a full-depth honeycomb-sandwich structure that terminates on a trailing-edge strip. Bonded doublers reinforce the area where the blade is attached to the grip. Inertia weights at the midspan and the tip are used for proper placement of the rotor's natural frequencies. In its general configuration, the hub is similar to that of the OH-58A, but the size, strength, and stiffness of the hub and the mast are increased to accommodate the longer-chord blade.

The four-bladed tail rotor is 69 inches in diameter. The blades have double-swept tips, and a chord of 6.33 inches. The tip speed is 530 feet per second.

2. Drive System

The system is rated at 317 horsepower for takeoff and 270 horsepower for continuous operation at an engine speed of 6000 rpm. Although it is similar in arrangement to that of the primary configuration (VI.C.2), almost all its components are new. The new mast and the tail-rotor drive shafting have greater torque capacities, the reduction ratios of the main transmission and the tail-rotor gearbox are higher, and the main drive shaft is shortened to accommodate the new reduction units. The new main transmission has a 20.9-to-1 reduction ratio, which increases the torque to the main rotor over that of the OH-58A at the same engine power. This increase in torque necessitates the use of a new, larger-diameter mast.

The all-new tail-rotor drive system is also similar in arrangement to that of the OH-58A, but it is designed to transmit 87 horsepower continuously at 6000 engine rpm. The gearbox has a 3.41-to-1 reduction ratio--49 percent higher than that of the OH-58A.

3. Powerplant

The powerplant, an Allison 250-C20 engine derated to 317 horsepower, is the same as that in the primary operational version (VI.C.3).

4. Control System

The control system is similar to that of the primary operational configuration (VI.C.4). However, the servo-actuators and

controls between the actuators and the main rotor are new, principally because of the larger-diameter mast and the higher control loads induced by the wide-chord rotor blades.

5. Airframe

The OH-58A airframe is strengthened in this configuration to accommodate the higher gross weight and the greater thrust capability of the main and tail rotors. The gross weights and maximum thrusts of the two aircraft are compared in Table XXVIII. The 20-percent increase in main-rotor thrust makes it necessary to strengthen the pylon-support structure and the box beam that forms the overhead structure of the cabin. Because of the increased gross weight, the crosstubes of the skid gear are strengthened, and the tail boom is strengthened to accommodate the greater thrust of the tail rotor. All these changes are accomplished by increasing the gauges of sheet metal or the thicknesses of machined parts.

The only other significant airframe change results from the increase of tail-rotor diameter from 62 to 69 inches. To maintain the clearance between the main and tail rotors, the length of the tail boom is increased by 3.5 inches.

Since most of these changes add weight aft of the center of gravity, 70 pounds of nose ballast and supporting structure is required. The basic structure of the fuselage needs no strengthening for this weight; only local structural carry-through is added.

TABLE XXVIII. GROSS WEIGHT AND ROTOR THRUST, OH-58A AND ALTERNATE OPERATIONAL CONFIGURATION

		OH-58A	Alternate Operational Configuration
Gross Weight	lb	3000	3400
Maximum Main-Rotor Thrust	lb	7500	9000
Maximum Tail-Rotor Thrust	lb	350	535

6. Weight and Balance

Weight and balance data for the alternate operational configuration are derived from current data on the production Model OH-58A. Changes in the weight and center of gravity are summarized in Table XXIX, the group weight statement in Table XXX, and weight and balance calculations in Table XXXI.

TABLE XXIX. WEIGHT AND MOMENT CHANGES, ALTERNATE OPERATIONAL CONFIGURATION

Group	Change	Weight (lb)	Moment (in.-lb)
Rotor	Substitute 30.95-in.-chord main-rotor assembly	+204	+21,828
Tail	Substitute four-bladed, 69-in.-diameter tail rotor	+ 11	+ 4,224
	Increase fin area for increased main-rotor torque	+ 3	+ 1,068
Body	Increase tail-boom skin gauge from 0.040 to 0.063 for increased tail-rotor thrust	+ 10	+ 2,730
	Extend tail boom 3 in.	+ 1	+ 338
Alighting Gear	Add strength to accommodate increased gross weight	+ 5	+ 500
Flight Controls	Increase strength of rotating controls to accommodate increased gross weight	+ 5	+ 545
	Modify boost cylinders and supports to accommodate increased control loads	+ 4	+ 328
Engine Section	Add spray-on sound-absorption material to cowl	+ 20	+ 2,640
	Add sound baffles	+ 1	+ 132
Propulsion	Change to 400-hp Allison 250-C20 engine	+ 20	+ 2,840
	Add exhaust silencers	+ 40	+ 6,200
	Increase engine-oil-cooler size to accommodate larger engine	+ 2	+ 344
	Modify drive train for reduced rotor speed and increased torque:		
	Main transmission	+ 20	+ 2,260
	Rotor mast	+ 5	+ 540
	Tail-rotor drive shaft	+ 3	+ 684
	Tail-rotor gearbox	+ 6	+ 2,112

TABLE XXIX - Continued			
Group	Change	Weight (lb)	Moment (in.-lb)
Electrical	Relocate battery to nose	-	- 3,250
Furnishings and Equipment	Add required nose ballast	+ 70	+ 1,120
Miscellaneous	Relocate tail rotor, gearbox, cover and fin 3 in. aft for increased-diameter tail rotor	-	+ 135
	Total Changes	+430	+47,183

TABLE XXX. GROUP WEIGHT STATEMENT, ALTERNATE OPERATIONAL CONFIGURATION		
Group	Weight (lb)	
Rotor		484
Tail		45
Body		337
Alighting Gear		39
Flight Controls		132
Engine Section		56
Propulsion		519
Engine Installation	156	
Air Induction	11	
Exhaust	44	
Fuel	39	
Lubricating	29	
Controls	10	
Starting	18	
Drive	212	
Instruments		54
Electrical		81
Avionics		97
Furnishings and Equipment		112
Air Conditioning		24
Unusable Fuel		6
Undrainable Fuel		3
Undrainable Oil		1
Weight Record Adjustment		23
Empty Weight		2013

TABLE XXXI. WEIGHT AND BALANCE, ALTERNATE OPERATIONAL CONFIGURATION			
	Weight (lb)	Arm (in.)	Moment (in.-lb)
Empty Weight, OH-58A	1583	118.2	187,110
Changes	+ 430		+ 47,183
Empty Weight, Alternate Operational Version	2013	116.4	234,293
Add Crew	+ 400	65.0	+ 26,000
Add Mission Equipment	+ 200	107.0	+ 21,400
Add Removable Armor	+ 111	75.7	+ 8,403
Add Engine Oil	+ 11	180.0	+ 1,980
Add Fuel	+ 455	116.6	+ 53,053
Gross Weight, Observation Mission	3190	108.2	345,129
Add Armament	+ 237		+ 25,413
Remove Fuel to 428 Lb	- 27		- 3,362
Gross Weight, Scout Mission	3400	108.0	367,180
CG Limits: Fuselage Stations 105.2 to 114.2			

7. Performance

The performance of the alternate operational configuration in observation and scout missions is summarized in Table XXXII. Payload for the observation mission includes 200 pounds of mission equipment and 111 pounds of removable armor. For the scout mission, an additional 237 pounds of armament is carried. The comparisons with the OH-5A are not based on gross weight and range but on equal payload and fuel. At the observation-mission weight of 3187 pounds the hovering ceiling is 11,100 feet on a standard day and 3900 feet at 95°F. Maximum speed is 116 knots.

The effect of the double-swept-tip planform of the main-rotor blades is accounted for in the calculation of power required. The parasite drag of the OH-58A is increased by 1.0 square foot of equivalent drag area to account for the addition of the

exhaust silencers and their supporting structure. For the scout configuration (armed), an additional 1.5 square feet of equivalent drag area is added for the fair d weapon installation.

Power available and fuel flow for the T63-A-700 engine at 5000 rpm are computed using the Allison-supplied engine-performance program. The installation losses employed (Table XXXIII) are those of the OH-58A, except for the exhaust-pressure rise, which is increased by 3.3 inches of water to account for the exhaust silencer.

TABLE XXXII. PERFORMANCE SUMMARY, ALTERNATE OPERATIONAL CONFIGURATION

		Observation Mission	Scout Mission
Gross Weight	lb	3190	3400
Crew	lb	400	400
Payload	lb	311	548
Fuel	lb	455	428
Hovering Ceiling, OGE			
Standard Day	ft	11,100	9000
95 F	ft	3900	2400
Maximum Speed, SLS			
Military Rated Power	kt	116	111
Normal Rated Power	kt	109	104
Maximum Rate of Climb, Maximum Power	ft/min	1500	1300
Maximum Endurance, SLS Day*	hr	3.22	2.96
Speed for Maximum Endurance, SLS Day	kt	51	52
Range, SLS Day*			
Normal Rated Power	nm	217	203
Long-Range Cruise	nm	227	210
Cruise Speed, SLS Day	kt	100	100
Rotor-Thrust Coefficient, SLS Day		0.126	0.134

* 10-pct fuel reserve, 5-pct increase in specification fuel flow

TABLE XXXIII. INSTALLATION LOSSES, ALTERNATE OPERATIONAL CONFIGURATION	
Inlet-Pressure Loss (including particle separator)	4.0 in. of water
Inlet-Temperature Rise	2.5°F
Exhaust-Pressure Rise	4.8 in. of water
Power Extraction (generator)	2.0 hp

The rotor-thrust coefficients t_c (Table XXXII) are for the mission weight and for unaccelerated flight conditions, on a sea-level-standard day. Because the main rotor's chord is not constant, an equivalent aerodynamic chord based on thrust must be used in calculating t_c.[15] For this configuration, it is 25.9 inches. Since thrust coefficient and blade stall are related, t_c is a measure of g-capability.

VII. COMPARISONS WITH OH-58A

The quiet-helicopter configurations are compared with the OH-58A in terms of their performance and their noise to show the effects of applying quieting features to the OH-58A. The performance of the test configurations is compared with that of the OH-58A in the LOH observation mission. The gross weights at which the operational configuration can carry the fuel and payload for the LOH observation and scout missions are the basis for comparing their performance. The noise levels of all configurations vary considerably with flight condition, aspect, and distance. Performance curves and tabulated noise data for assessing the effects of quieting features in other missions are also presented.

A. PERFORMANCE

1. Test Configurations

Table XXXIV summarizes the performance comparisons of the test configurations. Mission performance and the ratios of empty weight and useful load to gross weight are shown for three conditions: with payload and range the same as those of the OH-58A, with the hover ceiling and payload the same as those of the OH-58A, and with maneuvering capability the same as that of the OH-58A. With the same payload and range, the OH-58A can hover OGE on a 95°F day at 1700 feet, the primary test configuration at 800 feet, and the alternate test configuration not at all. Keeping the hover ceilings and payloads constant reduces the range of the primary test configuration by 54 nautical miles, and that of the alternate configuration by 125 nautical miles. When maneuver capability (as evidenced in the thrust coefficient) is held constant, the useful load of the primary test configuration is reduced from 1177 to 331 pounds.

Figure 36 shows that at a given gross weight, the hover ceilings of the test configurations are within 200 feet of that of the OH-58A. The maximum continuous speed of the primary configuration (Figure 37) is 3 to 5 knots lower than that of the OH-58A; its available power is less because of the reduction in engine speed. The alternate configuration is limited to 105 knots, but at gross weights above 2800 pounds, the limit is determined by maximum continuous power. Its maximum speed is 7 to 11 knots less than that of the OH-58A.

The specific range (Figure 38) of the primary configuration is as much as 14 percent greater than that of the OH-58A at minimum-power speed, and 2 to 3 percent greater at long-range cruise speed. At maximum continuous speed, however, it is about 5 percent less. The alternate configuration compares

TABLE XXXIV. PERFORMANCE COMPARISONS, TEST CONFIGURATIONS, OBSERVATION MISSION*

		OH-58A	Primary			Alternate		
			I**	II**	III**	I**	II**	III**
Gross Weight	lb	2760	2856	2750	2010	3007	2760	2610
Empty Weight	lb	1583	1679	1679	1679	1811	1811	1811
Useful Load								
Engine Oil	lb	11	11	11	11	11	11	11
Fuel	lb	455	455	349	120	474***	227	77
Crew	lb	400	400	400	200	400	400	400
Payload	lb	311	311	311	0	311	311	311
Empty Weight/Gross Weight	-	0.574	0.588	0.611	0.836	0.602	0.656	0.694
Useful Load/Gross Weight	-	0.426	0.412	0.389	0.164	0.398	0.344	0.306
Hover Ceiling, OGE, 95°F Day	ft	1700	800	1700	8600	-	1700	3100
Range At Long-Range-Cruise Speed	nm	245	245	191	71	245	120	41
Maximum-Continuous Speed	kt	113	107	108	113	104	105(V_{ne})	105(V_{ne})
Maximum Endurance	hr	3.49	3.45	2.65	0.94	3.70	1.33	0.46
Rotor-Thrust Coefficient (t_c)	-	0.142	0.202	0.195	0.142	0.164	0.150	0.142
Maneuver Capability at Maximum-Continuous Speed	g	2.03	1.40	1.45	1.93	1.63	1.76	1.86

*With particle separator
**I: OH-58A range and payload; II: OH-58A hover ceiling; III: OH-58A rotor-thrust coefficient
***Exceeds OH-58A capacity

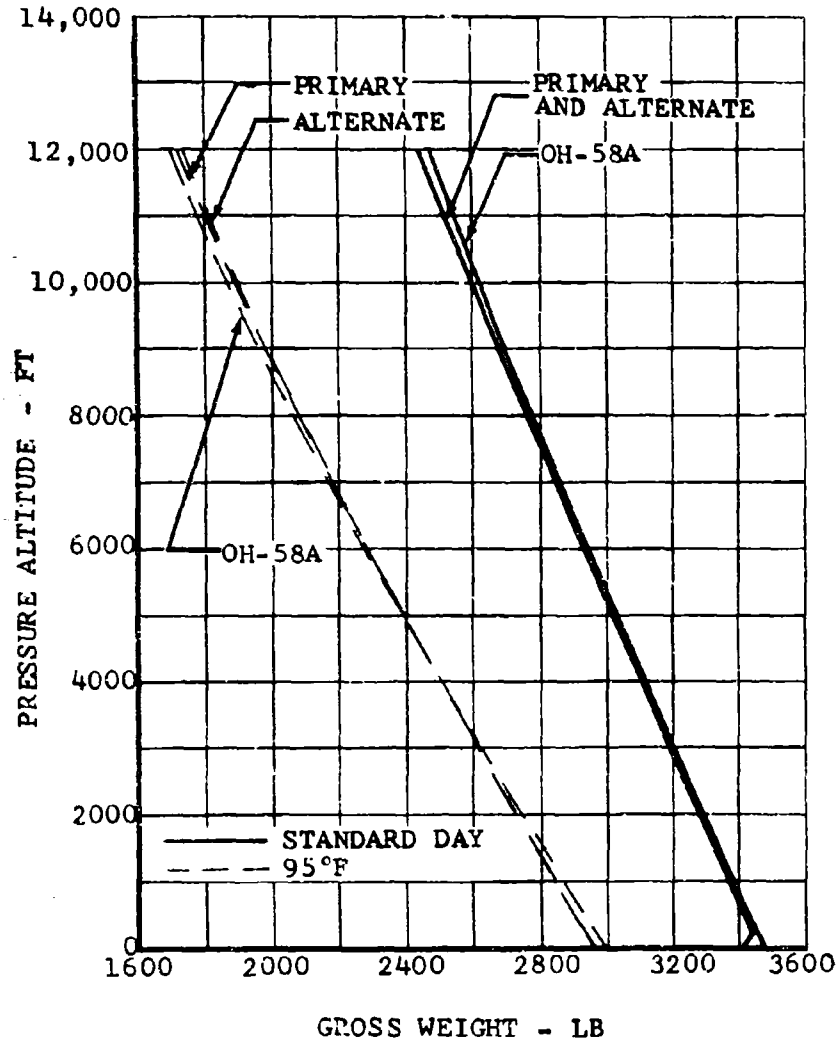

Figure 36. Hovering Ceilings, Test Configurations.

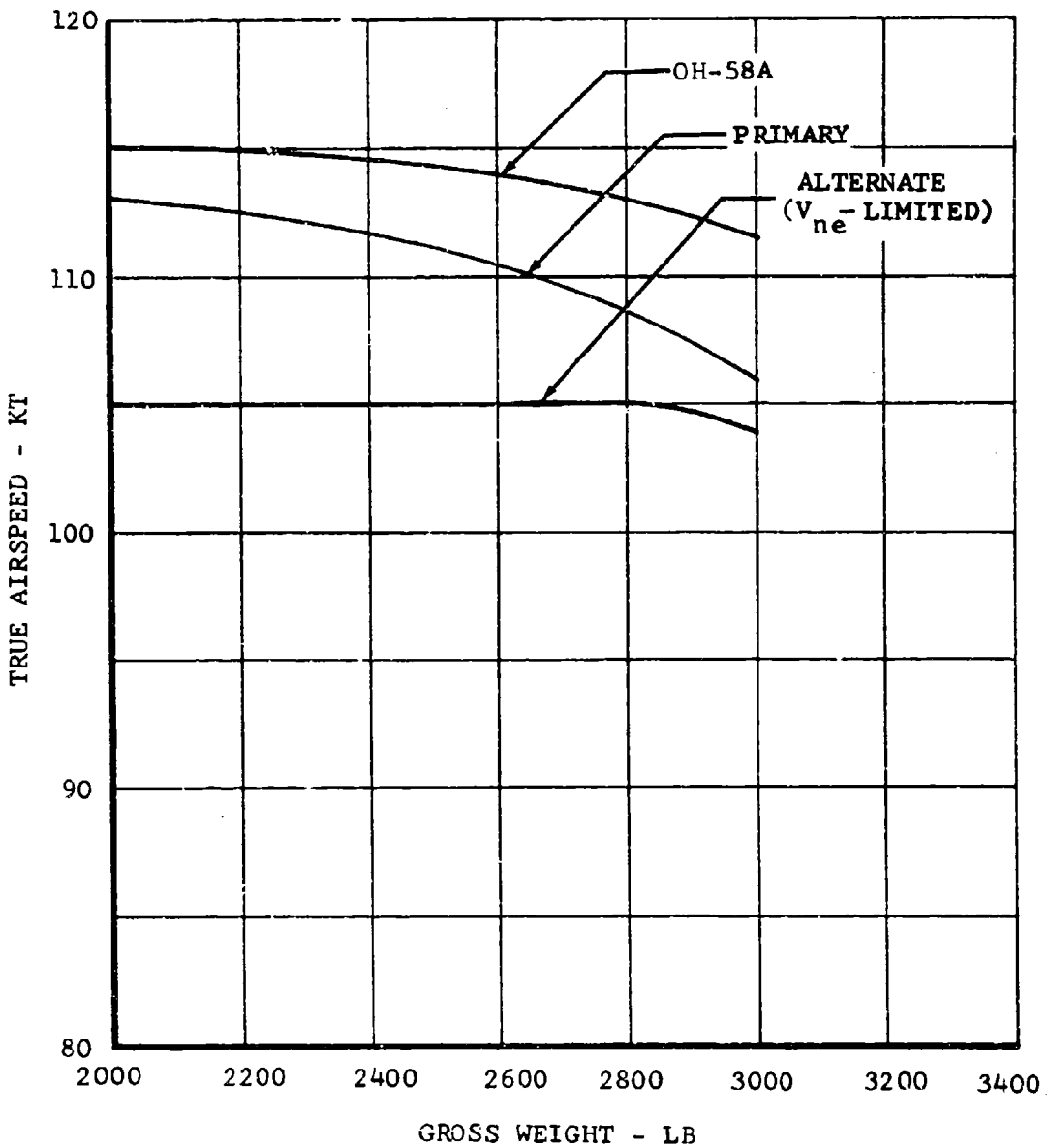

Figure 37. Speed at Maximum Continuous Power, Test Configurations.

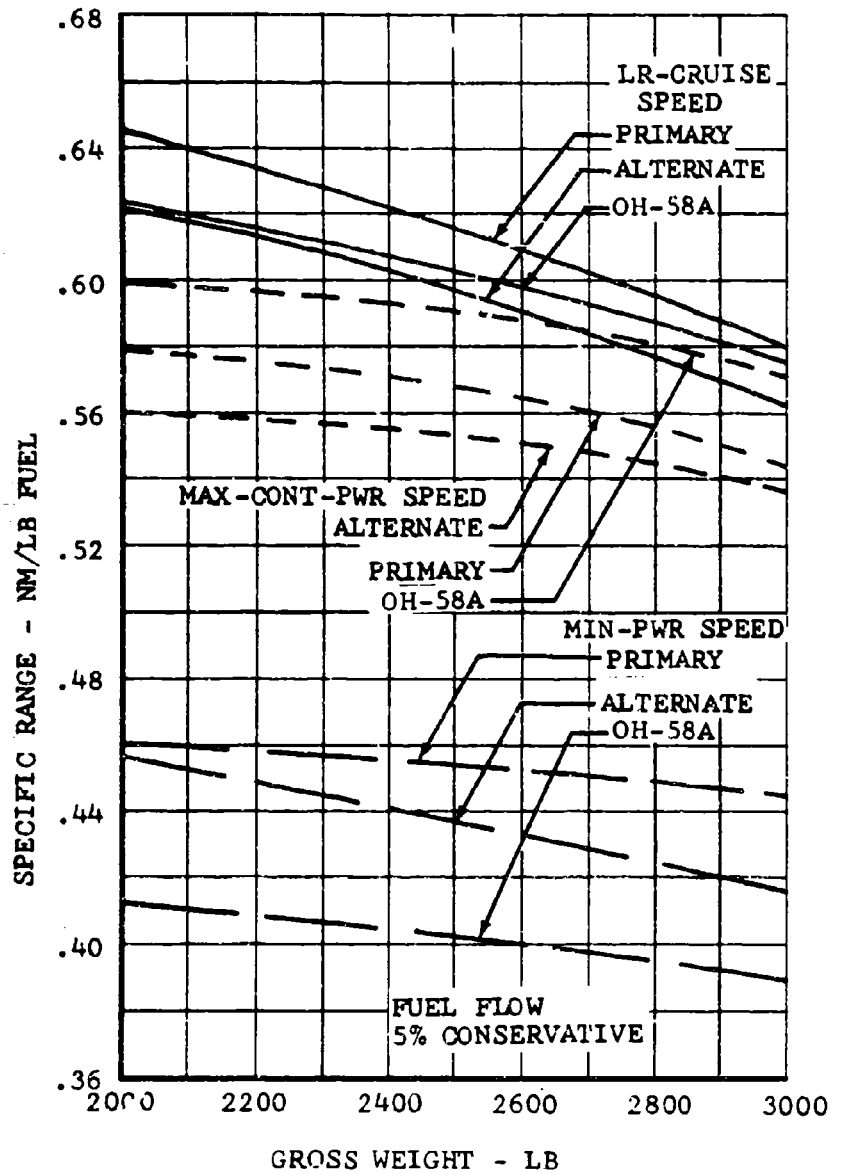

Figure 38. Specific Range, Test Configurations.

similarly with the OH-58A. At minimum-power speed, the specific range of the alternate configuration is 7 to 10 percent greater; at long-range-cruise speed, it is 2 percent greater; at maximum continuous speed, it is 8 percent less.

Figures 39 through 41 show payload-range for maximum continuous, long-range-cruise, and minimum-power speeds at design gross weight, and at long-range-cruise speed for the gross weight at which each configuration can hover OGE under the same conditions as the OH-58A--1700 feet on a 95°F day.

2. Operational Configurations

Performance of the two operational configurations in the LOH observation and scout missions is compared in Table XXXV with that of the OH-58A. The primary configuration's hovering ceiling is 3000 feet higher than that of the OH-58A, but its range, speed, and endurance are virtually unchanged. The alternate configuration's hovering ceilings for the two missions are 2200 and 2300 feet higher than those of the OH-58A. Its speed and endurance are not appreciably affected, but its range is slightly reduced. The increases in empty weight are significant: 15 percent for the primary and 27 percent for the alternate configuration.

The hovering ceilings of the alternate configuration (Figure 42) are slightly higher than those of the primary configuration, and both are substantially higher than those of the OH-58A. The greatest difference in the speeds at maximum continuous power (Figure 43) is 6 knots.

The specific-range data in Figure 44 are compared with the OH-58A data in Figure 38. At long-range-cruise speed and design gross weight, the primary configuration (3220 pounds) and the OH-58A (3000 pounds) have the same specific range, but that of the alternate configuration (3400 pounds) is 6.5 percent lower. Figures 45 and 46 show payload-range for the operational configurations comparable to the OH-58A curves in Figure 39.

For a range of 100 nautical miles at design gross weight and long-range-cruise speed, the OH-58A has a payload of 820 pounds; the primary configuration, 770 pounds; and the alternate configuration, 780 pounds. For a 200-nautical-mile range, these payloads are reduced to 635, 585, and 580 pounds. At observation-mission gross weights (payload of 311 pounds, 455 pounds of fuel), the OH-58A's range is 245 nautical miles, the primary configuration's is 241 nautical miles, and the alternate configuration's is 227 nautical miles.

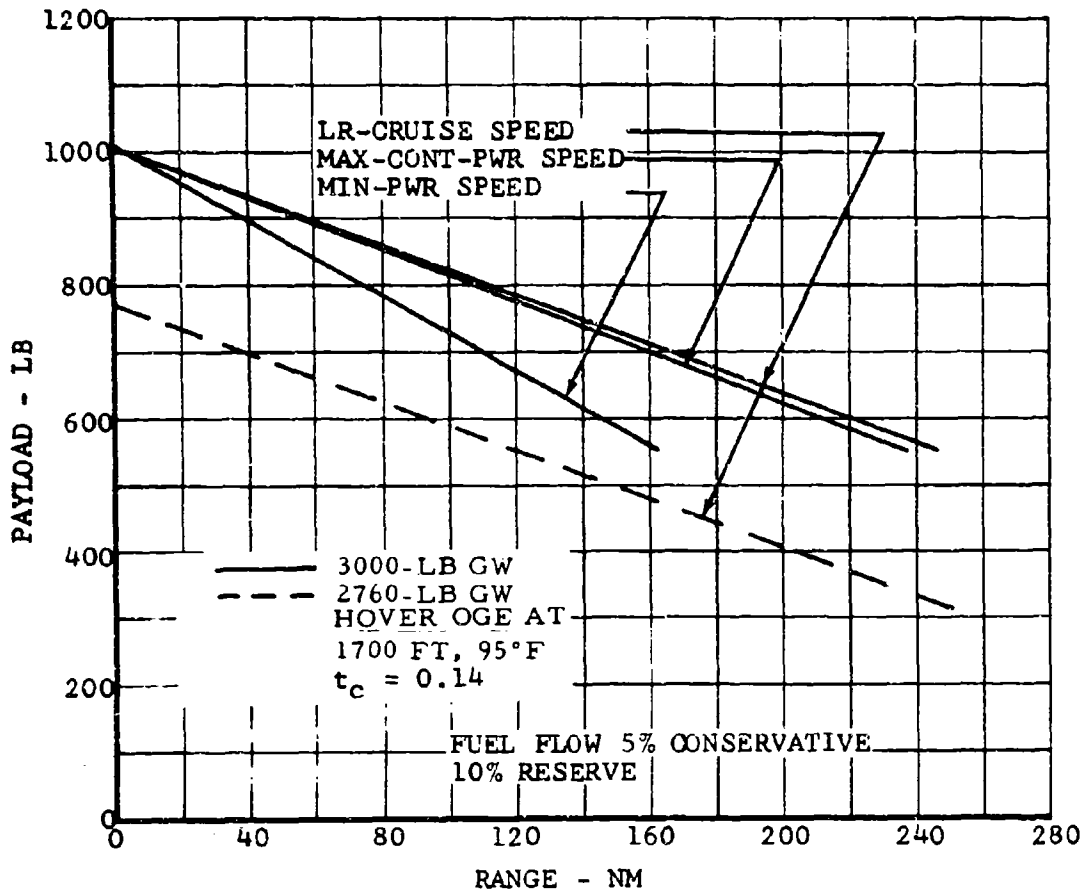

Figure 39. Payload-Range, OH-58A.

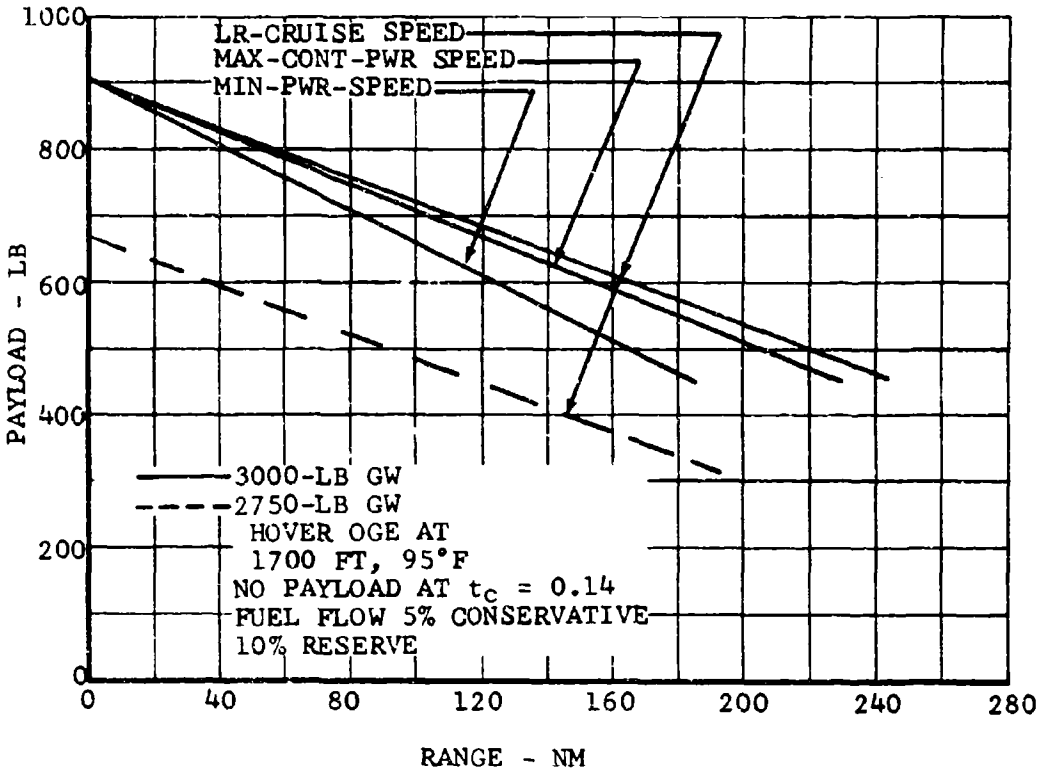

Figure 40. Payload-Range, Primary Test Configuration.

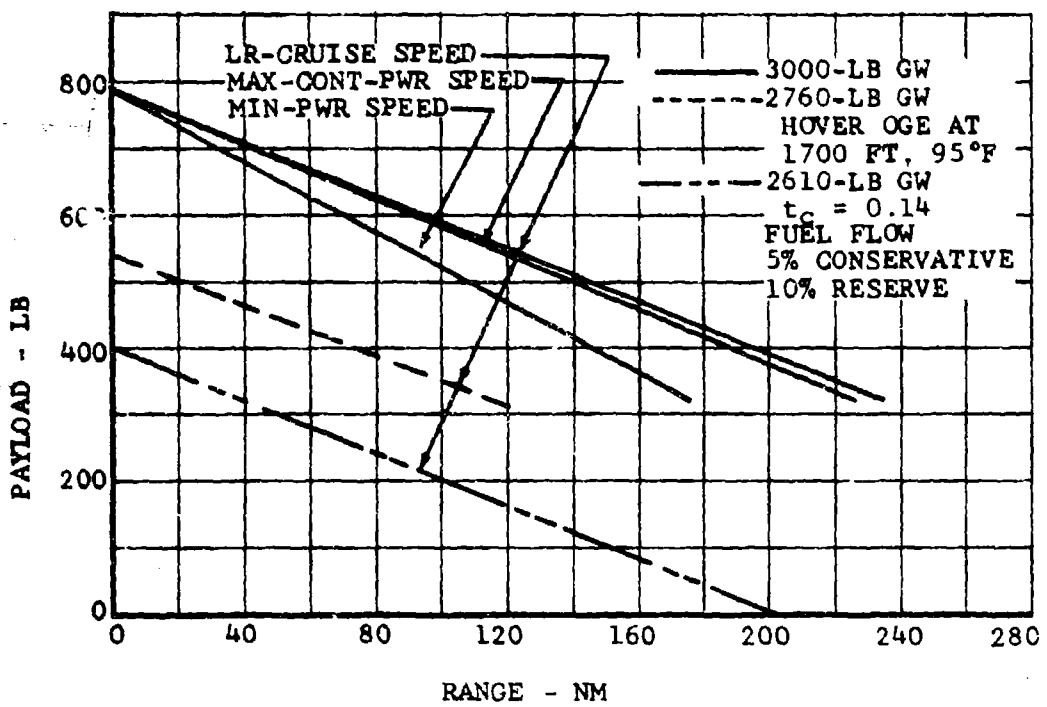

Figure 41. Payload-Range, Alternate Test Configuration.

TABLE XXXV. PERFORMANCE COMPARISONS, OPERATIONAL CONFIGURATIONS*

		OH-58A		Primary		Alternate	
		Observation Mission	Scout Mission	Observation Mission	Scout Mission	Observation Mission	Scout Mission
Gross Weight	lb	2760	2970	3008	3218	3190	3400
Empty Weight	lb	1583	1583	1831	1831	2013	2013
Useful Load							
Engine Oil	lb	11	11	11	11	11	11
Fuel	lb	455	428	455	428	455	428
Crew	lb	400	400	400	400	400	400
Payload	lb	311	548	311	548	311	548
Empty Weight/Gross Weight	-	0.574	0.533	0.609	0.569	0.630	0.593
Useful Load/Gross Weight	-	0.426	0.467	0.391	0.431	0.370	0.407
Hover Ceiling, OGE, 95°F	ft	1700	100	4700	3100	3900	2400
Range at Long-Range-Cruise Speed	nm	245	226	241	223	227	210
Maximum-Continuous Speed	kt	113	109	115	111	109	104
Maximum Endurance	hr	3.49	3.13	3.40	3.10	3.22	2.96
Rotor-Thrust Coefficient (t_c)	-	0.142	0.153	0.136	0.145	0.126	0.134
Maneuver Capability at Maximum-Continuous Speed	g	2.03	1.91	2.02	1.92	2.05	1.99

*With particle separator

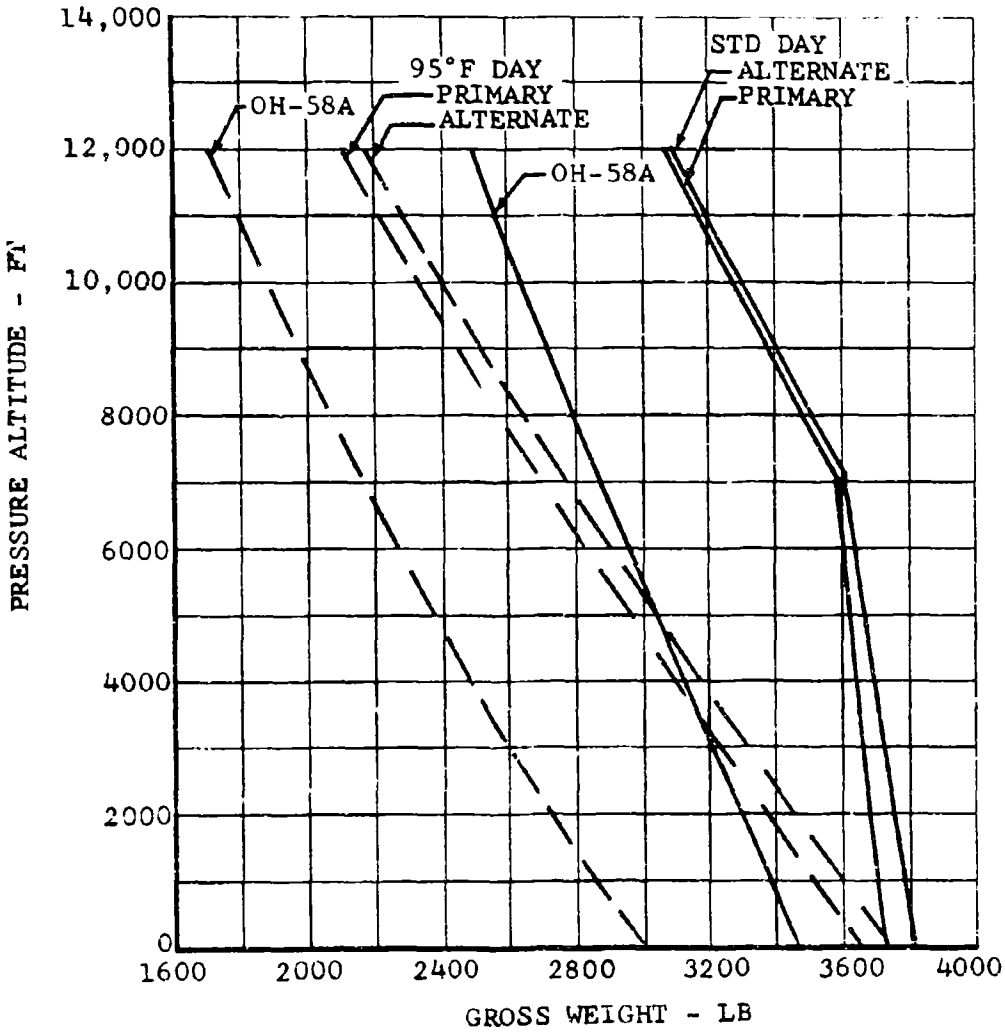

Figure 42. Hovering Ceilings, Operational Configurations.

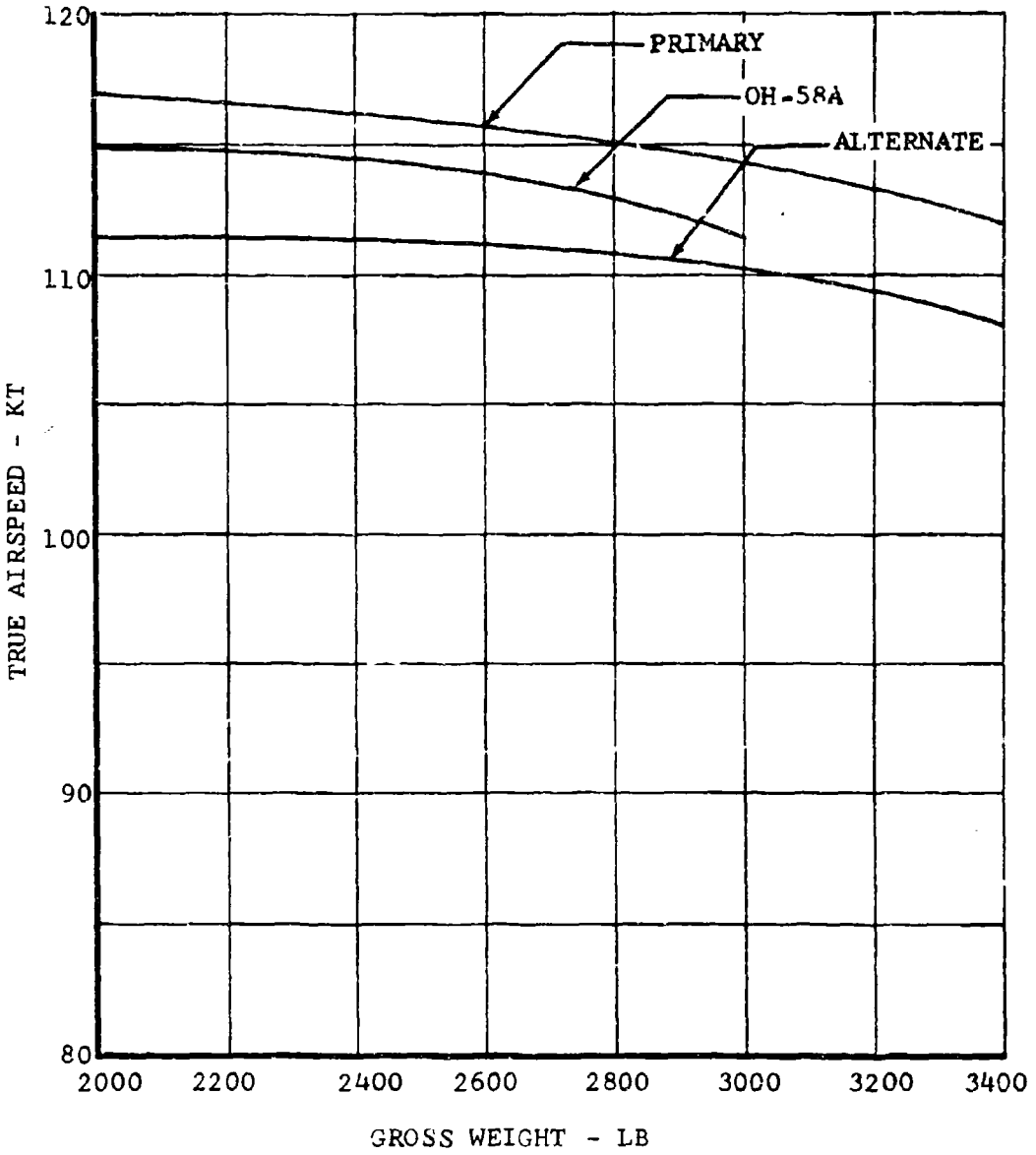

Figure 43. Speed at Maximum-Continuous Power, Operational Configurations.

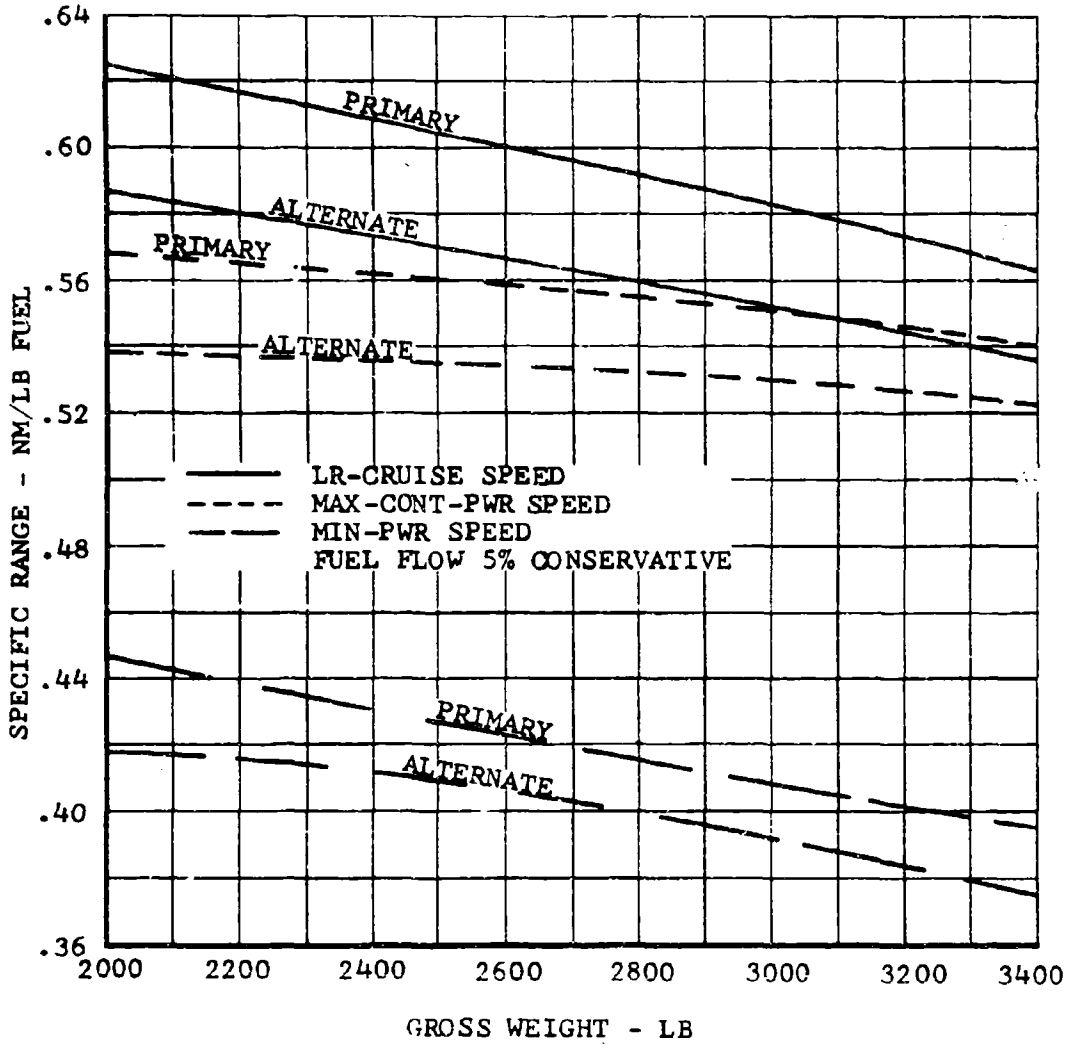

Figure 44. Specific Range, Operational Configurations.

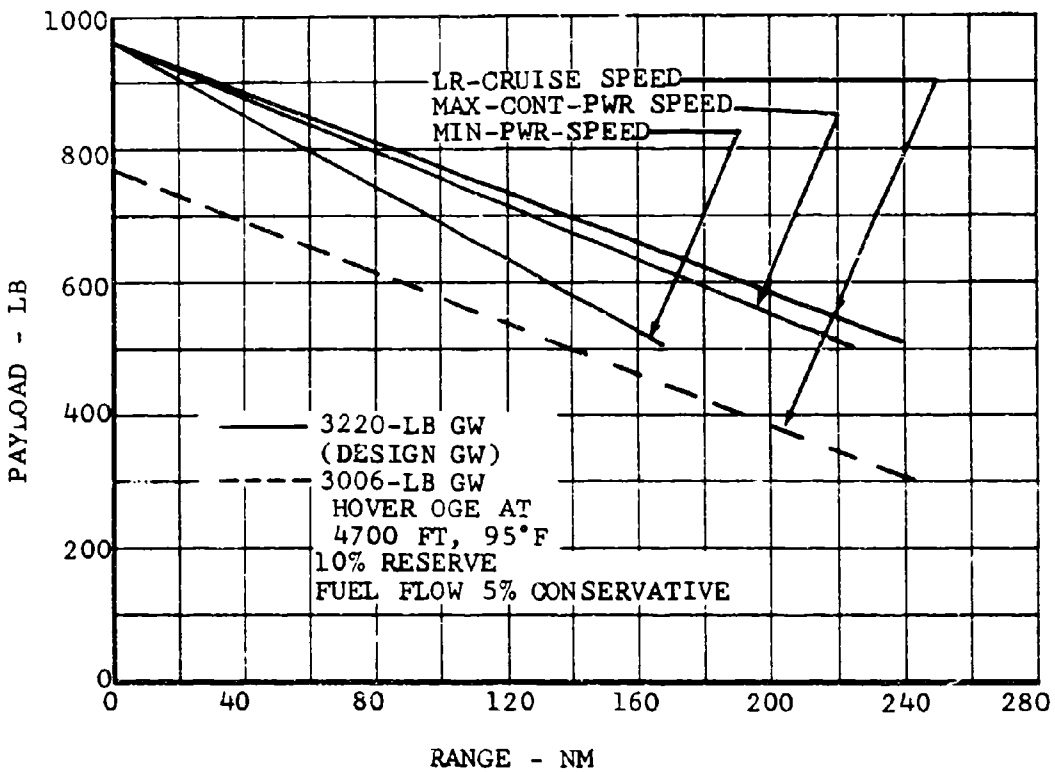

Figure 45. Payload-Range, Primary Operational Configuration.

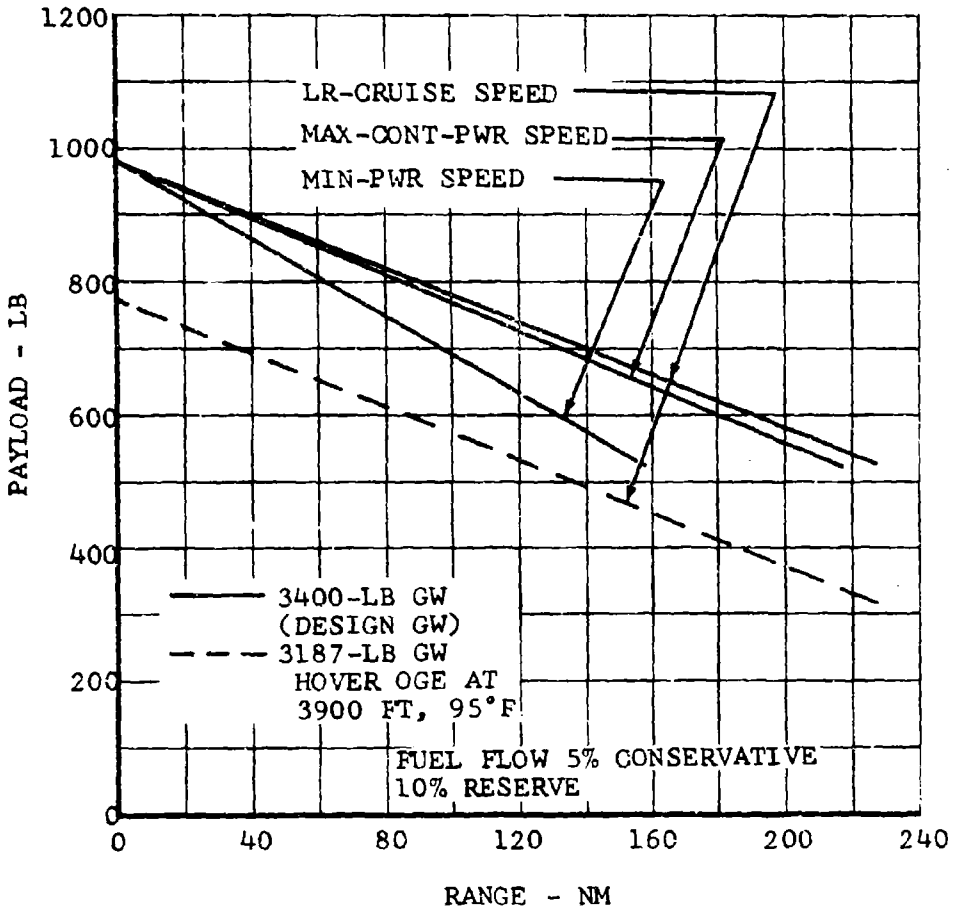

Figure 46. Payload-Range, Alternate Operational Configuration.

B. NOISE COMPARISONS

The perceived noise levels predicted for all four configurations are compared with those of the OH-58A in Tables XXXVI and XXXVII, for hover and for forward speeds up to 113 knots at azimuths of 0, 90, 180, and 270 degrees. To illustrate how the weight of a helicopter affects its noise, the tables also show the perceived noise levels predicted for the two test configurations when they are operating at near-minimum gross weights (see Tables XVI and XX).

Noise levels 200 feet from the primary test configuration in hover at design gross weight are 6 to 9 PNdb below those of the OH-58A. The reduction is as much as 13 PNdb directly in front of the helicopter in forward flight at its maximum speed. The reductions are more pronounced at 4000 feet: in hover, the primary test configuration is 10 to 11 PNdb quieter than the OH-58A, but in high-speed forward flight, it is 23 PNdb quieter in front of the helicopter. At design gross weight, the alternate test configuration is about 3 PNdb quieter under all conditions than the primary configuration. The perceived noise levels of the two operational configurations are approximately the same as those of the test configurations.

The gross weight at which a helicopter operates has significant effects on its noise. For example, when the useful load of the primary test configuration is reduced to lower its gross weight from 3000 to 2000 pounds, the predicted noise levels at 0 degrees and 4000 feet are 7 PNdb lower in hover and about 6 PNdb lower in forward flight than they are when the helicopter operates at design gross weight.

As a measure of the significance of perceived noise levels, these levels are related in Figure 47 to a scale of "noisiness". The curve represents subjective judgments of a 100-Hertz tone when its sound-pressure level is reduced from an original level of 50 db. For example, the primary test configuration's 10-PNdb reduction in hover would be perceived as a 50-percent reduction in noisiness.

TABLE XXXVI. PERCEIVED NOISE LEVELS AT 200 FEET (PNdb)

Azimuth (deg)	Velocity (kt)	OH-58A	Test Version				Operational Version	
			Primary Config		Alternate Config		Primary Config	Alternate Config
		3000-Lb GW	3000-Lb GW	2000-Lb GW	3000-Lb GW	2300-Lb GW	3220-Lb GW	3400-Lb GW
Hover								
0	-	91.1	84.9	81.3	81.9	79.6	81.6	80.4
90	-	91.8	83.2	80.0	80.2	78.2	81.8	80.6
180	-	91.2	83.6	80.1	80.0	77.7	81.6	80.5
270	-	92.6	83.9	80.4	80.6	78.4	82.1	80.9
Forward Flight								
0	45	90.6	82.0	76.9	77.3	76.1	81.0	79.6
	102	91.3	-	-	-	-	-	-
	108	-	-	-	75.6	-	-	78.5
	113	91.8	78.4	75.4	-	76.8	80.7	-
90	45	88.6	83.2	80.7	80.4	78.0	81.5	80.1
	102	89.1	-	-	-	-	-	-
	108	-	-	-	79.7	-	-	80.0
	113	91.3	82.1	79.5	-	77.1	81.1	-
180	45	89.6	82.6	79.4	79.0	77.4	81.5	79.7
	102	90.6	-	-	-	-	-	-
	108	-	-	-	79.6	-	-	80.2
	113	91.3	83.0	79.2	-	78.1	81.8	-
270	45	87.6	82.7	79.9	79.4	77.3	81.1	80.0
	102	88.7	-	-	-	-	-	-
	108	-	-	-	79.9	77.8	-	80.3
	113	90.1	82.9	80.2	-	-	81.2	-

TABLE XXXVII. PERCEIVED NOISE LEVELS AT 4000 FEET (PNdb)

Azimuth (deg)	Velocity (kt)	OH-58A	Test Version				Operational Version	
			Primary Config		Alternate Config		Primary Config	Alternate Config
		3000-Lb GW	3000-Lb GW	2000-Lb GW	3000-Lb GW	2300-Lb GW	3220-Lb GW	3400-Lb GW
Hover								
0	-	50.8	40.3	33.5	37.8	29.7	38.6	37.7
90	-	54.2	44.1	37.4	41.3	36.4	43.8	42.2
180	-	53.4	42.4	35.1	40.1	34.7	40.1	38.4
270	-	58.7	48.3	40.4	44.0	38.9	46.4	45.1
Forward Flight								
0	45	50.4	31.4	25.6	28.6	25.3	28.2	27.4
	102	54.3	-	-	-	-	-	-
	108	-	-	-	32.8	-	-	30.7
	113	56.5	33.4	27.1	-	26.4	31.6	-
90	45	51.1	32.6	25.8	30.9	25.2	35.4	34.1
	102	49.6	-	-	-	-	-	-
	108	-	-	-	31.1	-	-	27.8
	113	50.9	32.8	27.1	-	26.8	29.3	-
180	45	48.7	29.7	25.3	27.3	25.1	30.1	28.2
	102	48.4	-	-	-	-	-	-
	108	-	-	-	26.8	-	-	25.7
	113	48.4	28.3	25.1	-	25.1	27.9	-
270	45	54.6	33.4	26.1	29.3	25.1	32.0	29.8
	102	53.9	-	-	-	-	-	-
	108	-	-	-	28.1	-	-	28.3
	113	54.9	30.4	25.6	-	25.7	29.4	-

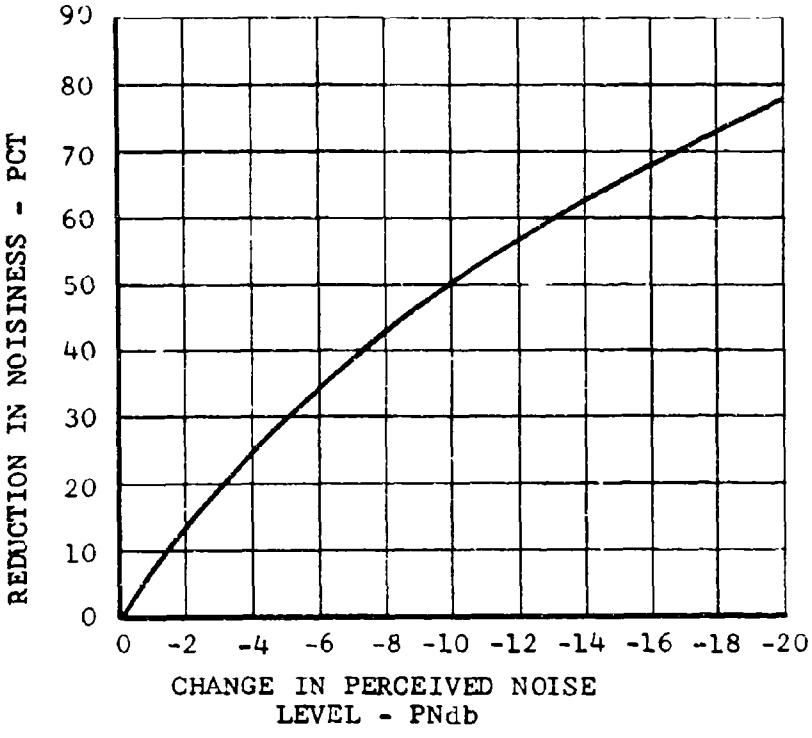

Figure 47. Noisiness as a Function of Perceived Noise Level.

VIII. DESIGN MODIFICATIONS AND TEST PROGRAM

A program is defined to confirm the predicted noise reductions for a test/demonstrator version of a quiet-modified OH-58A. The program is for either the primary test configuration (which uses modified OH-58A main-rotor blades) or the alternate test configuration (which uses modified UH-1D main-rotor blades operating at a reduced tip speed). No major changes in the drive system, powerplant, or airframe are required for either configuration. The primary configuration has the maximum possible noise reduction of the overall noise level with minimum modification and cost. The alternate configuration provides an additional reduction of main-rotor impulsive noise.

In the program for the primary configuration, the need for modification to the main-rotor tip will be determined by measuring noise with and without the tip modifications. The engine silencer will be developed. Noise tests will be conducted on the ground and in flight to measure noise of the quiet helicopter and to compare its noise with that of the OH-58A. Aural-detection tests will be conducted to determine detection range under simulated observation-helicopter operating conditions.

Regardless of which configuration is chosen for the test program, it would be possible to subsequently test the other configuration in a follow-on program at less than total-program cost for both programs separately. Some additional changes are required to run the two programs sequentially, but the same basic tail-rotor design, tail-rotor gearbox, engine exhaust silencers, and cowling modifications are common to both programs.

Design, limited component and ground tests, and a 10-hour flight-test program will be performed for the test version. Design work will be required for the rotor modifications, the new tail-rotor gearbox, and the engine-and-transmission-silencing modifications. A 5-hour bench test to check out the new tail-rotor gearbox, using the existing 206A tail-rotor-gearbox test stand, will be required. It is assumed that a bailed helicopter will be available for the program. Ground runs of the complete helicopter, the helicopter with main rotor and engine only, and with tail rotor and engine only will be made to verify structural integrity and to measure noise. Flight-load measurements will be made for the flight conditions required during noise tests. Selected main- and tail-rotor blade and hub stations will be instrumented. The noise test program will consist of an exhaust-silencer evaluation, a component-noise test, hover-and-flyover noise measurements, and aural-detection tests and analyses. Noise of the test helicopter will be analyzed and compared with that of the OH-58A. The plan of performance is shown in Figure 48.

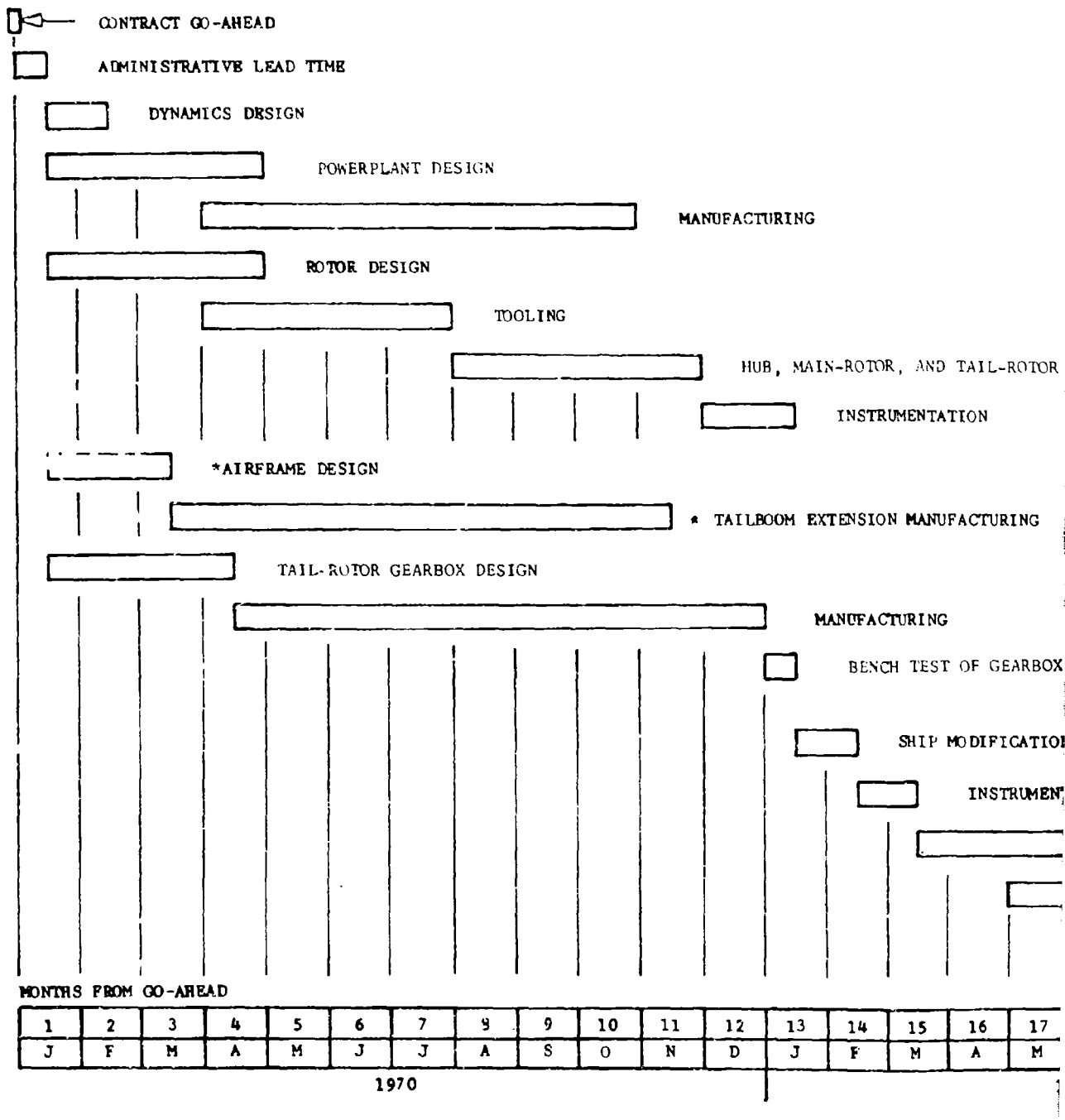

Figure 58. Test Program, Plan of Performance.

A

' DESIGN

MANUFACTURING

N

TOOLING

HUB, MAIN-ROTOR, AND TAIL-ROTOR MANUFACTURING

INSTRUMENTATION

* TAIL-BOOM EXTENSION AND LONGER DRIVE SHAFT USED ONLY IN ALTERNATE CONFIGURATION

* TAILBOOM EXTENSION MANUFACTURING

RBOX DESIGN

MANUFACTURING

BENCH TEST OF GEARBOX

SHIP MODIFICATION

INSTRUMENTATION

GROUND TEST AND FLIGHT TESTS

DATA REDUCTION

FINAL REPORT

8	9	10	11	12	13	14	15	16	17	18	19	20	21	22
A	S	O	N	D	J	F	M	A	M	J	J	A	S	O

1971

am, Plan of Performance.

23

B

A. ENGINE-SILENCER EVALUATION

The helicopter will be ground-run with the main- and tail-rotor drive shafts disconnected. Noise will be measured at 200 feet from the aircraft, with the engine running at the maximum N_{II} speed attainable with four exhaust-pipe configurations: the standard OH-58A exhaust deflector, the exhaust-noise silencer as designed, the silencer with some sections removed, and a silencer shell with the same skin and internal flow but without reactive or absorptive chambers or material. Noise will be measured at 100, 400, 800, and 1600 feet with the silencer as designed, in order to determine engine-noise falloff with distance.

B. COMPONENT TESTS

In these tests, sections of the drive shafts, either to the main rotor or to the tail rotor, will be removed. Tail-rotor-and-engine and main-rotor-and-engine tests will be conducted with the helicopter tied down. Noise will be measured for a range of thrusts of each rotor at its operating tip speed. Microphones will be placed 100 and 200 feet from the tail rotor, and the tests will be conducted with the microphones at five azimuths from the rotor. For the main rotor, tests will be at a range of 200 feet and at the azimuth for minimum engine noise in the frequency range of main-rotor vortex noise. Tests will also be conducted with a standard, unmodified OH-58A main rotor operating at a tip speed of 600 or 530 feet per second, depending on the test configuration chosen. A comparison of the noise of the standard and the modified rotors is expected to show the importance of the tip modification.

Noise of the complete helicopter will be measured for a range of thrusts at operating tip speeds, at a range of 200 feet, and at bearings of 0, 90, 180, and 270 degrees. All tests will be conducted in winds no greater than 5 knots, during hours when the background noise at the site is minimal. When possible, the noise tests will be combined with the helicopter buildup and ground-run tests prior to load-level flight tests. Engine-on time for all the component-noise tests is estimated at 4 hours.

C. HOVER AND FLYOVER NOISE MEASUREMENTS

Noise will be recorded at ground ranges of 200, 400, 800, 1600, and 3200 feet from the helicopter hovering at an altitude of 200 feet. At the 200-foot range, measurements will be made at 0, 90, 180, and 270 degrees. At the other ranges, measurements will be made only at selected azimuths. The tests will be conducted over nearly level, grass-covered terrain at the Bell Helicopter Company Flight Test Center.

Noise will be measured during flyovers and flybys of the test vehicle at an altitude of 200 feet, at airspeeds of 50 knots, 100 knots, and maximum speed. Flyovers will be directly over the microphone, and flybys will be 200 feet on either side.

Fifteen-second tape-recorded records are required for each hover data-point. Each flyover and flyby test run will be duplicated, from opposite directions.

D. AURAL-DETECTION TESTS

The test vehicle and an unmodified OH-58A will be subjected to aural-detection tests. The operating conditions will be:

- Head-on approach at 50 knots, 100 knots, and maximum speed
- Low, slow approach, climb to observe, descent back to nap-of-the-earth approach, and repeat, at successively closer distances

For the head-on approach tests, each helicopter will fly over a predefined course at a constant speed. Observers will be stationed at points along the flight path. Using stop watches, they will note the time at which they hear the helicopter and the time of its flyover. The intervals measured by the observers will be averaged. From these intervals and the helicopter's speed, the detection distances will be calculated. The airspeeds at which detection distances are least, and the differences in detection distances for the test helicopter and the OH-58A, will be determined.

A test day will be selected on which the wind is blowing 5 mph or less. The intervals between flights over the course will be kept as small as practicable so as to minimize the effects of atmospheric changes. An area with a reasonably constant background-noise level will be selected. Background noise, wind, temperature, and atmospheric humidity data will be measured periodically.

For the observation-flight conditions, observers will be placed on and about the flight path, and they will be instructed not to attempt visual detection. Markers will be placed along the course at which the aircraft will climb to an altitude of 200 feet to simulate observation maneuvers. The pilot will communicate his altitude, position, and maneuvers to a ground controller, and the observers will advise the controller when they hear the helicopter.

These tests will start at distances up to 3 miles from the observers. Procedures will be developed using a standard OH-58A.

E. ACOUSTICAL INSTRUMENTATION

Noise will be recorded on magnetic tape. The data-acquisition system will consist of a Nagra audio tape recorder, a Bruel and Kjaer Type 4131 condenser microphone system, a power supply, a wind screen, cables and a tripod. The recording system will be calibrated before and after each test, using the Bruel and Kjaer Type 4220 pistonphone.

The data-reduction system will consist of the General Radio Type 1551 octave-band analyzer, the Bruel and Kjaer Model 2107 constant-percentage band analyzer, the Bruel and Kjaer Model 2305 graphic level recorder, and an oscilloscope.

F. REPORT

A final report on the noise test program will be prepared.

LITERATURE CITED

1. Kryter, K. D., and Pearsons, K. S., SOME EFFECTS OF SPECTRAL CONTENT AND DURATION ON PERCEIVED NOISE LEVEL, Journal of Acoustical Society of America, Vol. 35, No. 6, 1963.

2. Lowson, M. V., and Ollerhead, J. B., STUDIES OF HELICOPTER ROTOR NOISE, Wyle Laboratories Inc.; USAAVLABS Technical Report 68-60, U.S. Army Aviation Materiel Laboratories, Fort Eustis, Virginia, May 1968, AD 684394.

3. Lowson, M. V., THOUGHTS ON BROADBAND NOISE RADIATION BY A HELICOPTER, Wyle Laboratories Research Staff WR 68-20, Wyle Laboratories Inc., Huntsville, Alabama, December 1968.

4. Schlegel, R. G., King, R. J., and Mull, H. R., HELICOPTER ROTOR NOISE GENERATION AND PROPAGATION, Sikorsky Aircraft; USAAVLABS Technical Report 66-4, U.S. Army Aviation Materiel Laboratories, Fort Eustis, Virginia, October 1966, AD 645884.

5. Sutherland, L. C., and Wyle Laboratories Research Staff, SONIC AND VIBRATION LOADING OF GROUND FACILITIES - A DESIGN MANUAL, WR 68-2, Wyle Laboratories Inc., Huntsville, Alabama, 1968.

6. Wiener, F. M., and Keast, D. N., EXPERIMENTAL STUDY OF THE PROPAGATION OF SOUND OVER GROUND, Journal of Acoustical Society of America, Vol. 31, 1959, p. 724.

7. Kneser, H., THE INTERPRETATION OF THE ANOMALOUS SOUND-ABSORPTION IN AIR AND OXYGEN IN TERMS OF MOLECULAR COLLISIONS, Journal of Acoustical Society of America, Vol. 5, 1933.

8. Guest, S. H., and Adams, B. B., METHODS OF DETERMINING THE EXCESS ATTENUATION FOR GROUND-TO-GROUND NOISE PROPAGATION, Progress of NASA Research Relating to Noise Alleviation of Large Subsonic Jet Aircraft, NASA SP-189, October 1968, pp. 453-492.

9. Prevoznik, E. J., T63 REGENERATIVE ENGINE PROGRAM, Allison Division, General Motors; USAAVLABS Technical Report 68-9, Addendum 1, U.S. Army Aviation Materiel Laboratories, Fort Eustis, Virginia, May 1968, AD 675444.

10. Gutin, L. Y., ON THE SOUND FIELD OF A ROTATING PROPELLER, Translated as NACA TM-1195, National Advisory Committee for Aeronautics, Washington, D.C., October 1948.

11. Cox, C. R., ROTOR NOISE MEASUREMENTS IN WIND TUNNELS, Proceedings, Third CAL/AVLABS Symposium, Aerodynamics of Rotary Wing and V/STOL Aircraft, Vol. 1, June 1969.

12. Cox, C. R., FULL-SCALE HELICOPTER ROTOR NOISE MEASUREMENTS IN AMES 40- BY 80-FOOT WIND TUNNEL, Bell Helicopter Company Report 576-099-052, Bell Helicopter Company, Fort Worth, Texas, July 1967.

13. Spencer, R. H., et al, TIP VORTEX CORE THICKENING FOR APPLICATION TO HELICOPTER ROTOR NOISE REDUCTION, Vertol Division, The Boeing Company; USAAVLABS Technical Report 66-1, U.S. Army Aviation Materiel Laboratories, Fort Eustis, Virginia, September 1966, AD 644317.

14. Gossett, M. H., T63/250 NOISE DATA, Letter to Bell Helicopter Company, Oklahoma City Zone Office, Allison Division, General Motors Corporation, 20 September 1968.

15. Gessow, A., and Myers, G. C., Jr., AERODYNAMICS OF THE HELICOPTER, Macmillan, New York, 1952, pp 86-88.

APPENDIX,
DRAWINGS

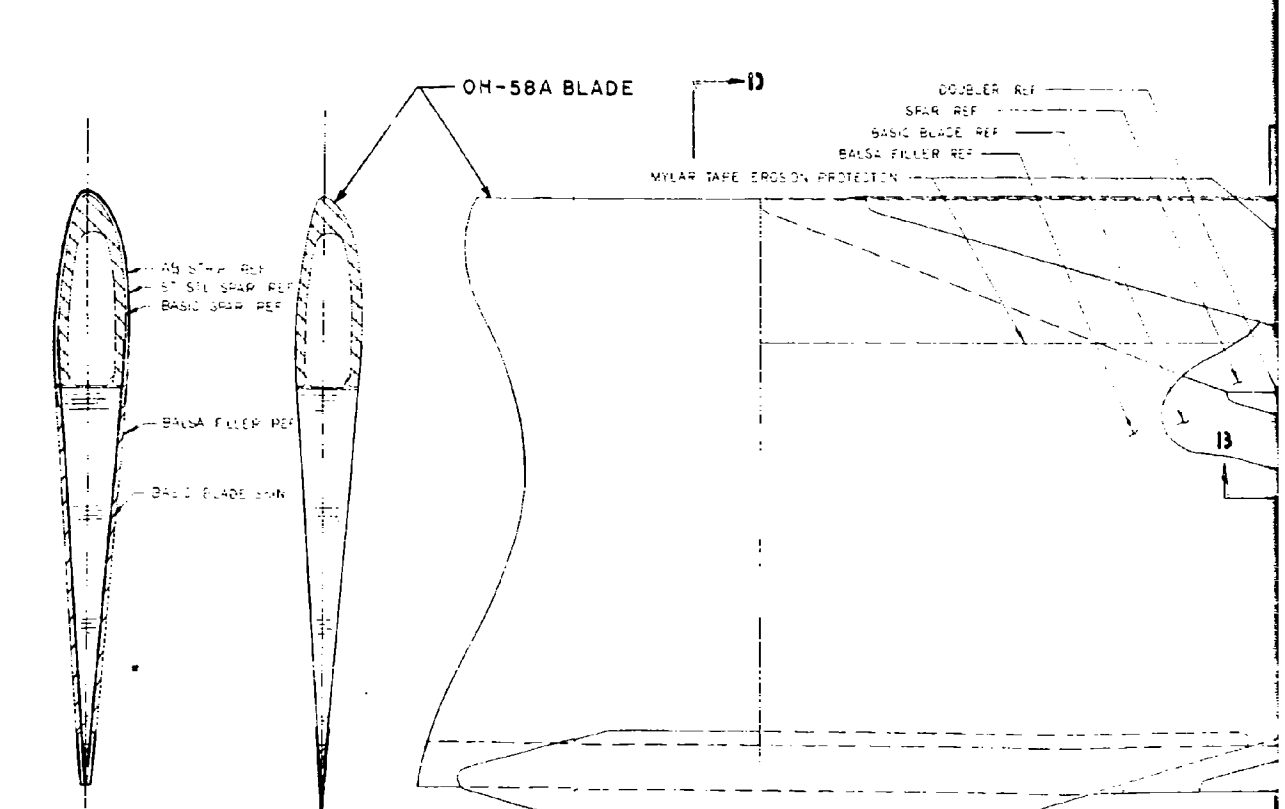

Figure 49. Tapered-Tip CH-58A Main-Rotor Blade.

A

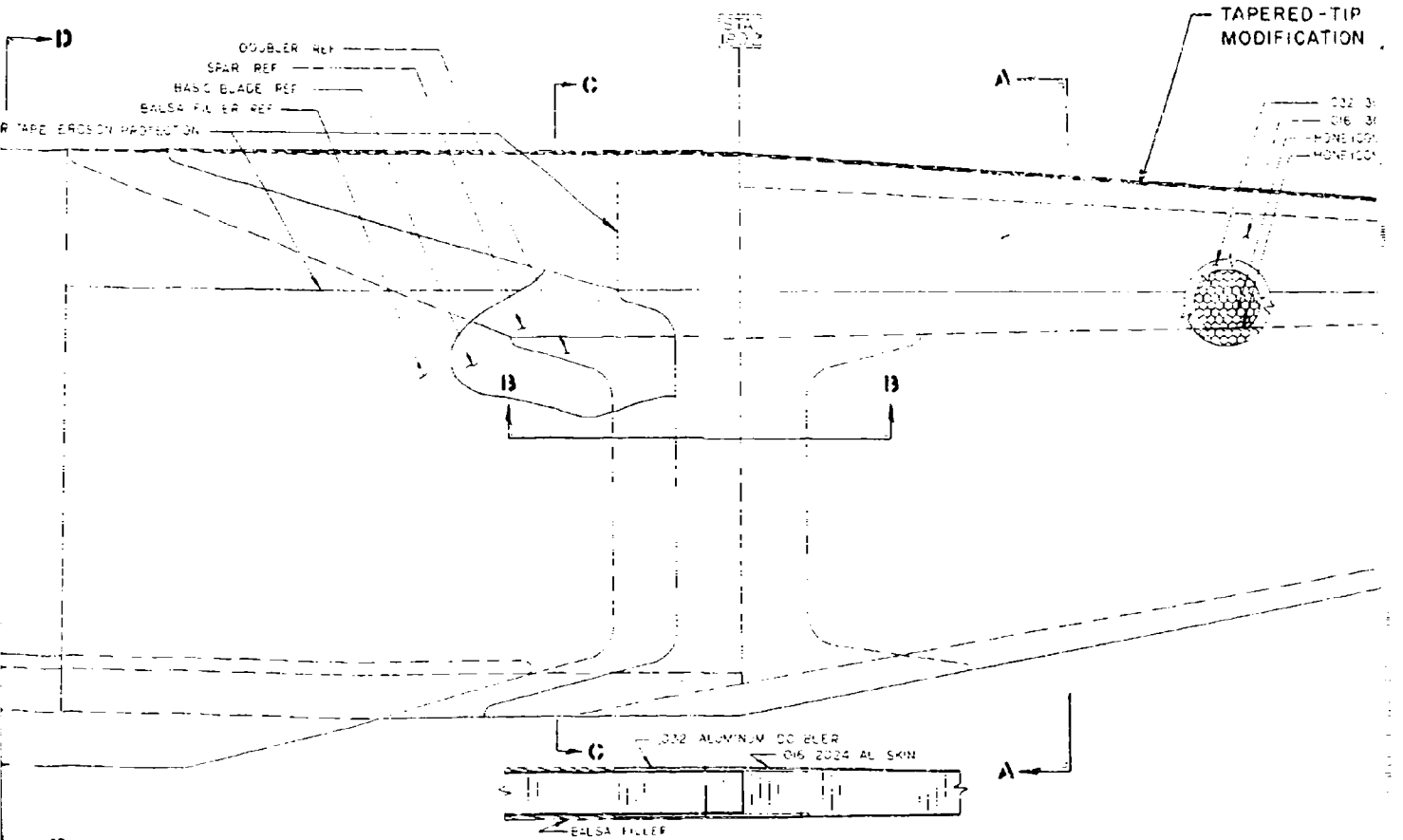

SECTION **B-B**
STOCK THICKNESS X2 FOR CLARITY

Rotor Blade.

A

B

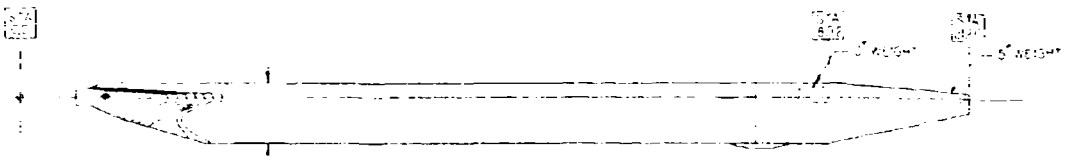

—13.00 TAPERED—TIP BLADE
SCALE 1/10

TAPERED-TIP
MODIFICATION

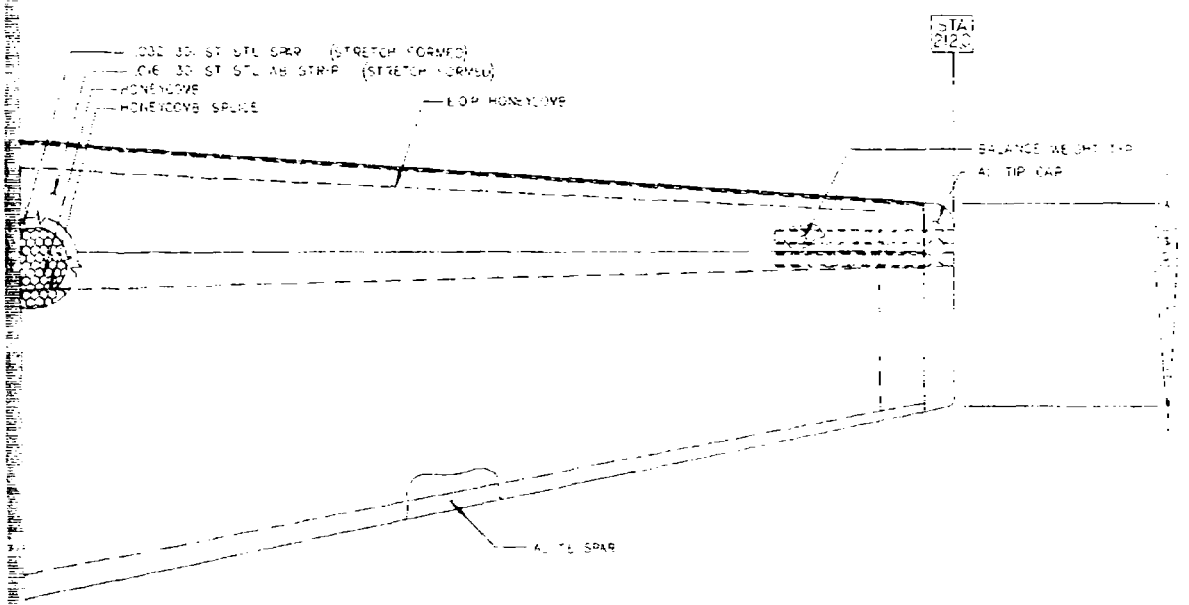

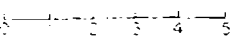

C

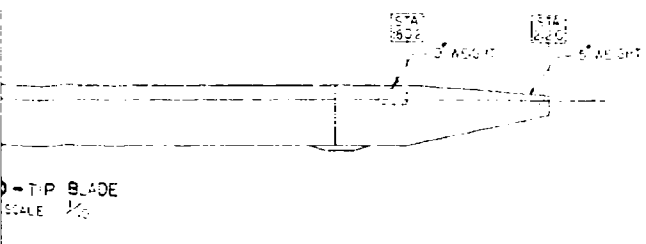

- TIP BLADE
SCALE 1/2

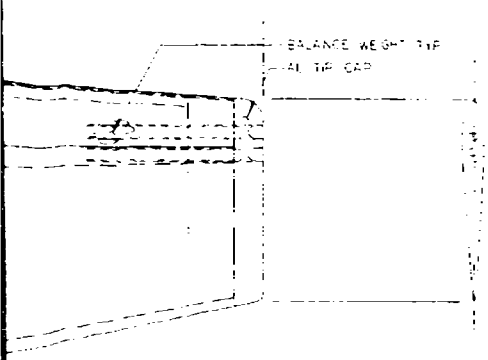

SECTION A-A

SCALE

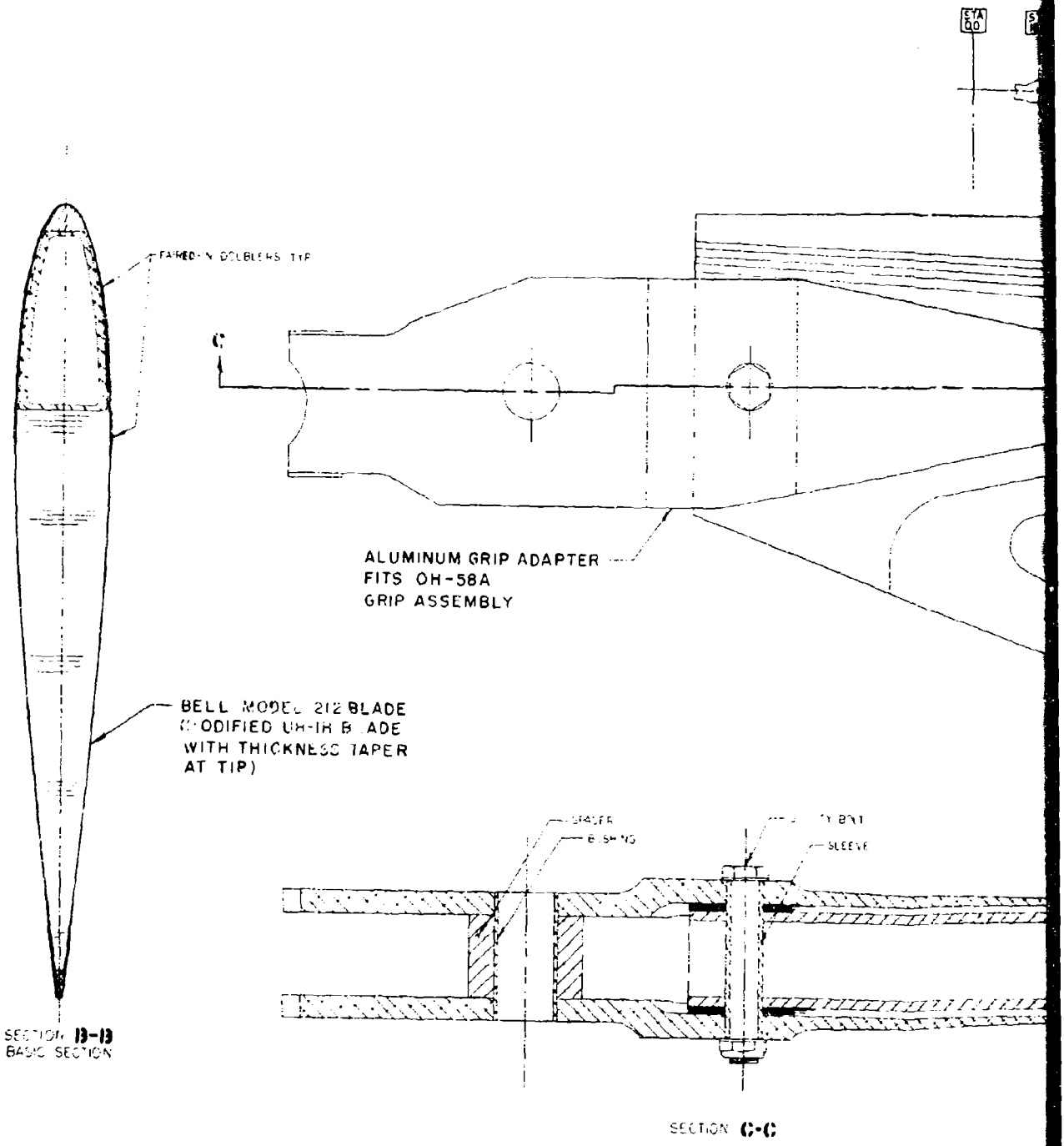

Figure 50. Modified UH-1 Main-Rotor Blade.

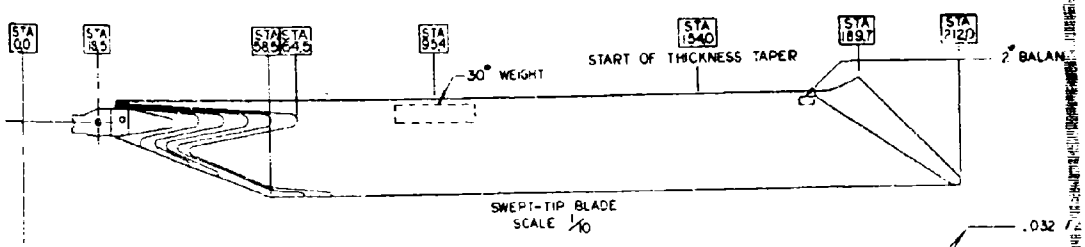

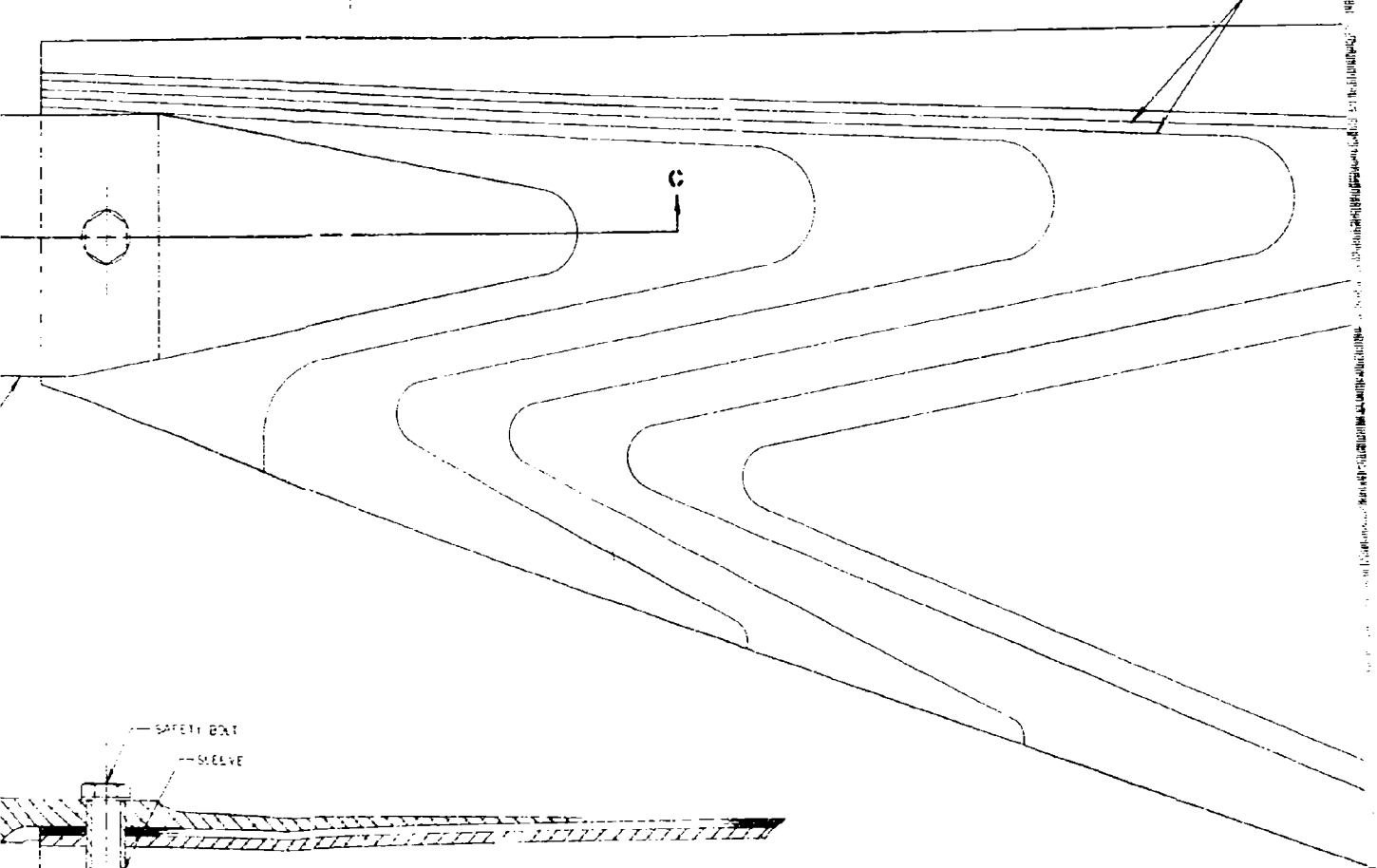

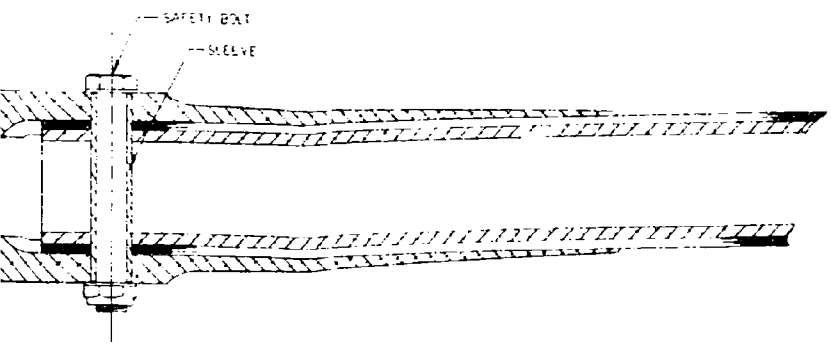

SECTION C-C

e.

B

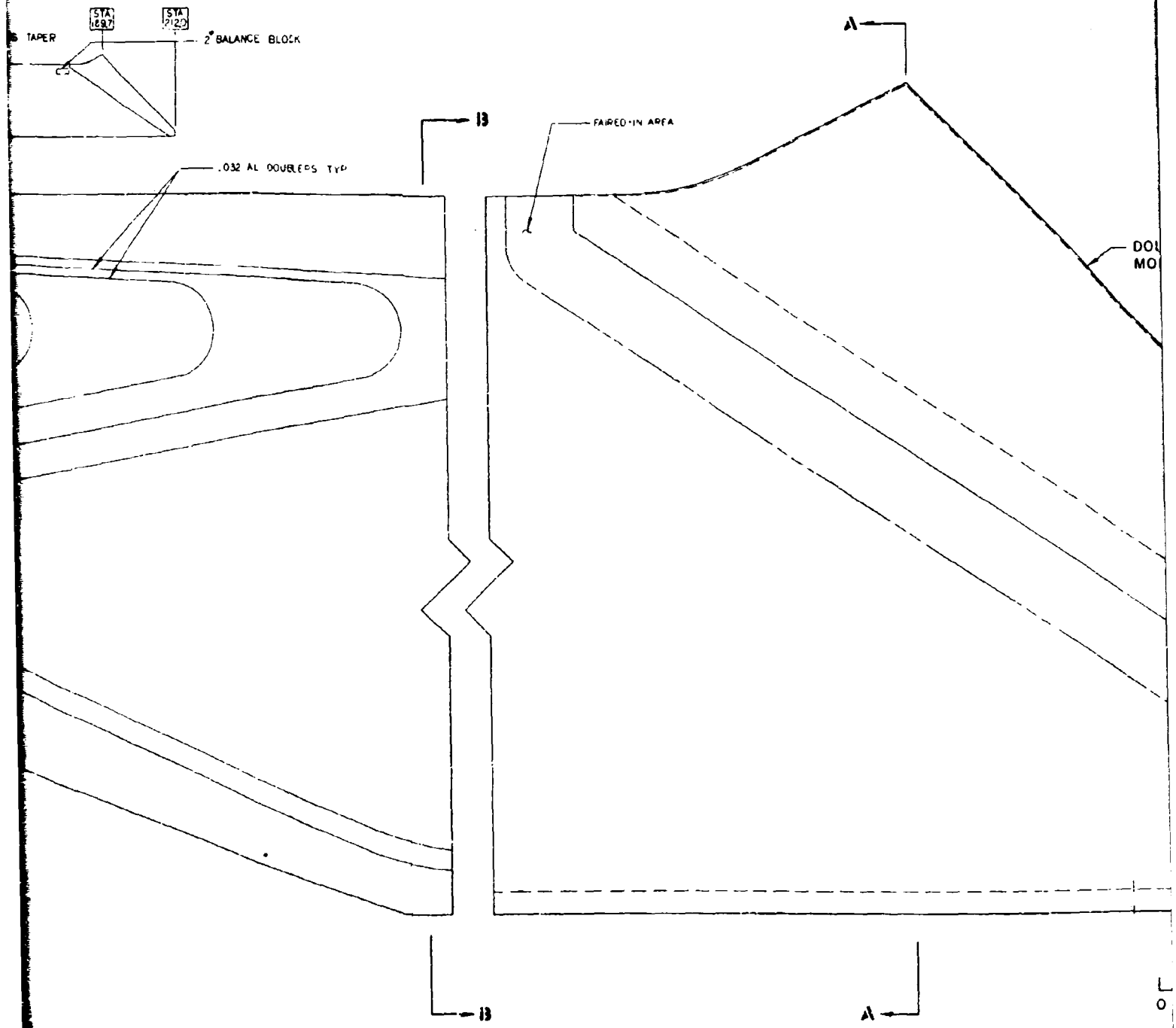
STA 289.7
STA 212.0
TAPER
2" BALANCE BLOCK
.032 AL DOUBLERS TYP
FAIRED-IN AREA
B
B
A
A

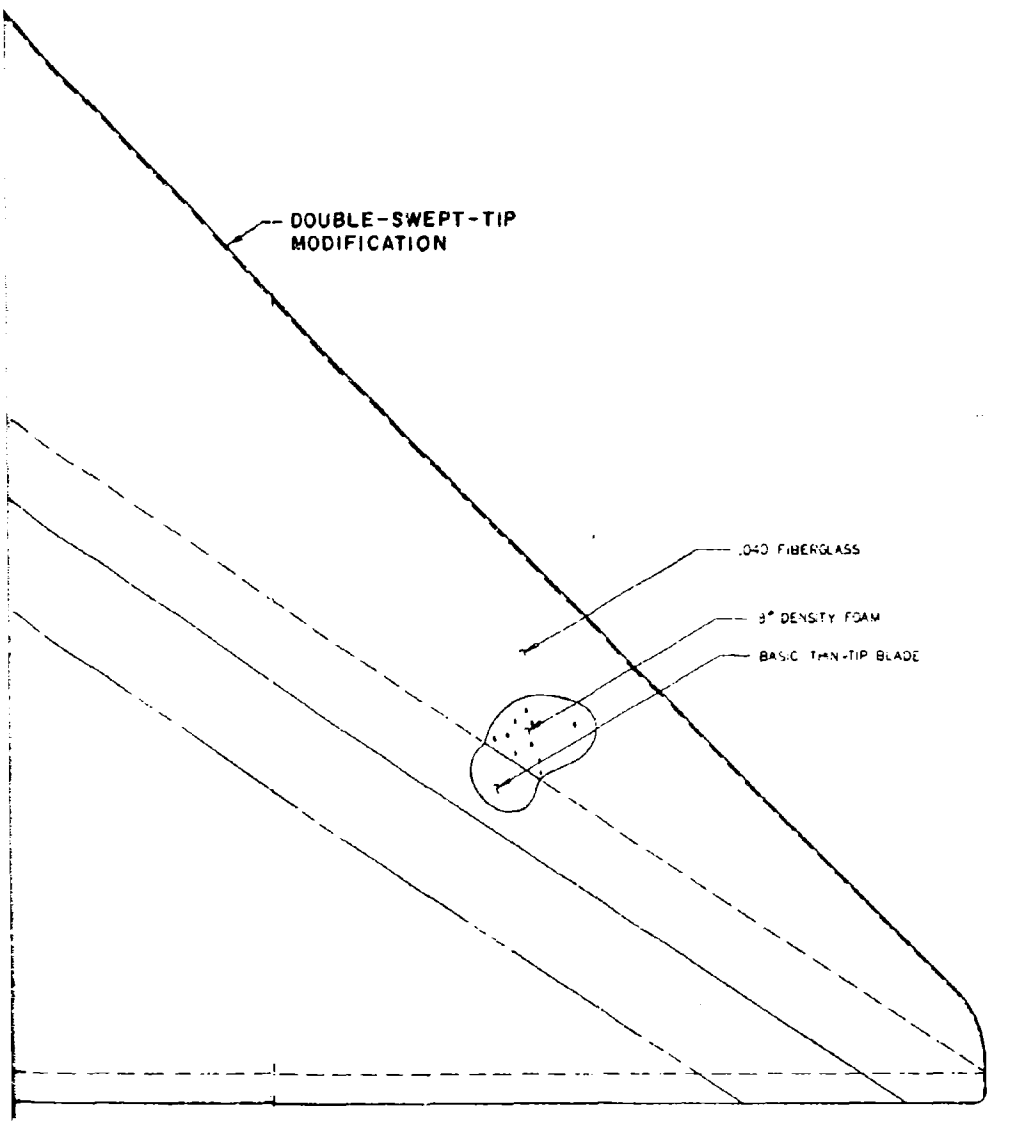

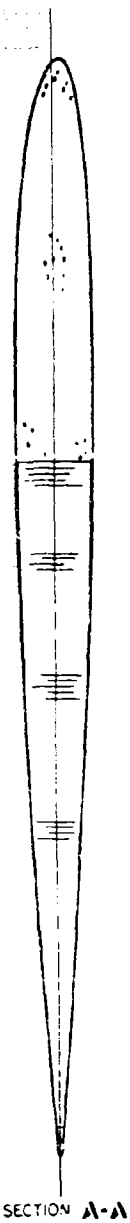

SECTION A-A

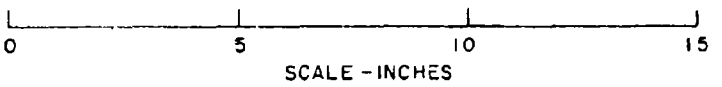

MOD OF MAIN ROTOR
QUIET HELICOPTER CH 54 A
AT CARTER
299 960 033

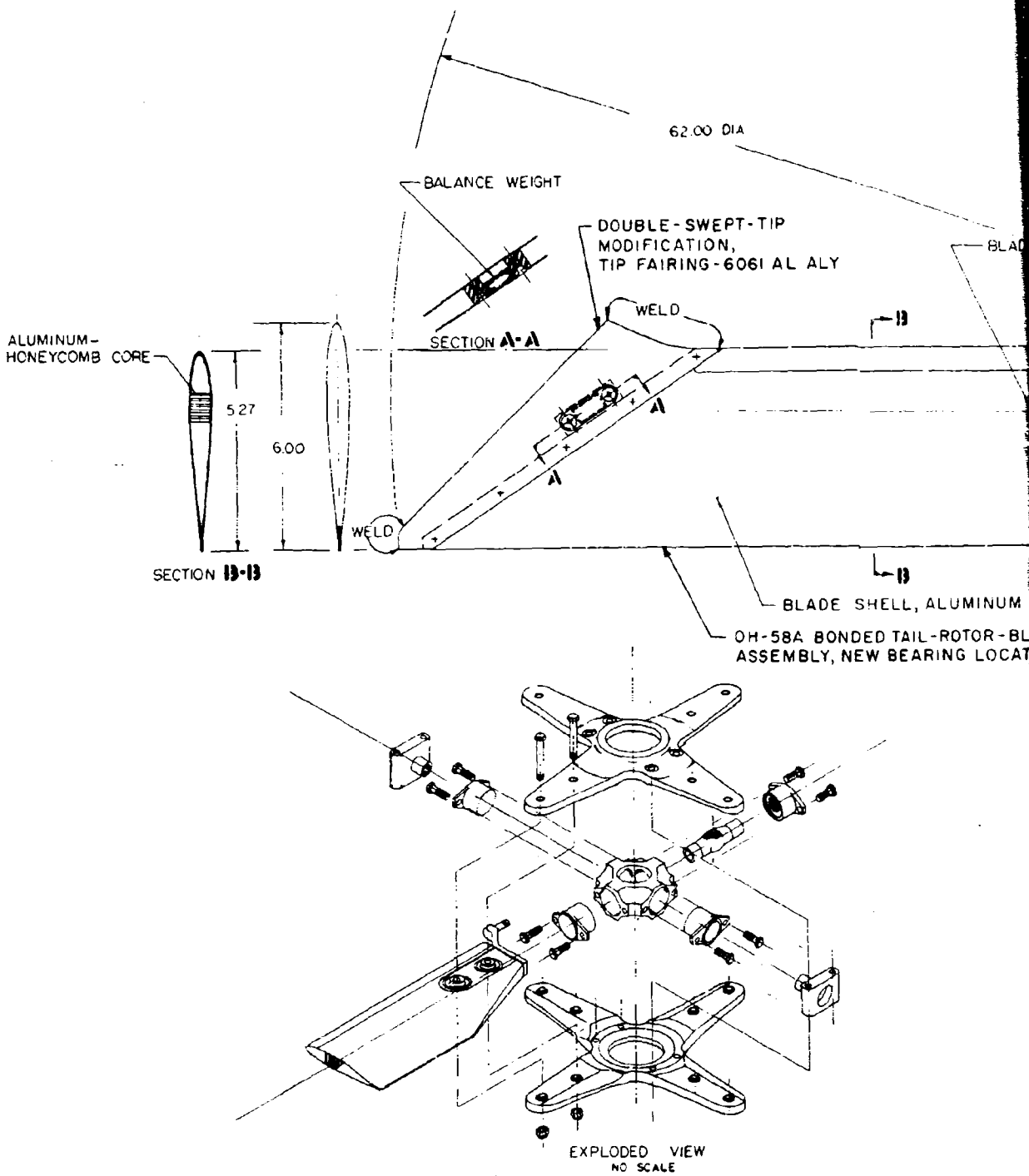

Figure 51. Four-Bladed Tail Rotor.

A

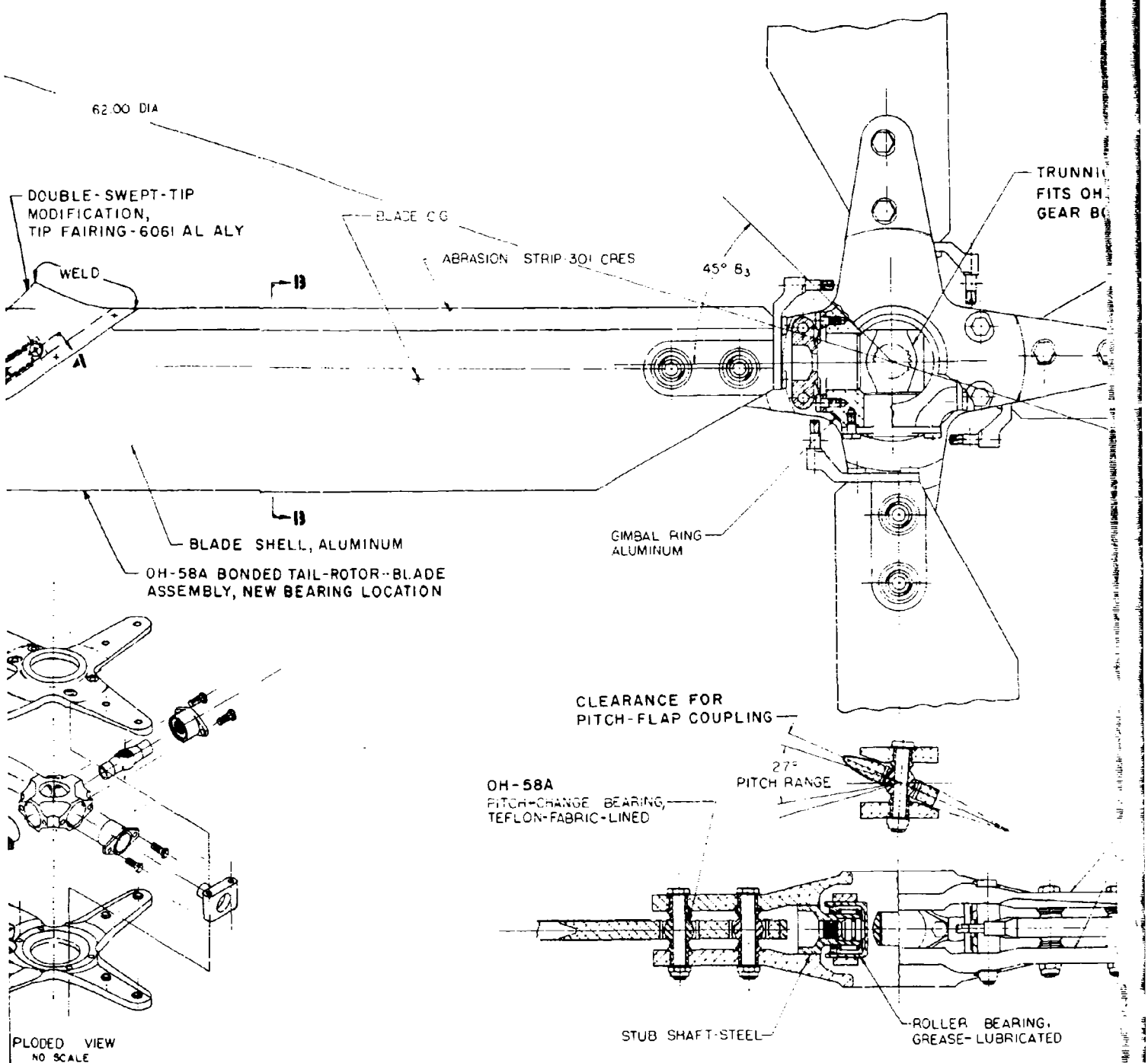

PLODED VIEW
NO SCALE

tor.

B

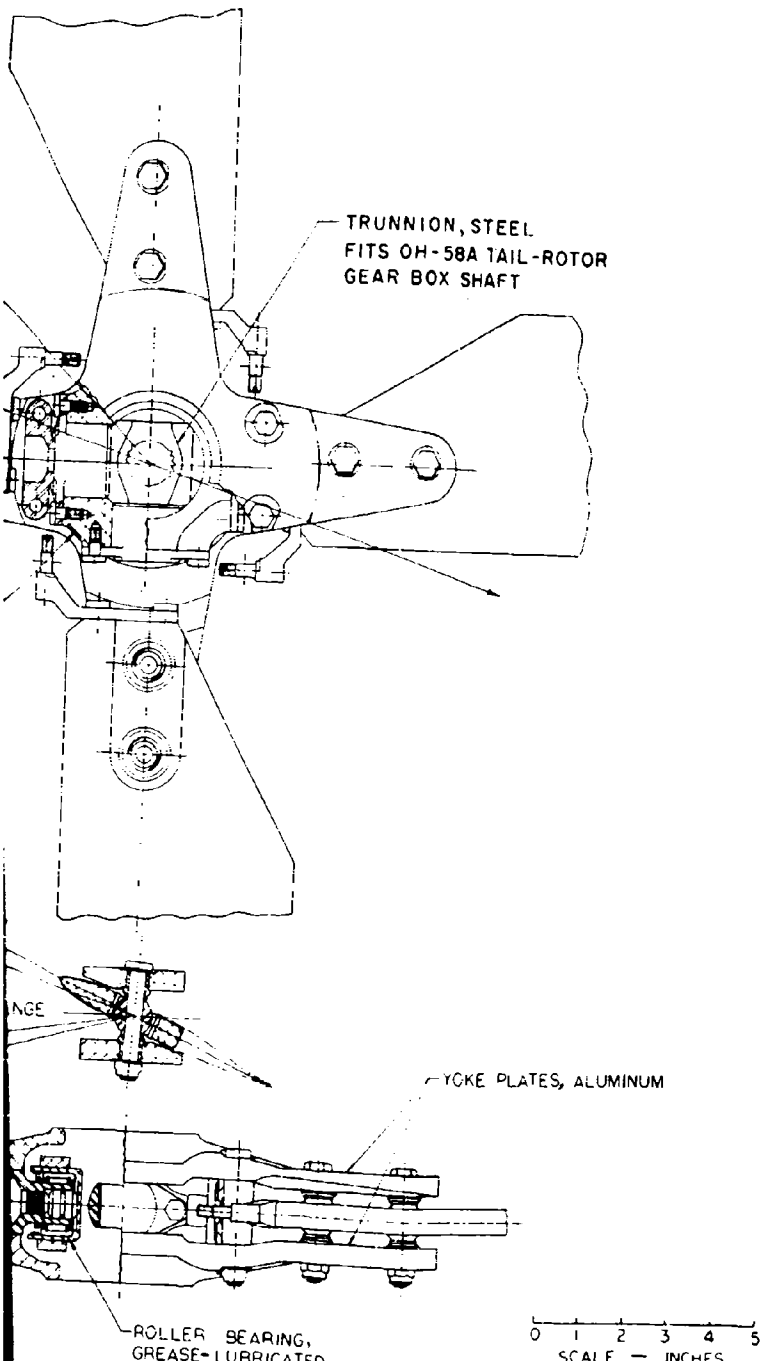

TAIL ROTOR-4 BLADES
QUIET HELICOPTER CH-58A

COVINGTON	7-7-69	HUGHES
[illegible]		299-960-034

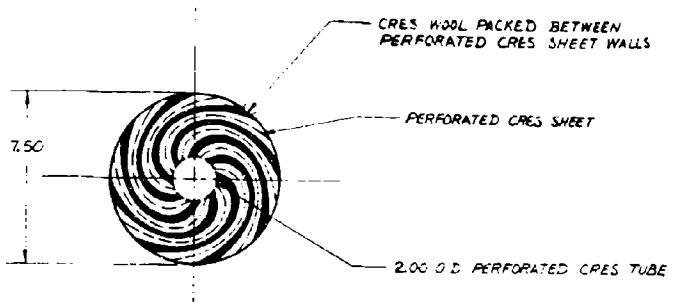

SECTION C-C
SCALE: 1/2

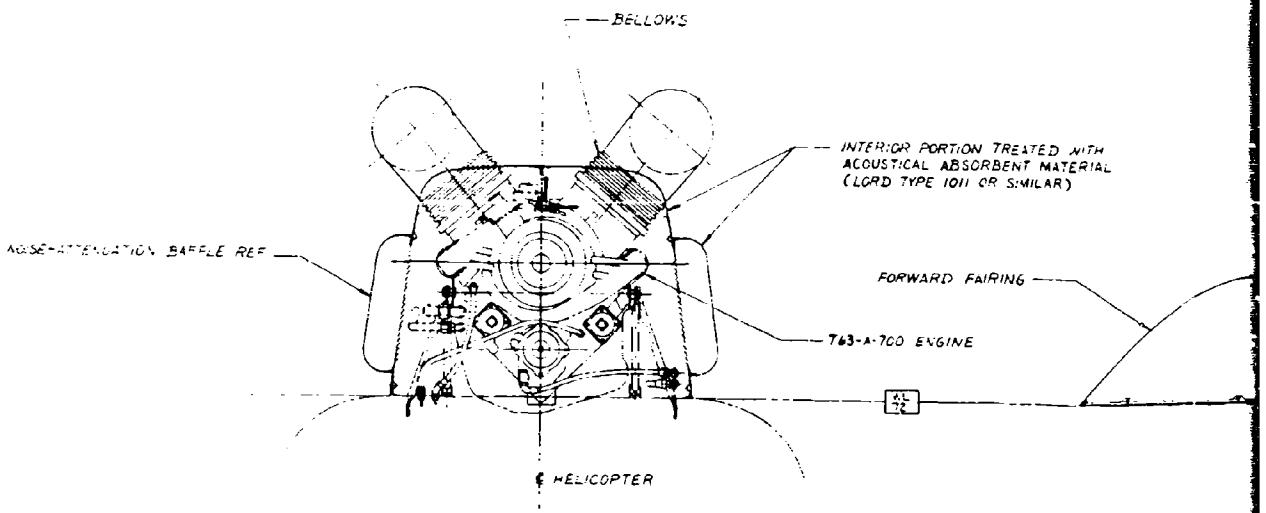

SECTION A-A

Figure 52. Powerplant Installation.

A

WOOL PACKED BETWEEN
RATED CRES SHEET WALLS

FORATED CRES SHEET

D PERFORATED CRES TUBE

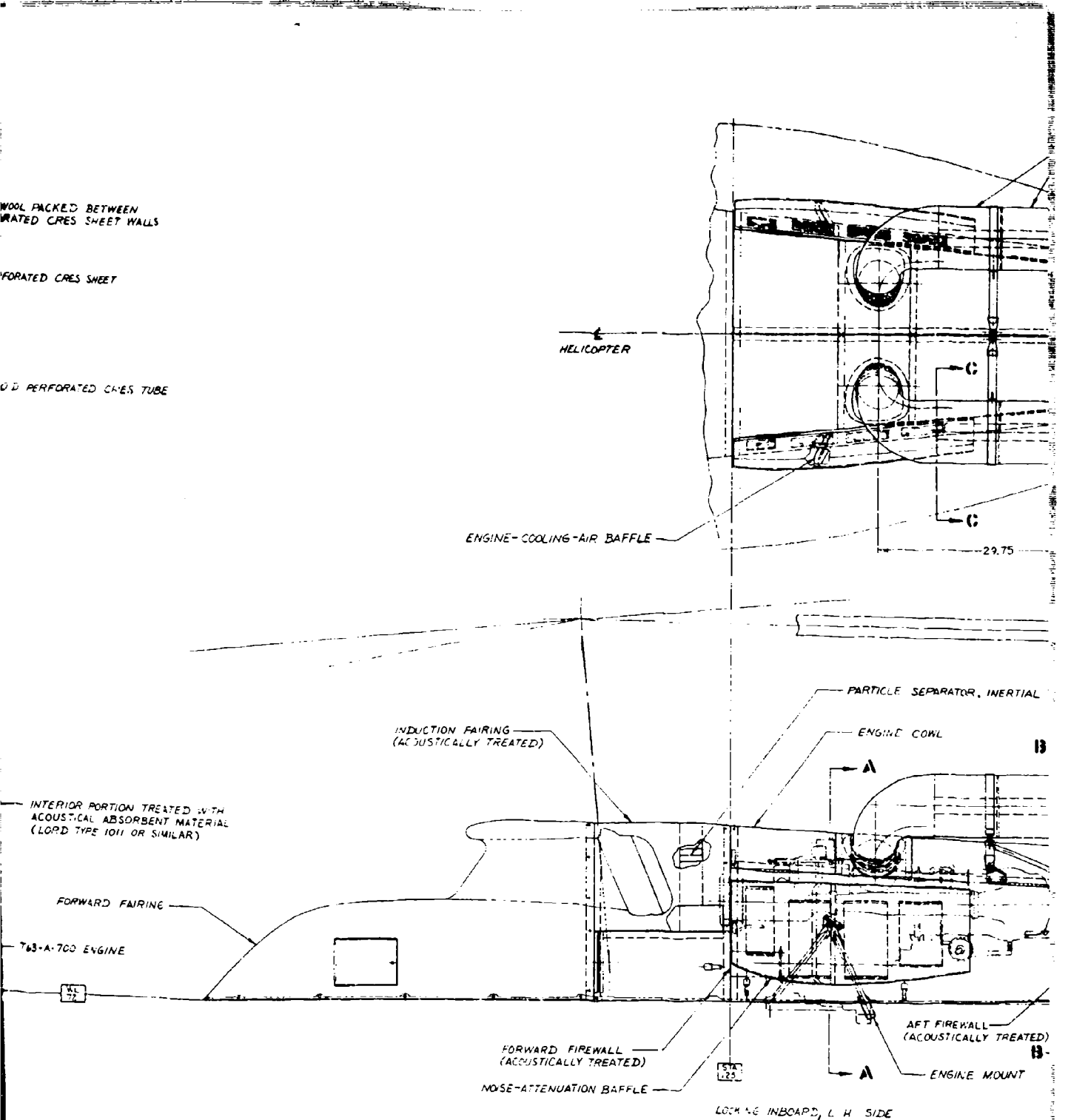

B

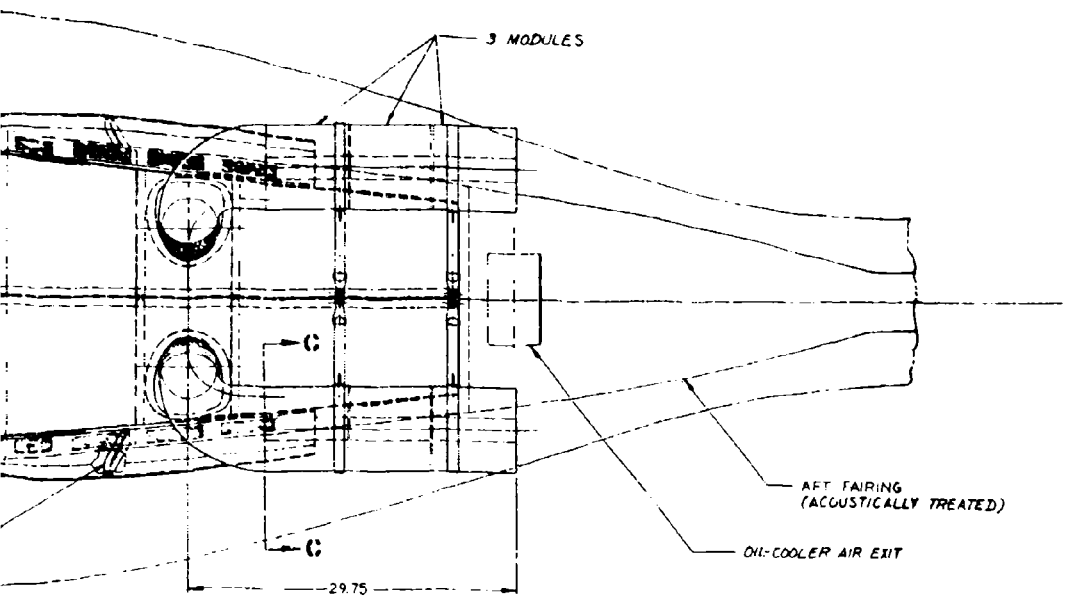

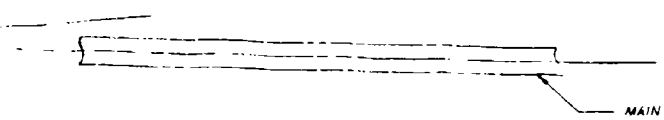

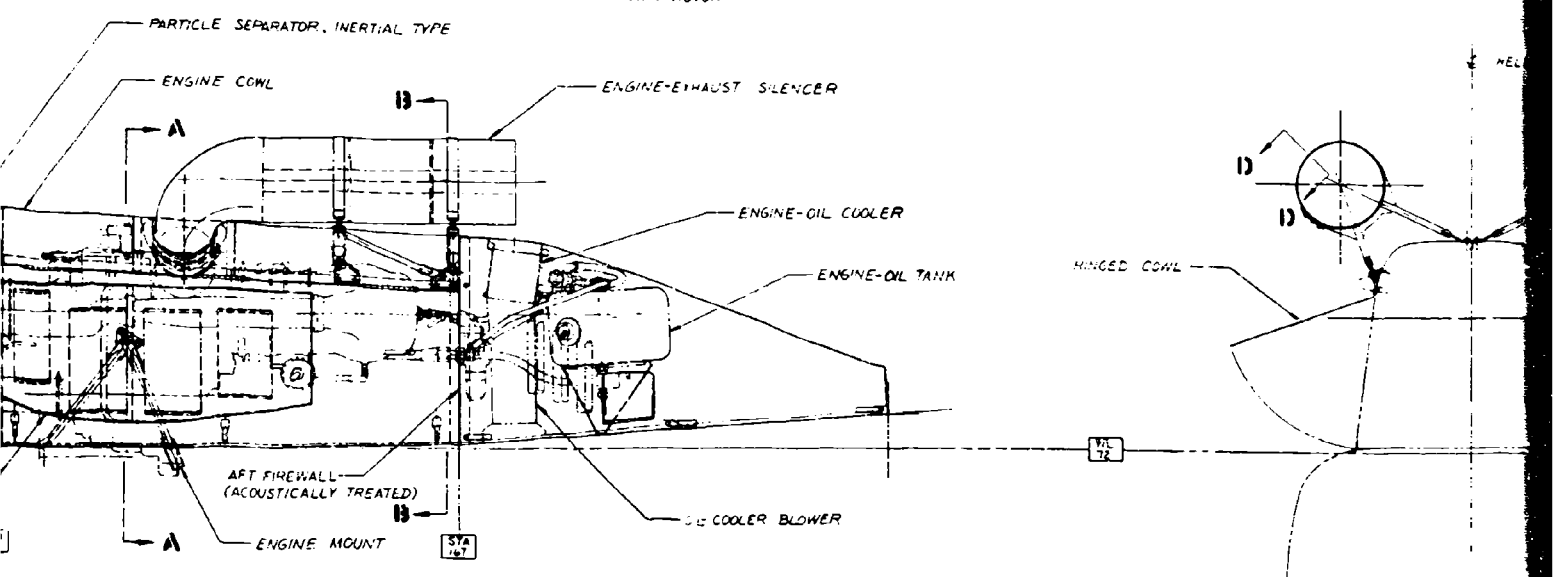

WING INBOARD, L H SIDE

SECTION B-

B

C

TED)

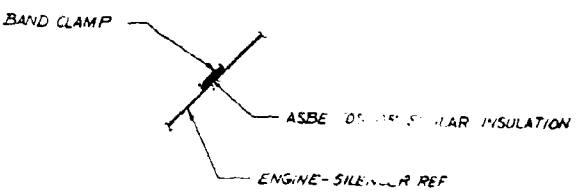

SECTION 1)-1)
SCALE : 1/2

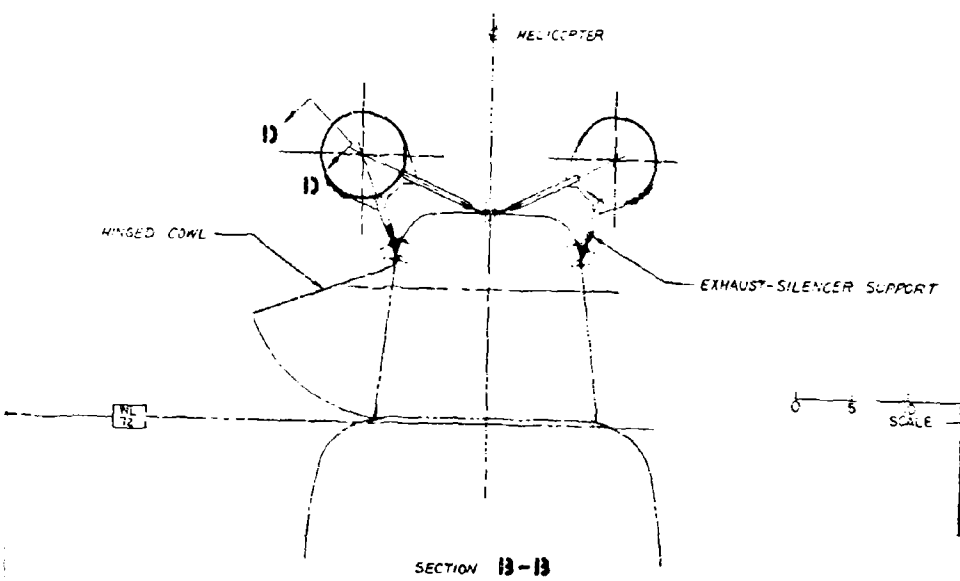

SECTION 3-3

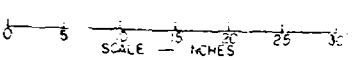

POWER PLANT INSTALLATION "DJET" HELICOPTER DH-58A		
		299-960-035

D

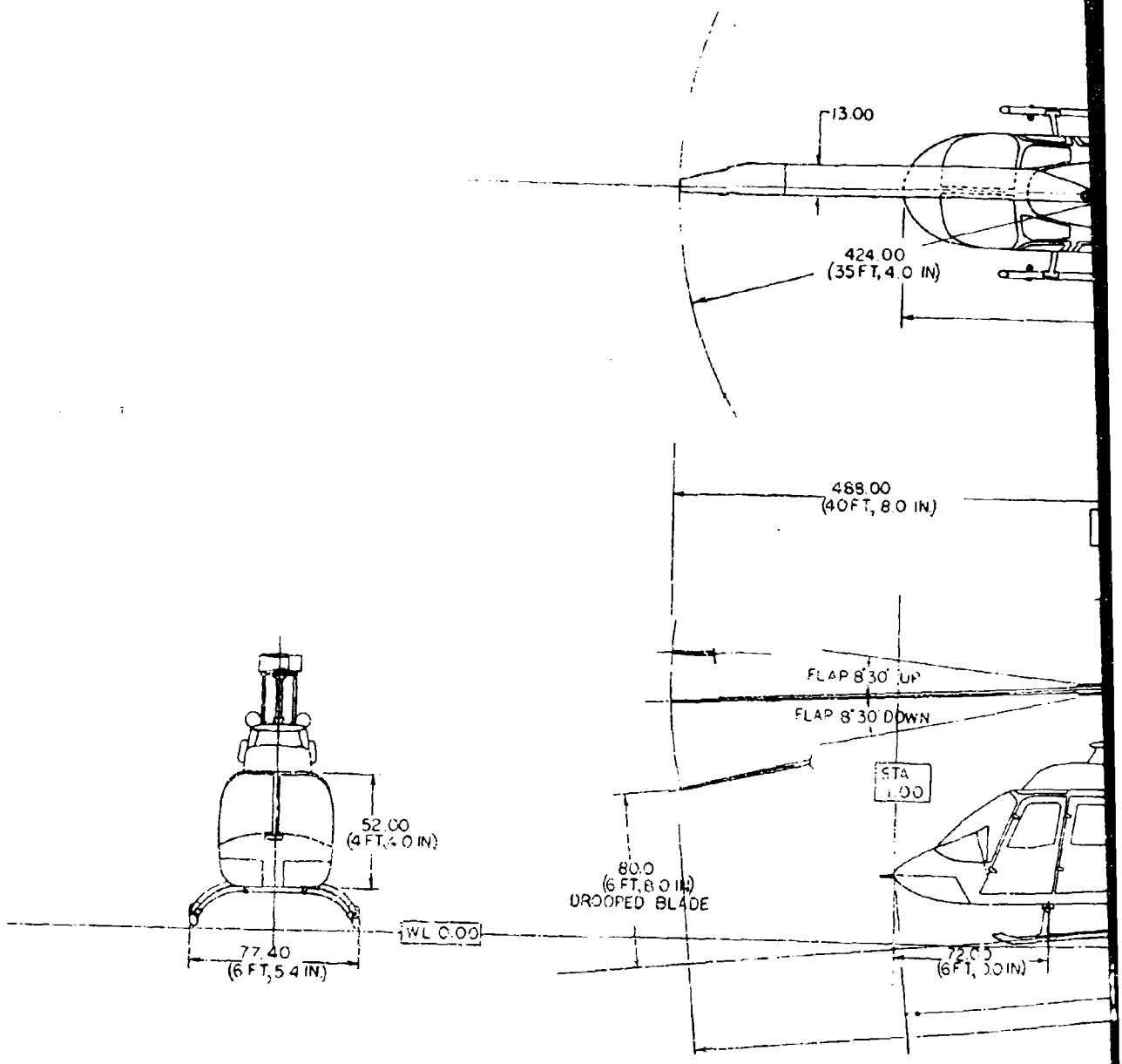

Figure 52. Three-View, Quiet Helicopter.

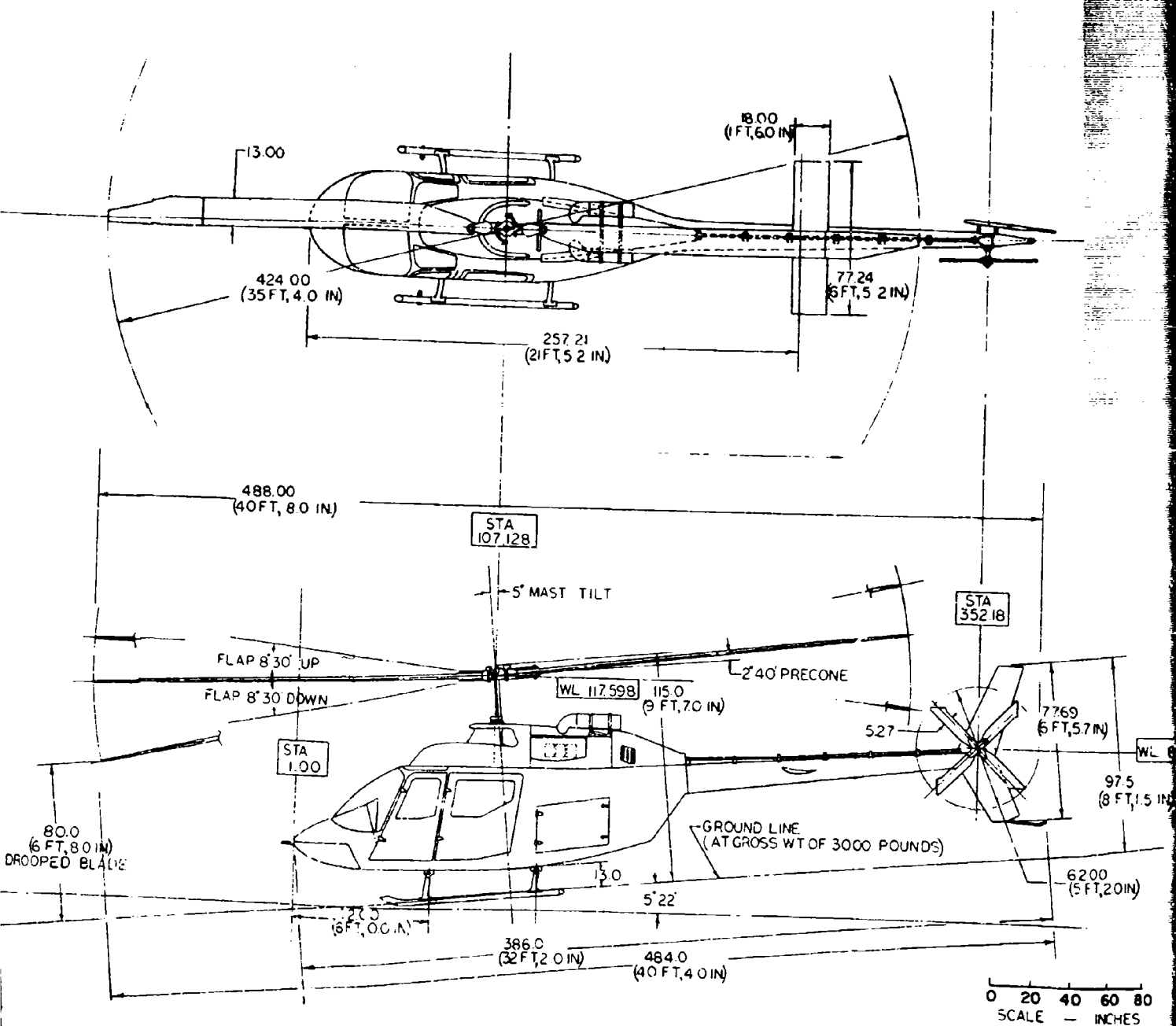
13.00
18.00
(1 FT, 6.0 IN)
424.00
(35 FT, 4.0 IN)
77.24
(6 FT, 5.2 IN)
257.21
(21 FT, 5.2 IN)
488.00
(40 FT, 8.0 IN)
STA
107.128
5° MAST TILT
STA
352.18
FLAP 8° 30' UP
FLAP 8° 30' DOWN
2° 40' PRECONE
WL 117.598
115.0
(9 FT, 7.0 IN)
STA
1.00
5.27
77.69
(6 FT, 5.7 IN)
97.5
(8 FT, 1.5 IN)
80.0
(6 FT, 8.0 IN)
DROOPED BLADE
GROUND LINE
(AT GROSS WT OF 3000 POUNDS)
13.0
5° 22'
72.0
(6 FT, 0.0 IN)
62.00
(5 FT, 2.0 IN)
386.0
(32 FT, 2.0 IN)
484.0
(40 FT, 4.0 IN)
0 20 40 60 80
SCALE — INCHES

elicopter.

B

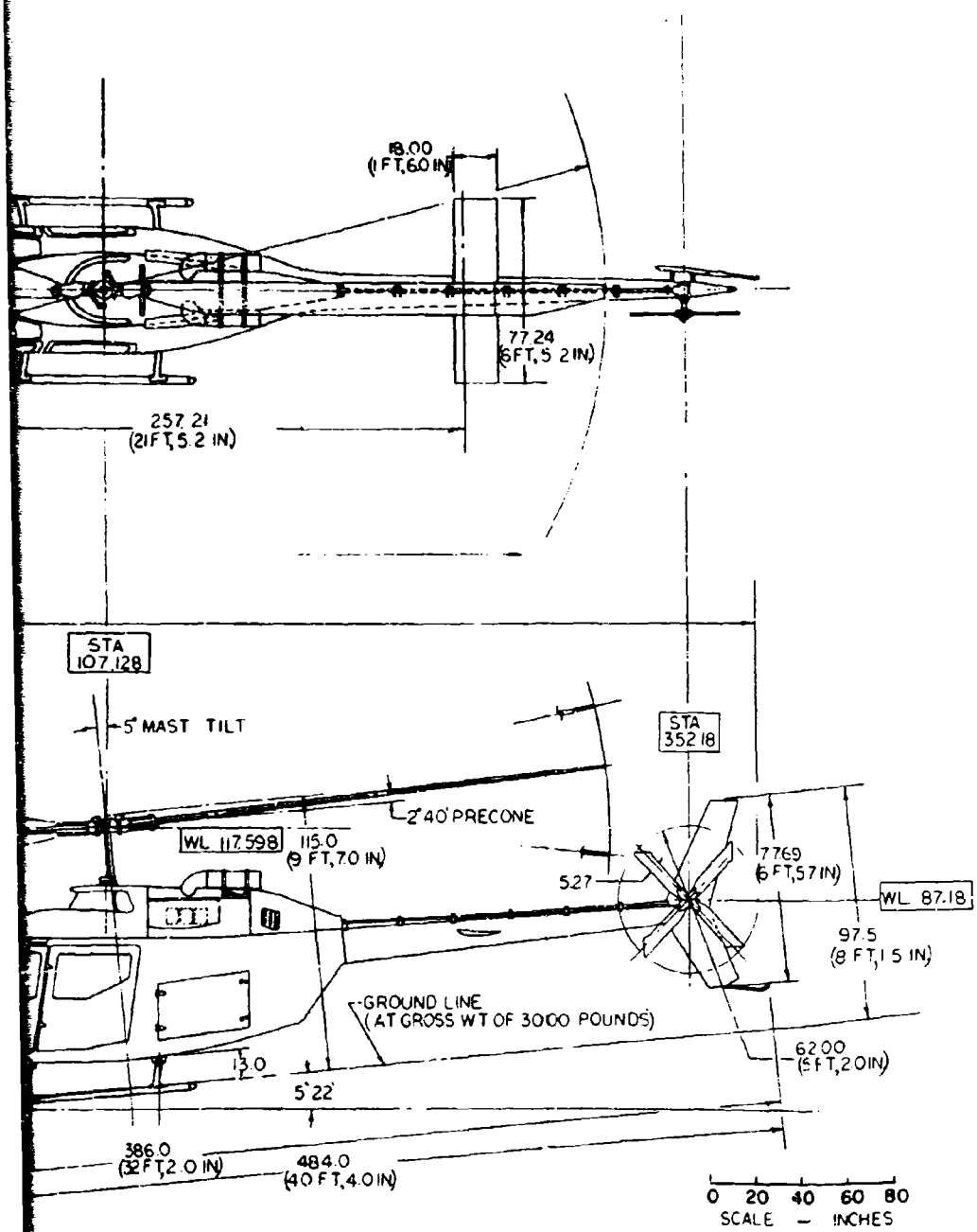

THREE VIEW			
QUIET HELICOPTER OH-58A			
R.D. KARANIAN	8-3-70	1/20	
EM	299-960 035		

B

C

Unclassified
Security Classification

DOCUMENT CONTROL DATA - R & D

(Security classification of title, body of abstract and indexing annotation must be entered when the overall report is classified)

1. ORIGINATING ACTIVITY (Corporate author)	2a. REPORT SECURITY CLASSIFICATION
Bell Helicopter Company P. O. Box 482 Fort Worth, Texas 76101	Unclassified 2b. GROUP

3. REPORT TITLE

A PRELIMINARY DESIGN STUDY OF A QUIET LIGHT OBSERVATION HELICOPTER

4. DESCRIPTIVE NOTES (Type of report and inclusive dates)

Final Report

5. AUTHOR(S) (First name, middle initial, last name)

Eugene L. Brown
Charles R. Cox
Dennis R. Halwes

6. REPORT DATE	7a. TOTAL NO. OF PAGES	7b. NO. OF REFS
December 1969	147	16

8a. CONTRACT OR GRANT NO.	9a. ORIGINATOR'S REPORT NUMBER(S)
DAAJ02-68-C-0095 b. PROJECT NO. Task 1F162203A14801 c. d.	USAAVLA Technical Report 69-99 9b. OTHER REPORT NO(S) (Any other numbers that may be assigned this report) Bell Report 299-099-526

10. DISTRIBUTION STATEMENT

This document is subject to special export controls, and each transmittal to foreign governments or foreign nationals may be made only with prior approval of U. S. Army Aviation Materiel Laboratories, Fort Eustis, Virginia 23604.

11. SUPPLEMENTARY NOTES	12. SPONSORING MILITARY ACTIVITY
	U. S. Army Aviation Materiel Laboratories Fort Eustis, Virginia 23604

13. ABSTRACT

This report presents the results of a preliminary design study and an analytical investigation of noise-reduction measures for the OH-58A Light Observation Helicopter (LOH). The purpose was to establish what degree of quieting is possible and what penalties in performance and mission capabilities are associated with the application of noise-reduction measures.

Design data are presented for four configurations. Two are test/demonstrator versions suitable for a flight-test program to verify the predicted noise reductions. The other two configurations incorporate design changes to give an operational quiet LOH the same payload and performance as the OH-58A.

Perceived noise levels are affected by the helicopter's flight conditions and gross weight and the observer's aspect and distance. Perceived levels 200 feet from the test configurations at design gross weight are at least 5 PNdb, and as much as 13 PNdb, lower than those of the OH-58A. The minimum level at this distance is 77 PNdb. At 4000 feet, the reductions are greater--ranging from 10 to 26 PNdb, for a minimum perceived noise level of 28 PNdb. The resulting noise levels are still above the initial design goals by 12 and 8 PNdb, respectively.

Design data, performance, and noise levels for all the study configurations are summarized. A program of design modification and tests to confirm the predicted noise reductions is presented.

DD FORM 1 NOV 68 1473 REPLACES DD FORM 1473, 1 JAN 64, WHICH IS OBSOLETE FOR ARMY USE.

Unclassified
Security Classification

14. KEY WORDS	LINK A		LINK B		LINK C	
	ROLE	WT	ROLE	WT	ROLE	WT
Quiet Light Observation Helicopter						
Noise Reduction						
Noise Measurement						
Noise Analysis						
Aural Detection						
Engine Silencer						
Rotor Noise						
Rotational Noise						
Engine Noise						
Drive-System Noise						
Acoustical Instrumentation						
Perceived Noise Level						
Noisiness						